ABSTRACT

LIU, TAO. Continuous Precipitation Polymerization of Acrylic Acid in Supercritical Carbon Dioxide. (Under the Direction of George W. Roberts and Joseph M. DeSimone)

Precipitation polymerization of acrylic acid in supercritical carbon dioxide ($scCO_2$) has received considerable attention during the last decade. By replacing water and organic solvents with $scCO_2$, this technique eliminates the costly polymer drying and purification processes required by conventional poly(acrylic acid) (PAA) production.

The present thesis provides detailed study on continuous precipitation polymerization of acrylic acid in $scCO_2$ in a continuous stirred tank reactor (CSTR) using 2, 2'-azobis (2, 4-dimethyl-valeronitrile) (V-65B) as the free-radical initiator. The reaction temperature was between 50 and 90 °C, the pressure was 207 bar, and the average residence time was between 12 and 40 minutes. The product polymer was a white, dry, fine powder that dissolved in water. A wide range of polymer molecular weights (5 to 200 kg/mol) was obtained.

The effect of the operating variables on the polymerization rate and on the polymer molecular weight was evaluated. The polymerization showed distinct characteristics of precipitation polymerization. Three simple kinetic models have been developed to describe this polymerization, and the models have been compared with the experimental results for rate of polymerization and viscosity average molecular weight. The first model, the "solution polymerization model", is based on the assumption that all of the polymerization reactions take place in the fluid phase, and that no reaction takes place in the polymer phase. In the second model, the "surface polymerization model", chain initiation is assumed to occur in the fluid phase, but chain propagation and chain termination occur in a thin zone on the surface

of the polymer particles. The third model, the "particle polymerization model", is similar to the "surface polymerization model", except that chain propagation and chain termination take place uniformly throughout the polymer particles. The surface polymerization model and the particle polymerization model both provided a much better fit of the data from the CSTR than the solution polymerization model. However, the data from a batch reaction calorimeter showed the particle polymerization model described the polymerization behavior better.

Scanning electron micrographs showed that three types of polymer particles were obtained: coagulum of primary particles of about 100 nanometers in size, irregular particles of 5-20 micrometers, and spherical particles of 10-100 micrometers. It is believed that the glass transition temperature of the polymer in the CSTR, T_g, was much lower than the glass transition temperature of the pure polymer, T_{g0}, due to the plasticization effect of $scCO_2$. It is speculated that the polymer coagulum was produced when the polymerization temperature, T_P, was below T_g, the irregular particles were produced when T_P was close to T_g, and the spherical particles were produced when T_P was above T_g. The absorption of CO_2 into PAA was measured with a quartz crystal microbalance. The T_g depression by $scCO_2$ was calculated from the Chow's equation. The calculated results lent strong support to the proposed particle formation mechanism.

Cross-linking polymerization of acrylic acid in $scCO_2$ was studied in a batch reactor at 50 °C and 207 bar with tetraallyl pentaerythritol ether and triallyl pentaerythritol ether as the cross-linkers and V-65B as the free radical initiator. All polymers were white, dry, fine powders. As the cross-linker concentration increased, the polymer glass transition temperature first decreased, and then increased. Viscosity measurements showed that the polymer thickening effect strongly depended on the degree of cross-linking. By adjusting the

cross-linker concentration, water-soluble and water-insoluble PAAs were synthesized. The water-insoluble PAA could be neutralized by ammonia gas and sodium hydroxide alcohol solution to make superabsorbent polymers.

CONTINUOUS PRECIPITATION POLYMERIZATION OF ACRYLIC ACID IN SUPERCRITICAL CARBON DIOXIDE

by

Tao Liu

A dissertation submitted to the faculty of North Carolina State University in partial fulfillment of the requirements for the Degree of Doctor of Philosophy in the Department of Chemical and Biomolecular Engineering

Raleigh, NC
March 21, 2005

Approved by:

George W. Roberts (co-chair)	Joseph M. DeSimone (co-chair)
Saad A. Khan	Alan E. Tonelli

BIOGRAPHY

Tao Liu was born in 1971 in Huantai, Shandong Province, China. He went to Zhejiang University of Technology, Hangzhou, Zhejiang Province, China, in September 1990 and obtained his B.S. in fine chemical engineering in July 1994. He then attended Beijing University of Chemical Technology, Beijing, China, in September 1994 and received his M.S. in chemical engineering in June 1997. After the completion of his M.S., Liu joined the Department of Chemical Engineering of Beijing General Research Institute of Mining and Metallurgy, where he served as a research engineer for three years. In August 2000, the author came to North Carolina State University to pursue his Ph.D. After one year of course work, he joined the Kenan Center for Utilization of CO_2 in Manufacturing and started his research on precipitation polymerization in supercritical carbon dioxide. He was co-advised by Dr. George W. Roberts and Dr. Joseph M. DeSimone. He received a M.S. in chemical engineering in December 2002.

ACKNOWLEDGEMENTS

I would like to express my deep gratitude to my advisors, Dr. George W. Roberts and Dr. Joseph M. DeSimone, for their constant advice, suggestions, knowledge, and understanding. Without them, this thesis would never have been possible. Also, I want to thank them for all the rewarding opportunities that I experienced as part of their research groups.

I would like to thank my colleagues at the Kenan CO_2 Center for their help. I would specifically like to thank Nael Zaki and Jaehoon Kim for the discussions and advice, Chunmei Shi for her expertise in automatic viscometer, Amy Zweber, Yazan Hussain and Vito Carla for their help in the study of CO_2 absorption into polymer.

I want to thank Dr. Saad A. Khan's group, Ahmed Eissa, Shamsheer Mahammad, David Frankowski, Angelica Sanchez, and Lauriane Scanu, for their help in DSC, GPC and DSR measurements. I also want to thank my friends, Bin Wei, Haiou Yang, Yangxing Li, and Xiangwu Zhang for always having the equipments that I needed.

Finally, I would like to thank my family for all their love, support, encouragement, and faith.

TABLE OF CONTENTS

Page

LIST OF TABLES

Page

LIST OF FIGURES

Page

CHAPTER 1

INTRODUCTION

1.1 Motivation and Objectives

Unsaturated monomers usually are polymerized in aqueous or organic media. However, increasing concern about the negative environmental impact of volatile organic compounds and organic-containing aqueous waste has prompted a search for environmentally benign polymerization media. The use of supercritical carbon dioxide ($scCO_2$) for this purpose has received considerable attention during the last decade [e.g., 1, 2]. In fact, DuPont recently introduced the first commercial fluoropolymers manufactured in $scCO_2$ [3].

Carbon dioxide (CO_2) has an easily accessible critical point (T_c = 31.1 °C, P_c = 73.8 bar). It is readily available, inexpensive, nontoxic, nonflammable, chemically inert under most conditions, and environmentally benign. When $scCO_2$ is used as the polymerization media, there is no chain transfer to solvent. Moreover, CO_2 can eliminate the need for costly polymer drying processes. The products from a polymerization conducted in CO_2 are completely dry after depressurizing to remove the CO_2 [2].

Many monomers and organic initiators are soluble in $scCO_2$. However, only amorphous fluoropolymers and silicones are soluble enough to permit solution polymerization in $scCO_2$ [1]. For other systems, a heterogeneous polymerization technique must be used. There are four basic heterogeneous polymerization processes: suspension polymerization, emulsion polymerization, dispersion polymerization, and precipitation polymerization. The first three require CO_2-philic surfactants. Some approaches to the design

and synthesis of such surfactants are described in three recent publications [4-6]. Effective CO_2-philic surfactants are expensive, and are difficult and costly to remove from the product polymer. Therefore, precipitation polymerization in $scCO_2$ has an inherent raw-material cost advantage over the other heterogeneous polymerization processes, and is most suitable for applications where pure polymers are required.

Polymer particles precipitate from the continuous phase during any precipitation polymerization. Radicals can be trapped in the polymer particles when they precipitate, or can be formed in the particles as a result of partitioning of a free-radical initiator between the two phases. Monomer then can diffuse into the polymer particles, allowing chain propagation to continue. The radical ends in the polymer phase are less accessible to each other, so that the rate of termination in the particles is greatly decreased. The result is an increase in the overall rate of polymerization and a corresponding increase in the polymer molecular weight. Thus, precipitation polymerization can allow both high polymerization rates and high molecular weights, even with a relatively unreactive monomer [7].

There is some controversy concerning the importance of propagation in the polymer particles during precipitation polymerizations in $scCO_2$. In their studies of the continuous precipitation polymerization of vinylidene fluoride (VF_2) in $scCO_2$, DeSimone, Roberts and coworkers [8-10] developed a model based on the assumption that initiation, propagation, and termination all took place homogeneously in the supercritical fluid, and that no reaction took place in the polymer particles. This model was able to describe all of the important features of the polymerization including the kinetics and the existence of a bimodal molecular weight distribution at some experimental conditions. Ahmed et al. [10] speculated that the lifetime of a radical in the supercritical fluid might be much smaller than the time

scale for polymer precipitation. If so, the concentration of radicals trapped in polymer particles when they precipitated would be small, and their impact on polymerization rate and polymer properties might not be significant. It also is possible that the polymerization rate in the polymer particles is low because of the low solubility of VF_2 in poly(vinylidene fluoride) in the presence of $scCO_2$ [11]

Nevertheless, a homogeneous solution polymerization model probably cannot describe the behavior of most precipitation polymerization systems, because the precipitated polymer frequently is an important locus of polymerization. For example, in the polymerization of acrylonitrile in water, Moore and Parts found that the rate of polymerization and polymer molecular weight were reduced if the polymer particles were continuously eliminated from the reaction by centrifuging [12]. The rate of a precipitation polymerization usually depends on the monomer concentration to a power higher than 1, whereas a classical solution polymerization is first-order in monomer. The dependence of the rate of a precipitation polymerization on the initiator concentration also can be different from that of a classical solution polymerization, where the order with respect to initiator is 0.5. For example, the precipitation polymerization of acrylonitrile in benzene at 50 °C, initiated by 2, 2'–azobis(isobutyronitrile) (AIBN), had an order with respect to monomer of about 1.7. The order with respect to initiator varied from 0.89 when the initiator concentration was 10^{-4} mol/L to 0.33 when the initiator concentration was 10^{-2} mol/L [13].

Acrylic acid polymers and copolymers are widely used as dispersants, thickeners, flocculants, and superabsorbent polymers (SAPs). Poly(acrylic acid) (PAA) commonly is prepared by solution polymerization, although suspension polymerization, inverse emulsion polymerization, and precipitation polymerization in organic media also are used [14]. In

solution polymerization, water usually is the solvent and a costly drying process is necessary. The other three processes are carried out in organic media. The use of surfactants and/or organic solvents inevitably leads to chemical contamination of the polymer. For applications where extremely clean PAA or PAA derivatives are desired (e.g. thickeners in toothpaste and cosmetics), costly purification and drying processes often are necessary.

Acrylic acid is moderately soluble in $scCO_2$, while PAA is insoluble. Precipitation polymerization in $scCO_2$ may offer an attractive alternative to conventional processes for PAA, in that the final polymer is virtually free of contamination. Unreacted monomer and initiator are easily removed from the polymer by extraction with $scCO_2$.

Precipitation polymerization of acrylic acid in CO_2 was first reported in a French patent [15] in 1968. The U. S. version of this patent [16] appeared in 1970. The precipitation polymerization of several vinyl compounds, including acrylic acid, in liquid and supercritical CO_2, was demonstrated in these patents. In 1986, a Canadian patent [17] described the synthesis of water-soluble PAA in $scCO_2$. In 1987, the synthesis of acrylic-acid-type thickeners in $scCO_2$ was discussed in a U. S. patent application [18]. A similar study was also reported in a European patent application [19] in 1988. More recently, DeSimone and coworkers [20] studied acrylic acid polymerization in $scCO_2$, and used ethyl mercaptan as a chain transfer agent to control the polymer molecular weight. Finally, Xu et al. [21] explored the effect of cosolvents on the polymerization of acrylic acid in $scCO_2$.

The first objective of this thesis is to study the continuous precipitation polymerization of acrylic acid in $scCO_2$ using a continuous stirred tank reactor (CSTR). The effect of the major chemical and operating variables on polymerization rate and on polymer

molecular weight will be evaluated. The polymerization kinetics will be studied and kinetic models that describe the polymerization behavior will be developed.

A continuous process has been reported for precipitation polymerization of VF_2 in $scCO_2$, using a CSTR [8-10]. This process also has been applied to the synthesis of PAA [22]. While batch reactors are useful for the production of small-to-intermediate volume polymers, continuous reactors are more suitable for the production of high-volume, commodity polymers. Compared to batch processes, continuous processes have many advantages, including: (1) smaller and cheaper reactors; (2) easier recycle of CO_2 and unreacted monomer, and; (3) time-invariant reaction conditions, and hence more uniform polymer properties. In addition, the polymer produced in $scCO_2$ with a CSTR may have properties that are different and advantageous relative to polymer produced in conventional processes [8, 9].

Although the precipitation polymerization of acrylic acid in $scCO_2$ has been known for many years, a systematic kinetics study has not been reported. The polymerization kinetics is important for the optimization and control of commercial production, because it tells us how the reaction conditions will affect the rate of polymerization and the molecular weight of polymer [23, 24]. Polymerization is usually highly exothermic. Uncontrolled reaction can cause operation difficulties and even safety issues. The molecular weight and molecular weight distribution (MWD) determine the applications of polymer. People prefer to get the required molecular weight and MWD at the reaction stage, because it is difficult to change them after reaction.

The second objective of this thesis is to study the preparation of SAPs with $scCO_2$ technology. SAPs usually are cross-linked, partially neutralized, water-insoluble PAA [25].

They are the largest use of PAA, accounting for 73% of the PAA consumption in 2000 [26]. The U.S. demand for SAPs is estimated at 800 million pounds in 2003, and it is expected to grow at an average annual rate of 5% during 2003 – 2008 [27].

The most prevalent commercial process to make SAPs is cross-linking copolymerization of acrylic acid and metal acrylates in water [25]. The polymerization produces a hydrogel intermediate containing a large amount of water, because the monomer concentration in the polymerization ranges from about 16% to about 43% on a weight basis. Commercially, about 2 to 5 kg of water must be removed by evaporation for 1 kg of polymer produced. Suspension polymerization in organic solvents, usually in high molecular weight aliphatic hydrocarbons (C10 – C14), is also used to make SAPs [25]. Because of the better heat transfer in this process, a much higher monomer concentration can be used in the polymerization phase. Therefore, the drying cost is reduced. However, this advantage is negated by the low polymerization phase ratio (ratio of dispersed phase to continuous phase), which limits to 1:1 or less.

Not like acrylic acid, metal acrylates (e.g. sodium acrylate, ammonium acrylate and calcium acrylate) are not soluble in $scCO_2$, even in the presence of cosolvents. Therefore, it is difficult to copolymerize metal acrylates and acrylic acid in $scCO_2$. A novel method consist of two steps to make SAPs will be developed in this thesis. In the first step, water-insoluble polymer will be synthesized by precipitation cross-linking polymerization of acrylic acid in $scCO_2$. The effect of polymerization variables on polymer properties will be investigated. In the second step, the water-insoluble polymer will be partially neutralized to make SAPs. Various neutralization methods will be studied.

1.2 Overviews of Contents of This Thesis

This thesis focuses on the precipitation polymerization of acrylic acid in $scCO_2$, including experimental work and theoretical studies.

Chapter 2 presents literature review. The general features of precipitation polymerization are described first. Then the previous studies on precipitation polymerization of acrylic acid in $scCO_2$ are summarized.

Chapter 3 describes the experimental studies on continuous precipitation polymerization of acrylic acid in $scCO_2$ in a CSTR. The effects of the operating variables on the polymerization rate and on the polymer molecular weight are evaluated. The observed kinetics suggests that the polymerization takes place in both the supercritical fluid and the precipitated polymer particles.

Chapter 4 presents the kinetic analysis of precipitation polymerization of acrylic acid in $scCO_2$. Kinetics modeling and calorimetric study show that the polymer phase is the main polymerization locus. A polymerization model assuming chain initiation takes place only in continuous phase while chain propagation and chain termination takes place only in and homogeneously throughout the polymer particles predicts the experimental results well.

Chapter 5 describes the morphology of the polymer made by continuous precipitation polymerization of acrylic acid in $scCO_2$. Three types of polymer particles are prepared. A particle formation mechanism is proposed. It is speculated that the polymer morphology mainly depends on the polymerization temperature.

Chapter 6 shows the efforts to synthesize cross-linked acrylic acid polymers. By adjusting the polymerization variables, especially the cross-linker concentration, water-

soluble and water-insoluble polymers are synthesized. The effect of cross-linking on polymer properties is evaluated.

Chapter 7 presents the novel methods to make SAPs with $scCO_2$ technology. Water-insoluble PAA, which is made by precipitation cross-linking polymerization of acrylic acid in $scCO_2$, is neutralized by ammonia gas and sodium hydroxide alcohol solution to make SAPs.

Chapter 8 summarizes the conclusions of all the results and recommends future works.

1.3 References

1. DeSimone, J. M.; Maury, E. E.; Menceloglu, Y. Z.; McClain, J. B.; Romack, T. J.; Combes, J. R. Science 1994, 265, 356-359.
2. Kendall, J. L.; Canelas, D. A.; Young, J. L.; DeSimone, J. M. Chemical Review 1999, 99, 543-563.
3. Dupont Product News March 6, 2002: "DuPont Introduces First Fluoropolymers Made with Supercritical CO_2 Technology". http://www1.dupont.com/NASApp/dupontglobal/corp/index.jsp?page=/news/products_today.html&type=Product_News&year=2002
4. Lacroix-Desmazes, P.; Andre, P.; DeSimone, J. M.; Ruzette, A-V.; Boutevin, B. Journal of Polymer Science Part A: Polymer Chemistry 2004, 42, 3537-3552.
5. Ma, Z.; Lacroix-Desmazes, P. Journal of Polymer Science Part A: Polymer Chemistry 2004, 42, 2405-2415.

6. Galia, A.; Giaconia, A.; Iaia, V.; Filardo, G. Journal of Polymer Science Part A: Polymer Chemistry 2004, 42, 173-185.
7. Barrett, K. E. J.; Thomas, H. R. in Dispersion Polymerization in Organic Media; Barrett, K. E. J., Ed.; Wiley-Interscience: New York, 1974; Chapter 4, 116-118.
8. Charpentier, P. A.; DeSimone, J. M.; Roberts, G. W. Industrial and Engineering Chemistry Research 2000, 39, 4588-4596.
9. Saraf, M. K.; Gerard, S.; Wojcinski, L. W. II; Charpentier, P. A.; DeSimone, J. M.; Roberts, G. W. Macromolecules 2002, 35, 7976 – 7985.
10. Ahmed, T. S.; DeSimone, J. M.; Roberts, G. W. Chemical Engineering Science 2004, 59, 5139 – 5144.
11. Kennedy, K. A., "Characterization of Phase Equilibrium Associated with Heterogeneous Polymerizations in Supercritical Carbon Dioxide", Ph. D. Thesis, North Carolina State University (2003).
12. Moore, D. E.; Parts, A. G. Die Makromolekulare Chemie 1960, 37, 108-118.
13. Lewis, O. G.; King, R. M. In Addition and Condensation Polymerization Processes: a Symposium; Gould, R. F., Ed.; American Chemical Society: Washington D. C., 1969; pp 25-45.
14. Nemec, J. W.; Bauer, W. in Encyclopedia of Polymer Science and Engineering, 2nd ed.; Mark, H. F., Ed.; Wiley-Interscience: New York, 1988; vol.1, pp 211-231.
15. Fukui, K.; Fujii, K.; Kagiya, T.; Toriuchi, Y.; Yokota, H. (Sumitomo Chemical Company, Ltd. and Sumitomo Atomic Energy Industries, Ltd.). French Patent 1,524,533, April 1, 1968.

16. Fukui, K.; Fujii, K.; Kagiya, T.; Toriuchi, Y.; Yokota, H. (Sumitomo Chemical Company, Ltd. and Sumitomo Atomic Energy Industries, Ltd.). U. S. Patent 3,522,228, July 28, 1970.
17. Sertage, W. G. J.; Davis, P.; Schenck, H. U.; Denzinger, W.; Hartmann, H. (BASF Corporation). Canadian Patent 1,274,942, October 2, 1990.
18. Hartmann, H.; Denzinger, W. (BASF Corporation). U. S. Patent 4,748,220, May 31, 1988.
19. Herbert, M. W.; Huvard, G. S. (B.F. Goodrich Company). European Patent 0,301,532 (A2), February 1, 1989.
20. Romack, T. J.; Maury, E. E.; DeSimone, J. M. Macromolecules 1995, 28, 912-915.
21. Xu, Q.; Han, B.; Yan, H. Polymer 2001, 42, 1369-1373.
22. Charpentier, P. A.; Kennedy, K. A.; DeSimone, J. M.; Roberts, G. W. Macromolecules 1999, 32, 5973-5975.
23. Brooks, B. W. Industrial and Engineering Chemistry Research 1997, 36, 1158-1162.
24. Ray, W. H.; Soares, B. P.; Hutchinson, R. A. Macromol. Symp. 2004, 206, 1-13.
25. Graham, A. T.; Wilson, L. R. in Modern Superabsorbent Polymer Technology; Buchholz, F. L.; Graham, A. T. Ed.; Wiley – VCH: New York, 1998; Chapter 3, p69-118.
26. Will, R.; Sasano, T. in CEH Marketing Research Report; the Chemical Economics Handbook – SRI International, 2001; pp 582.000A-582.005J.
27. Lacson, J. G.; Lochner, U.; Toki, G. in CEH Marketing Research Report; the Chemical Economics Handbook – SRI International, 2004; pp 606.4000A-606.4004G.

CHAPTER 2

LITERATURE REVIEW

2.1 Kinetics of Precipitation Polymerization

2.1.1 Chemistry of Free Radical Vinyl Polymerization

Free radical vinyl polymerization is a chain reaction that consists of a sequence of three steps: initiation, propagation and termination.

A. Initiation:

$$I \xrightarrow{k_d} 2R^{\bullet} \tag{2-1}$$

$$R^{\bullet} + M \xrightarrow{k_i} P_1^{\bullet} \tag{2-2}$$

B. Propagation

$$P_n^{\bullet} + M \xrightarrow{k_p} P_{n+1}^{\bullet} \tag{2-3}$$

C. Termination

$$P_n^{\bullet} + P_m^{\bullet} \xrightarrow{k_t} products \tag{2-4}$$

The simplest vinyl polymerization process is homogeneous solution polymerization, in which the rates of initiation, propagation and termination are typically given by Equations 2-5, 2-6 and 2-7, respectively:

$$R_i = 2fk_d[I] \tag{2-5}$$

$$R_p = k_p\left(\frac{fk_d}{k_t}\right)^{1/2}[M][I]^{1/2} \tag{2-6}$$

$$R_t = 2k_t[P^{\bullet}]^2 \tag{2-7}$$

The kinetic chain length, ν, is then given by Equation 2-8.

$$\nu = \frac{R_p}{R_i} = \frac{k_p}{2(fk_d k_t)^{1/2}} \frac{[M]}{[I]^{1/2}} \tag{2-8}$$

As the reaction progresses, solution polymerization generally involves a pronounced increase in viscosity and evolution of heat. In the polymerization of certain monomers, either undiluted or in concentrated solution, auto-acceleration can eventually take place at high viscosities. This is particularly pronounced for polymerization of methyl methacrylate, methyl acrylate, and acrylic acid [1-9]. The viscosity increase demands higher power and stronger design for pumps and agitators. Other disadvantages of solution polymerization include: 1) need of inert solvent to avoid possible chain transfer to solvent; 2) lower yield per reactor volume; 3) reduction of reaction rate and average chain length; and 4) difficulty of complete solvent removal [10, 11].

Due to the disadvantages of solution polymerization, heterogeneous polymerizations are used in free-radical polymerization. There are four basic heterogeneous polymerization processes: suspension polymerization, emulsion polymerization, dispersion polymerization, and precipitation polymerization. The following discussions focus on the kinetics of precipitation polymerization of vinyl monomers. Unless a continuous process is specified, the discussions are for batch polymerization.

2.1.2 General Features of Precipitation Polymerization

In precipitation polymerization, monomer and initiator are dissolved in a liquid that is a non-solvent for the polymer. The reaction mixture is homogeneous at the outset and the polymerization is initiated in the homogeneous solution. Depending on the solvency of the medium for the resulting polymer radicals and polymer molecules, phase separation occurs at an early stage. This leads to the nucleation and formation of primary particles. The number of

particles gets constant at a very low monomer conversion. New primary particles produced in the continuous phase are deposited upon a large number of existing particles, which grow in size with time [12].

Because polymer radicals coalesce with polymer, radical activity can be trapped in the polymer particles. Although diffusion of monomer is still possible in both phases, occlusion makes the radical ends less accessible to each other in polymer phase. As a result, termination in the particles is greatly decreased, while the occluded radicals can undergo propagation largely unhindered. This results in an increase in the overall rate of polymerization and a corresponding increase in the overall molecular weight. Thus, precipitation polymerization allows attainment of both high reaction rates and high molecular weights, even from relatively unreactive monomer [13]. A typical precipitation polymerization begins slowly and gradually accelerates to a maximum rate followed by a diminution in rate as monomer is consumed.

Many polymers are produced by precipitation polymerization. Detailed polymerization kinetics depends very much on the nature of the monomer and the polymer matrix it forms. A review of some typical precipitation polymerization systems is presented below.

2.1.3 Precipitation Polymerization of Acrylonitrile

Polyacrylonitrile (PAN) does not dissolve in its own monomer. The bulk polymerization of acrylonitrile conforms to precipitation polymerization. It is believed that growing radicals at some stage become insoluble in the continuous phase, and there will be a finite probability that the active end of the radical will become shielded by coiling of the

molecule. Coalescence of polymer particles would be expected to greatly enhance the degree of shielding and it is the major factor in the occlusion of radicals [14]. The main effect of occlusion is to reduce the termination rate coefficient. Studies [15, 16] have shown a great increase of average lifetime of free radical beyond about 1% polymerization. This effect naturally leads to a progressive increase in the rate of reaction and a higher initiator order than normal [14]. In the study of Bamford and Jenkins [14], the rate of polymerization increased with time up to about 20% monomer conversion. Moreover, the order of initiator concentration in the expression of polymerization rate was 0.9, which is much greater than 0.5. In the study of Bengough [15], the initiator order was 0.5 in the very early stages of the polymerization (<0.1% monomer conversion) and it increases to 0.7 beyond about 1% monomer conversion. Lewis and King [16] showed that the monomer order is about 1.7 in the precipitation polymerization of acrylonitrile in benzene at 50 °C. In the study of Garcia-rubio and coworkers [17, 18], the acceleration in polymerization rate was not apparent at low initiator concentrations, but at high initiator concentration the rate of polymerization quickly increased to a maximum then fell to zero at a limiting conversion less than 100%. The duration of the autoacceleration, the value and position of the maximum polymerization rate depended strongly on temperature and initiator concentration. The higher the temperature and the initiator concentration, the lower the monomer conversion when the maximum polymerization rate appears. The limiting conversion with excess initiator was reached when the polymer-monomer solution became a glass.

With extreme degrees of occlusion, chain propagation can occur only with difficulty [14]. However, studies [19,20] have shown that only about 1-2 percent of the total number of radicals generated can be trapped in this way, even under favorable conditions. Moreover,

because extreme occlusion can completely prevent chain growth, long living radicals must contribute little toward the overall rate of polymerization.

As the temperature increases, the loosening of aggregates may allow and increase the amount of propagation before appreciable bimolecular termination is possible. Bamford and Jenkins [14] prepared a number of PAN samples using the same initiator concentration at different temperatures. Polymer thus obtained at 55 °C and above showed a smooth decrease of molecular weight with rise in temperature, as would be expected, but those prepared below 55 °C showed an increase in molecular weight with increase in temperature, indicating a faster rise of propagation than termination. Garcia-Rubio and coworkers also found a gradual increase in molecular weight with temperature in the range of 0 to 80 °C [17, 18].

It is believed that the number of particles becomes constant in the very early stage of polymerization [16]. Lewis and King [16] found that no new aggregates were formed beyond about 0.4% conversion in bulk polymerization of acrylonitrile. The aggregates of precipitated polymer particles were highly porous, which could be seen in electron micrographs. It was also found that particles from polymerization in benzene were more compact and dense in appearance than those from bulk polymerization.

Peelbes [21] proposed that three separate loci of polymerization exist during the precipitation polymerization of acrylonitrile. These are: the solution phase, the surface of polymer particles, and the interior of polymer particles. Accordingly, three types of polymerization are named: solution polymerization, surface polymerization and interior polymerization. It is believed that a polymer chain becomes insoluble in its early stage of growth. Most of the polymer is produced in the polymer phase [18].

The monomer concentration inside the polymer particle is low [22]. The solubility of acrylonitrile in PAN is about 10 wt% in the temperature range of 0 to 80 °C [17, 18]. In addition, monomer concentration gradients exist in the precipitated polymer particles, because the diffusion of monomer in glassy polymers is slow [17, 18]. Therefore, the particle surface is the main polymerization locus [16, 21, 22], especially when the initiator concentration is high and the temperature is low [17, 18]. However, interior polymerization should become indistinguishable from surface polymerization at high temperature, because the loosening of coalesced polymer particles at high temperature will make the diffusion of small molecules into polymer particles easier [21].

Precipitation polymerization of acrylonitrile can also be carried out in aqueous solution. Like in bulk polymerization, the polymer phase plays an important role in this process. The rate of polymerization and polymer molecular weight can be lowered by removal of the polymer particles by centrifugation of the polymerization system [23]. The studies of McCarthy et al. [24] and Nishida et al. [25] suggested the polymerization mainly occurred on the particle surface.

Elbing et al. [12] studied the precipitation polymerization of acrylonitrile in water at 50 °C using potassium persulphate as initiator. The particle number density in each run became constant at very early stages of reaction. The same value (1.56×10^{12} cm^{-3}) was found for four different initial concentrations of monomer and initiator. The study of McCarthy et al. [24] showed the average number of free radicals per particle was about 250. Radical capture efficiency by the particles was close to100%. Their study also showed the loss of free radicals from the particle surface was first order in the average number of free radicals. A plausible mechanism for this observation proposed by McCarthy et al. was that propagation

might place the free radical chain ends in such close proximity to the surface that further monomer addition was precluded on steric grounds: the absence of backbone rotations in the glassy state would freeze the stunted chain in these hindered nonpropagating conformations. Termination with another free radical (a second order process) might eventually take place, but this would be on a much slower time scale, and thus the loss of free radical activity would appear kinetically first order.

2.1.4 Precipitation Polymerization of Vinyl Chloride

Poly(vinyl chloride) (PVC) is insoluble in vinyl chloride. Therefore, the bulk polymerization of vinyl chloride also conforms to precipitation polymerization. Vinyl chloride follows the same behavior as acrylonitrile when polymerized at low temperature and high initiation rate [26]. However, at normal temperature they behave differently. In the bulk polymerization of acrylonitrile, the maximum polymerization rate occurs at low conversions, where both monomer and polymer phases are present in appreciable amounts [17]. In the bulk polymerization of vinyl chloride, the maximum polymerization rate occurs after the monomer phase has been consumed. This is because vinyl chloride, not like acrylonitrile, which has low solubility in PAN, has much higher solubility in PVC. During the entire life of the monomer phase, the polymer phase is saturated with monomer [27], and the two phases are in thermodynamic equilibrium. Thus the polymer phase composition remains constant [28].

The bulk polymerization of vinyl chloride can be divided into three stages [29]. At the first stage, the monomer conversion increases from zero until polymer particles precipitate. The polymerization takes place homogeneously. At 50 °C, polymer starts to

precipitate when monomer conversion gets to about 0.1%. At the second stage, monomer conversion increases to a critical value, x_c, where the free vinyl chloride disappears. At this stage, the polymerization proceeds in both the monomer and the polymer phases. The value of x_c is a function of temperature [27]. It is 80, 77 and 72% at 30, 50 and 70 °C, respectively. At the third stage, the polymerization proceeds in the polymer particles. If the reaction temperature is below the glass transition temperature (T_g) of the product polymer, diffusion of monomer to the propagation radical is extremely slow. As a result, the conversion has an upper limit less than 100%. The limit is estimated to be 96% at 55 °C, 93% at 30 °C and 90% at –10 °C [29].

In the bulk polymerization of acrylonitrile, the rate of chain transfer to monomer is so low that radical termination is mainly by mutual termination of occluded radicals in the polymer phase. In the precipitation polymerization of vinyl chloride, the initiator order is essentially 0.5, because of the high rate of chain transfer to monomer [30, 31]. An occluded radical in the polymer phase can chain transfer to monomer, which can diffuse back into the liquid phase. The radical termination mainly takes place in the liquid phase, and mutual termination of radicals in the polymer phase is therefore negligible [30].

2.1.5 Precipitation Polymerization of Vinyl Fluoride

Poly(vinyl fluoride) is not soluble in vinyl fluoride or any solvent at room temperature. If a solvent is used, it has two opposite effects on the polymerization. The increase of solvent concentration will increase the swelling of the polymer phase and consequently increase the monomer diffusion into the polymer phase. At the same time, it will decrease the monomer concentration. Therefore, the polymerization rate reaches a

maximum as the solvent fraction increases. Also, since chain transfer to solvent can take place, a small amount of solvent can considerably decrease the polymer molecular weight [32, 33].

A kinetics model has been developed for the precipitation polymerization of vinyl Fluoride [33]. The model assumes that the polymer phase is swelled by the solvent and monomer. The two phases are in equilibrium with each other. At a certain length, a propagating "mobile radical" in the continuous phase precipitates to the polymer phase and becomes a " fixed racial". A "fixed radical" can terminate by chain transfer to solvent or monomer, which becomes a "mobile radical" in the polymer phase. This new "mobile radical" can terminate another "fixed radical". According to this model, the solvent determines the rate of the reaction by its swelling of the polymer, and the degree of polymerization is mainly determined by transfer reactions.

2.1.6 Precipitation Polymerization of Vinylidene Fluoride

The studies of DeSimone, Roberts and coworkers [34-36] of the continuous precipitation polymerization of vinylidene fluoride (VF_2) in $scCO_2$ showed that the polymerization took place like a normal free radical solution polymerization. They developed a model based on the assumption that initiation, propagation, and termination all took place homogeneously in the continuous fluid phase, and that no reaction took place in the polymer particles. This model was able to describe all of the important features of the polymerization including the kinetics and the existence of a bimodal molecular weight distribution at some experimental conditions. It is believed that the lifetime of a radical in the supercritical fluid might be much smaller than the time scale for polymer precipitation [36]. If so, the

concentration of radicals trapped in polymer particles when they precipitated would be small, and their impact on polymerization rate and polymer properties might not be significant.

It also is possible that the polymerization rate in the polymer particles was low because of the low solubility of VF_2 in poly(vinylidene fluoride) (PVDF) in the presence of $scCO_2$. The Sanchez-Locombe equation of state predicts that the partition coefficient of VF_2 between PVDF and CO_2 phases is less than 0.5 at 75 °C above 15 MPa [37]. Considering this factor and the low volume fraction of the polymer phase, the polymerization in the polymer phase can be negligible.

2.1.7 Precipitation Polymerization of Acrylic Acid

Precipitation polymerization of acrylic acid usually is used to make high molecular weight polymers which find use in applications such as flocculents and thickeners [38-41]. Reichert and coworkers [42, 43] studied the precipitation polymerization of acrylic acid in toluene initiated by 2,2'-azobis(2,4-dimethyl valeronitrile) using an isothermal reaction calorimeter. In their study, autoaccelerated polymerizations were observed. The rate of polymerization showed a rapid acceleration to a maximum at a monomer conversion between 30% and 40%. Then the rate steadily decreased. Reichert and coworkers proposed a kinetic model that predicted the time evolution of the rate of polymerization well [43]. The model assumed: (1) Chain initiation occurred in the continuous phase; (2) Chain propagation and termination took place in the disperse phase; and (3) The monomer concentration in the continuous phase was equal to that in the disperse phase.

2.2 Precipitation Polymerization of Acrylic Acid in Supercritical Carbon Dioxide

2.2.1 Polymerization Processes

Acrylic acid is soluble in $scCO_2$ (Figure 2-1) [44], while PAA is insoluble [45]. Therefore, the polymerization of acrylic acid in $scCO_2$ conforms to precipitation polymerization. This process was first reported in a French patent in 1968 [46]. In this patent, the precipitation polymerization of several vinyl compounds, such as acrylic acid, styrene and vinyl chloride, in liquid and supercritical CO_2, was demonstrated. However, under the conditions set forth in this patent, only small hard PAA chunks could be obtained [47]. In 1986, the synthesis of water-soluble powdery PAA in $scCO_2$ was described in a Canadian patent application [48]. In 1987, the precipitation cross-linking polymerization of acrylic acid in $scCO_2$ was discussed in a U.S. Patent [49]. In this patent, water-soluble cross-linked PAA useful as thickening agents was synthesized. A similar study was also presented in a European Patent in 1988 [47]. More recently, DeSimone and coworkers [50] studied acrylic acid polymerization in $scCO_2$, and used ethyl mercaptan as a chain transfer agent to control the polymer molecular weight. Finally, Xu and coworkers [51, 52] explored the effect of cosolvents on the polymerization of acrylic acid in $scCO_2$.

Although most of the previous works were carried out in batch reactors, continuous polymerization processes were also reported. For example, Sertage and coworkers described the use of a continuous tubular reactor [48], and Roberts and coworkers [53] reported the use of a continuous stirred tank reactor for the synthesis of PAA in $scCO_2$. However, these studied were so preliminary that only very limited results are available.

In a typical batch polymerization experiment [50], deoxygenated acrylic acid is charged into a high-pressure reactor with magnetic agitation. If a cross-linker (e.g. allyl

pentaerythritol ether [47]) or a chain transfer agent (e.g. ethyl mercaptan [50]) is used, they are added along with acrylic acid. The reactor is then sealed and enough liquid CO_2 is added to form a homogeneous solution occupying approximately half of the reactor volume. The temperature is gradually increased to the desired value. Initiator is then blown into the reactor by high-pressure CO_2. More CO_2 is added into the reactor to achieve the desired pressure. The onset of polymerization can be observed after a short induction period, as the reaction mixture turns cloudy. Within minutes white solid particles appear in the reactor. The reaction time, depending on the reaction conditions, such as temperature and initiator species, can be quite short, say 0.5 hour, or very long, say more than 10 hours [47]. At the end of reaction, the CO_2 employed is easily removed from the resultant polymer by venting. The product of reaction is isolated as a dry, free-flowing powder. Usually, a monomer conversion above 90% can be achieved.

The pressure increases with monomer conversion in batch precipitation polymerization of acrylic acid in $scCO_2$ [54]. In fact, pressure change is common for polymerizations in $scCO_2$ [55-57]. It is caused by the non-ideal behavior of the monomer/CO_2 mixtures. Depending on the monomer, the pressure can increase or decrease [54, 56].

In the study of DeSimone and coworkers [50], the product polymer was large aggregates of primary particles smaller than 100nm in size. Xu and coworkers [51] also made polymer of similar morphology. In addition, they found the size of the primary particles could be varied by use of cosolvents in polymerization, such as ethanol and acetic acid.

2.2.2 Effects of Polymerization Variables

Inhibitors. Oxygen is a powerful inhibitor for the polymerization of acrylic acid. A small amount of oxygen (1-20 ppm) in CO_2 is useful to inhibit polymerization while the reactor is charged with carbon dioxide and brought to the desired pressure and temperature. With a small amount of oxygen, a short induction time is observed until the oxygen is consumed, whereupon polymerization begins. More oxygen causes excessively long induction periods [47].

The commercial monomer grade acrylic acid contains about 200 ppm 4-methoxyphenol (MEHQ), which is an inhibitor for free radical polymerization. Acrylic acid is usually used without removing MEHQ, but the effect of MEHQ on precipitation polymerization of acrylic acid in $scCO_2$ has not been reported.

Initiator. A lot of initiators, including peroxide initiators, azo initiators and redox initiators, have been used [46-54, 58]. Although in theory any free-radical initiator having sufficient solubility in $scCO_2$ is usable, the particular initiator employed depends upon the desired molecular weight and the temperature of polymerization [59].

For a typical free radical polymerization, the kinetic chain length is inversely dependent on the initiator concentration. Therefore, any attempt to increase the polymerization rate by increasing the initiator concentration comes at the expense of producing smaller polymer molecules. Hu et al. [54] investigated the effect of initiator concentration on molecular weight in precipitation polymerization of acrylic acid in $scCO_2$. Not surprisingly, the product molecular weight decreased as the initiator concentration increased.

Monomer. The work by Xu and coworkers showed that the polymer molecular weight and the polymer particle size increased with monomer concentration. They also found that the glass transition temperature of polymer increased with the polymer molecular weight [51].

Chain Transfer Agent. DeSimone and coworkers [50] performed a series of reactions in the presence of various amounts of chain transfer agent, ethyl mercaptan. Effective molecular weight control was achieved. The molecular weight of the product polymer decreased from 153 kg/mol to 2.9 kg/mol when the concentration of ethyl mercaptan increased from 0.0012 mol/l to 0.169 mol/l.

Cross-Linking. When a cross-linker is used, the properties of the product are critically dependent upon the ratio of acrylic acid to the cross-linker. If too little cross-linker is used, the polymer is insufficiently cross-linked for many uses. If too much cross-linker is used, the resultant polymer is over-cross-linked and cannot be used. The optimum ratio for a given set of conditions must be found by trial and error [47, 49]. The properties of the cross-linked polymer could be improved by utilizing semi-batch charging of cross-linker [47].

Reaction Pressure. DeSimone and coworkers [50] studied the batch precipitation polymerization of acrylic acid in $scCO_2$ at pressures ranging from 125 bar to 345 bar using AIBN as the free radical initiator. Analyses of products from reactions carried out at four different pressures indicated that there was no discernible pressure effect on product molecular weight, polydispersity index, particle size, or morphology within this pressure range. Xu and coworkers [51] investigated the effect of pressure on product molecular weight in the pressure range of 11.5 to 17 MPa, and found no obvious effect of pressure on molecular weight either.

While DeSimone and coworkers and Xu et al. carried out their experiments with monomer concentration of 10v%v, Hu and coworkers [54] used higher concentrations, from 10 to 30v%v. They found product molecular weight decreased slightly as pressure increased.

Herbert and Huvard reported the only study of the effect of pressure on the rate of polymerization. Their work showed that lower reaction pressure led to higher reaction yield in a fixed period of time [47].

Cosolvents. Adding cosolvents to the system can alter the solubilities of monomers in $scCO_2$, adjust the equilibrium constants of different reactions, improve the selectivity of reaction and increase the rate of reaction. Xu and coworkers [51] studied the effects of a few cosolvents on the precipitation polymerization of acrylic acid in $scCO_2$ at 335 K in the pressure range of 12-17 MPa. AIBN was used as the initiator. When acetic acid was used as the cosolvent, the AIBN decomposition rate increased with the acetic acid concentration. Therefore, the polymer molecular weight and glass transition temperature decreased with increasing cosolvent concentration. When ethanol was used as the cosolvent, the AIBN decomposition rate decreased as the ethanol concentration increased. Accordingly, the polymer molecular weight and glass transition temperature increased with cosolvent concentration [51].

Comparison of $ScCO_2$ with Conventional Solvents. Utilizing AIBN as a free radical initiator, DeSimone and coworkers [50] compared the PAA prepared in $scCO_2$ to those made in conventional solvents. Polymerization in conventional solvents produced lower molecular weights and smaller polydispersities because of chain transfer to solvents. The scanning electron micrographs of polymer prepared in dense CO_2 (345 bar) were quite

similar to those prepared in benzene, indicating that PAA prepared in $scCO_2$ compared favorably to those prepared in conventional solvents.

2.3 References

1. Soh, S.K.; Sundberg, D.C. Journal of Polymer Science: Polymer Chemistry Edition 1982, 20, 1299-1313.
2. Soh, S.K.; Sundberg, D.C. Journal of Polymer Science: Polymer Chemistry Edition 1982, 20, 1315-1329.
3. Soh, S.K.; Sundberg, D.C. Journal of Polymer Science: Polymer Chemistry Edition 1982, 20, 1331-1344.
4. Soh S.K.; Sundberg D.C. Journal of Polymer Science: Polymer Chemistry Edition 1982, 20, 1345-1371.
5. Stickler, M.; Panke, D. C. Journal of Polymer Science: Polymer Chemistry Edition 1984, 22, 2243-2253.
6. Vivaldo-Lima, E.; Hamielec, A. E.; Wood, P. E. Polymer Reaction Engineering 1994, 2, 17-85.
7. Bogunjoko, J.S.T.; Brooks, B.W. Die Makromol. Chem. 1983, 184, 1623-1643.
8. Bogunjoko, J.S.T.; Brooks, B.W. Die Makromol. Chem. 1983, 184, 1603-1621.
9. Brooks, B.W. Industrial & Engineering Chemistry Research 1997, 36, 1158-1162.
10. Elbewele, R.O. Polymer Science and Technology. CRC Press: Boca Raton, 2000, Chapter 10, p.249.
11. Dotson, N.A.; Galvan, R.; Laurence, R.L.; Tirrell, M. Polymerization Process Modeling, VCH Publishers, Inc.: New York, 1996; Chapter 3, p.105.

12. Elbing, L.E.; McCarthy, S.J.; Snowdon, S.; Coller, B.A.W.; Wilson, I.R. Journal of the Chemical Society: Faraday Transactions I 1986, 82, 943-952.
13. Berrett, K.E.J.; Thomas, H.R. in Dispersion Polymerization in Organic Media; Barrett, K. E. J., Ed.; Wiley-Interscience: New York, 1974; Chapter 4, 116-118.
14. Bamford, C.H.; Jenkins, A.D. Proceedings of the Royal Society of London, Series A, Methematical and Physical Science 1953, 216, 515-539.
15. Bengough W.I. Proceedings of the Royal Society of London, Series A, Methematical and Physical Science 1961, 260, 205-217.
16. Lewis, O.G.; King, R.M.J. in Addition and Condensation Polymerization Processes. 1969, American Chemical Society: Washington D. C. p. 25-45.
17. Garcia-Rubio, L.H.; Hamielec, A.E. Journal of Applied Polymer Science 1979, 23, 1397-1411.
18. Garcia-Rubio, L.H.; Hamielec, A.E.; Macgregor, J.F. Journal of Applied Polymer Science 1979, 23, 1413-1429.
19. Bamford, C.H.; Jenkins, A.D.; Ingram, D.J.E.; Symons, M.C.R. Nature 1955, 175, 894-895.
20. Guha, S.; Rao, T.R.G.; Mandrand, B. Journal of Applied Polymer Science Part B: Polymer Physics 2003, 41, 1192-1197.
21. Peebles, L.H. in Copolymerization, Ham, G.E., Ed., Interscience Publishers: New York, 1964; Chapter 9, 525-586.
22. Chio, K.Y. in Handbook of Radical Vinyl Polymerization, Mishra, M.K.; Yagci, Y. Ed.; Marcel Dekker, Inc.: New York, 1998; 299-365.
23. Moore, D.E.; Parts, A.G. Die Makromolekulare Chemie 1960, 37, 108-118.

24. McCarthy, S.J.; Elbing, E.E.; Wilson, I.R.; Gilbert, R.G.; Napper, D.H.; Sangster, D.F. Macromolecules 1986, 19, 2440-2448.
25. Nishida, R.; Poehlein, G.W.; Schork, F.J. Polymer Reaction Engineering 1995, 3, 397-420.
26. Tavan, M.; Palma, G.; Carenza, M.; Brugnaro, S. Journal of Polymer Science: Polymer Chemistry Edition 1974, 12, 411-432.
27. Xie, T.Y.; Hamielec, A.E.; Wood, P.E.; Woods, D.R. Polymer 1991, 32, 537-557.
28. Talamini, G.; Visentini, A.; Kerr, J. Polymer 1998, 39, 1879-1891.
29. Endo, K. Progress in Polymer Science 2002, 27, 2021-2054.
30. Abdel-Alim, A.; Hamielec, A.E. Journal of Applied Polymer Science 1972, 16, 783-799.
31. Mickley, H.S.; Journal of Polymer Science 1962, 60, 121-140.
32. Raucher, D.; Levy, M. Journal of Polymer Science: Polymer Chemistry Edition 1975, 13, 1339-1346.
33. Raucher, D.; Levy, M. Journal of Polymer Science: Polymer Chemistry Edition 1979, 17, 2663-2673.
34. Charpentier, P.A.; DeSimone, J.M.; Roberts, G.W. Industrial & Engineering Chemistry Research 2000, 39, 4588-4596.
35. Saraf, M.K.; Gerard, S.; Wojcinski, L.M.; Charpentier, P.A.; DeSimone, J.M.; Roberts G.W. Macromolecules 2002, 35, 7976-7985.
36. Ahmed, T.S.; DeSimone, J.M.; Roberts, G.W. Chemical Engineering Science 2004, 59, 5139-5144.

37. Kennedy, K.A. Ph.D. thesis, chemical engineering, North Carolina State University: Raleigh, 2003.
38. Brown, H.P. (B. F. Goodrich Company). U.S. Patent 2,798,053, July 2, 1957.
39. Huang, C.; Schlatzer, R.K. (B.F. Goodrich). U.S. Patent 4,509,949, April 9, 1985.
40. Schlatzer, R.K.J. (B. F. Goodrich). U.S. Patent 3,915,921, October 28, 1975.
41. Swift, G. in Encyclopedia of Polymer Science and Technology, Kroschwitz, J.I., Ed. Wiley-Interscience: New York, 2003. p. 79.
42. Avela A.; Poersch, H.; Reichert, K. Die Angewandte Makromolekulare Chemie 1990, 175, 107-116.
43. Poersch-Panke, H.; Avela, A.; Reichert, K. Die Angewandte Makromolekulare Chemie 1993, 206, 157-169.
44. Byun, H.S.; Hasch, B.M.; Mchugh, M.A. Fluid Phase Equilibria 1996, 115, 179-192.
45. Rindfleisch, F.; DiNoia, T. P.; McHugh, M.A. J. Phys. Chem. 1996, 100, 15581-15587.
46. Fukui, K.; Kagiya, T.; Yokota, H.; Toriuchi, Y.; Fujii, K. (Sumitomo Chemical Company, Ltd.). Japanese Patent 45-25305. August 21, 1970.
47. Herbert, M.W.; Huvard, G.S. (B. F. Goodrich Company). European Patent 0301532A2. Februry 1, 1989.
48. Sertage, W.G.J.; Davis, P.; Schenck, H.U.; Denzinger, W.; Heinrich, H. (BASF Corporation U.S.A.). Canada Patent 1 274 942, 1,274,942, October 2, 1990.
49. Hartmann, H.; Denzinger, W. (BASF Aktiengesellsschaft, Ludwigshafen, Fed. Rep. of Germany). United States Patent 4,748,220, May 31, 1988.
50. Romack, T.J.; Maury, E.E.; Desimone, J. M. Macromolecules 1995, 28, 912-915.

51. Xu, Q.; Han, B.; Yan, H. Polymer 2001, 42, 1369-1373.

52. Xu, Q.; Han, B.; Yan, H. Journal of Applied Polymer Science 2003, 88, 1876-1880.

53. Charpentier, P.A.; Kennedy, K.A.; DeSimone, J.M.; Roberts, G.W. Macromolecules 1999, 32, 5973-5975.

54. Hu, H.; Chen, M.; Li, J.; Cong, G. Acta Polymerica Sinica 1998, 6, 740-743.

55. DeSimone, J.M.; Maury, E.E.; Mehceloglu, Y.Z.; McClain, J.B.; Romack, T.J.; Combes, J. R. Science 1994, 265, 356-359.

56. Lepilleur, C.; Beckman, E. Macromolecules 1997, 30, 745-756.

57. Canelas, D.A.; DeSimone, J.M. Macromolecules 1997, 30, 5673-5682.

58. Dada, E.; Lau, W.; Merritt, R.F.; Paik, Y.H.; Swift, G. Synthesis of Poly(acrylic acid)s in Supercritical Carbon Dioxide. in Abstracts of Papers of the American Chemical Society, PMSE Part 2, March 24, 1996.

59. Division, L.; Corporation, P. Polymer Engineering and Science 1979, 19, 597-606.

Nomenclature

f	initiator efficiency
k_d	rate constant for initiator decomposition (s^{-1})
k_i	rate constant for chain initiation (s^{-1})
k_p	rate constant for chain propagation (L/mol-s)
k_t	rate constant for chain termination (L/mol-s)
I	free radical initiator
[I]	instantaneous initiator concentration (mol/L)
M	monomer
[M]	instantaneous monomer concentration (mol/L)
$[P^\bullet]$	instantaneous polymer radical concentration (mol/L)
$P_n^\bullet$	polymer radical with n monomer units
$R^\bullet$	free radical generated by initiator decomposition
R_i	rate of initiation (mol/L-s)
R_p	rate of propagation (mol/L-s)
R_t	rate of termination (mol/L-s)
ν	kinetic chain length

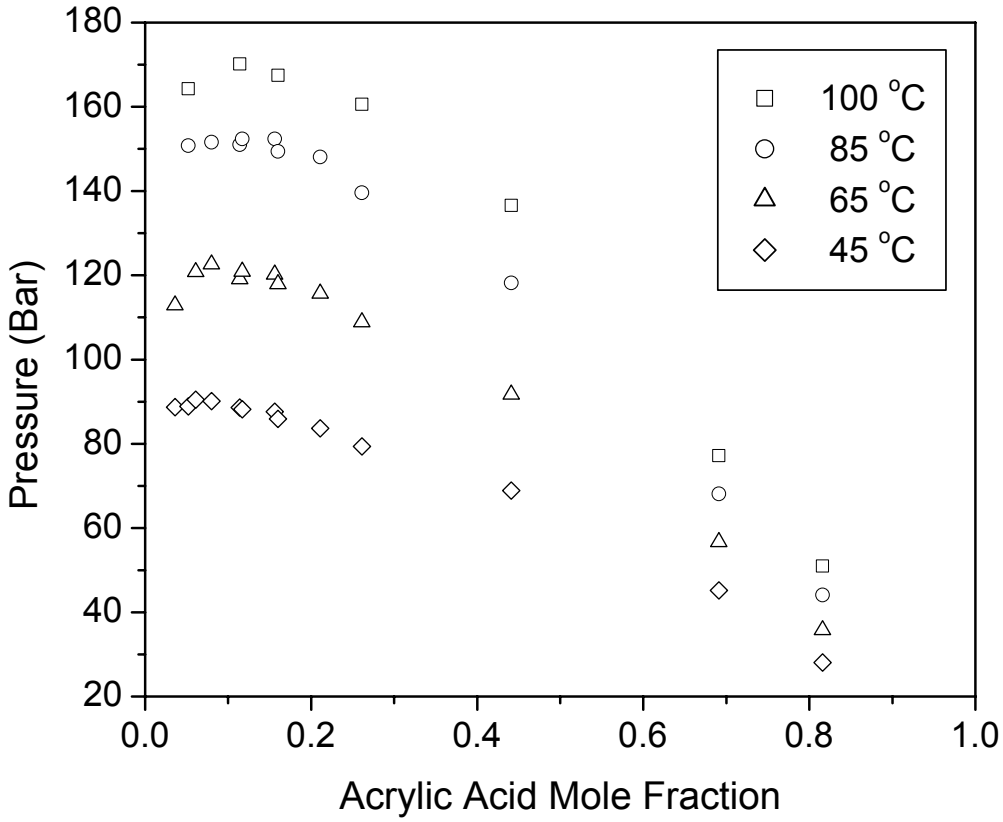

Figure 2-1. Pressure-composition isotherms for CO_2-acrylic acid system

CHAPTER 3

CONTINUOUS PRECIPITATION POLYMERIZATION OF ACRYLIC ACID IN SUPERCRITICAL CARBON DIOXIDE: POLYMERIZATION RATE AND POLYMER MOLECULAR WEIGHT

Tao Liu[1], Joseph M. DeSimone[1, 2], and George W. Roberts[1]

[1]Department of Chemical Engineering, Campus Box 7905, North Carolina State University, Raleigh, North Carolina 27695-7905

[2]Department of Chemistry, CB 3290, Venable and Kenan Laboratories, University of North Carolina at Chapel Hill, North Carolina 27599-3290

This is a manuscript submitted for publication in

Journal of Polymer Science Part A: Polymer Chemistry

November 2004

Abstract

The precipitation polymerization of acrylic acid in supercritical carbon dioxide was studied in a continuous stirred tank reactor using 2, 2'-azobis (2, 4-dimethyl-valeronitrile) as the free-radical initiator. The reactor temperature was between 50 and 90 °C, the pressure was 207 bar, and the average residence time was between 12 and 40 minutes. The product polymer was a white, dry, fine powder that dissolved in water. A wide range of polymer molecular weights (5 to 200 kg/mol) could be obtained. The effect of the operating variables on the polymerization rate and on the polymer molecular weight was evaluated. The observed kinetics suggests that polymerization took place in both the supercritical fluid and the precipitated polymer particles.

Keywords

acrylic acid, radical polymerization, kinetics, continuous polymerization, supercritical CO_2, water-soluble polymers

3.1 Introduction

Unsaturated monomers usually are polymerized in aqueous or organic media. However, increasing concern about the negative environmental impact of volatile organic compounds and organic-containing aqueous waste has prompted a search for environmentally-benign polymerization media. The use of supercritical carbon dioxide ($scCO_2$) for this purpose has received considerable attention during the last decade [e.g., 1,2]. In fact, DuPont recently introduced the first commercial fluoropolymers manufactured in $scCO_2$ [3].

Carbon dioxide (CO_2) has an easily accessible critical point (T_c = 31.1 °C, P_c = 73.8 bar). It is readily available, inexpensive, nontoxic, nonflammable, chemically inert under most conditions, and environmentally benign. When $scCO_2$ is used as the polymerization medium, there is no chain transfer to solvent. Moreover, CO_2 can eliminate the need for costly polymer drying processes. The products from a polymerization conducted in CO_2 are completely dry after depressurizing to remove the CO_2 [2].

Many monomers and organic initiators are soluble in $scCO_2$. However, only amorphous fluoropolymers and silicones are soluble enough to permit solution polymerization in $scCO_2$ [1]. For other systems, a heterogeneous polymerization technique must be used. There are four basic heterogeneous polymerization processes: suspension polymerization, emulsion polymerization, dispersion polymerization, and precipitation polymerization. The first three require CO_2-philic surfactants. Some approaches to the design and synthesis of such surfactants are described in three recent publications [4-6]. Effective CO_2-philic surfactants are expensive, and are difficult and costly to remove from the product polymer. Therefore, precipitation polymerization in $scCO_2$ has an inherent raw-material cost

advantage over the other heterogeneous polymerization processes, and is most suitable for applications where pure polymers are required.

Solid polymer particles precipitate from the continuous phase during any precipitation polymerization. Radicals can be trapped in the polymer particles when they precipitate, or can be formed in the particles as a result of partitioning of a free-radical initiator between the two phases. Monomer then can diffuse into the polymer particles, allowing chain propagation to continue. The radical ends in the polymer phase are less accessible to each other, so that the rate of termination in the particles is greatly decreased. The result is an increase in the overall rate of polymerization and a corresponding increase in the polymer molecular weight. Thus, precipitation polymerization can allow both high polymerization rates and high molecular weights, even with a relatively unreactive monomer [7].

There is some controversy concerning the importance of propagation in the polymer particles during precipitation polymerizations in $scCO_2$. In their studies of the continuous precipitation polymerization of vinylidene fluoride in $scCO_2$, DeSimone, Roberts and coworkers [8-10] developed a model based on the assumption that initiation, propagation, and termination all took place homogeneously in the supercritical fluid, and that no reaction took place in the polymer particles. This model was able to describe all of the important features of the polymerization including the kinetics and the existence of a bimodal molecular weight distribution at some experimental conditions. Ahmed et al. [10] speculated that the lifetime of a radical in the supercritical fluid might be much smaller than the time scale for polymer precipitation. If so, the concentration of radicals trapped in polymer particles when they precipitated would be small, and their impact on polymerization rate and polymer properties might not be significant. It also is possible that the polymerization rate in

the polymer particles is low because of the low solubility of vinylidene fluoride in poly(vinylidene fluoride) (PVDF) in the presence of $scCO_2$ [11].

Nevertheless, a homogeneous solution polymerization model probably cannot describe the behavior of most precipitation polymerization systems, because the precipitated polymer frequently is an important locus of polymerization. For example, in the polymerization of acrylonitrile in water, Moore and Parts found that the rate of polymerization and polymer molecular weight were reduced if the polymer particles were continuously eliminated from the reaction by centrifuging [12]. The rate of a precipitation polymerization usually depends on the monomer concentration to a power higher than 1, whereas a classical solution polymerization is first-order in monomer. The dependence of the rate of a precipitation polymerization on the initiator concentration also can be different from that of a classical solution polymerization, where the order with respect to initiator is 0.5. For example, the precipitation polymerization of acrylonitrile in benzene at 50 °C, initiated by 2, 2'–azobis(isobutyronitrile) (AIBN), had an order with respect to monomer of about 1.7. The order with respect to initiator varied from 0.89 when the initiator concentration was 10^{-4} mol/L to 0.33 when the initiator concentration was 10^{-2} mol/L [13].

Acrylic acid polymers and copolymers are widely used as dispersants, thickeners, flocculants, and superabsorbent polymers (SAP). Poly(acrylic acid) (PAA) commonly is prepared by solution polymerization, although suspension polymerization, inverse emulsion polymerization, and precipitation polymerization in organic media also are used [14]. In solution polymerization, water usually is the solvent and drying is necessary. The other three processes are carried out in organic media. The use of surfactants and/or organic solvents inevitably leads to chemical contamination of the polymer. For applications where extremely

clean PAA or PAA derivatives are desired (e.g. thickeners in toothpaste and cosmetics), costly purification and drying processes often are necessary.

Acrylic acid is moderately soluble in $scCO_2$, while PAA is insoluble. Precipitation polymerization in $scCO_2$ may offer an attractive alternative to conventional processes for PAA, in that the final polymer is virtually free of contamination. Unreacted monomer and initiator are easily removed from the polymer by extraction with $scCO_2$.

Precipitation polymerization of acrylic acid in CO_2 was first reported in a French patent [15] in 1968. The U. S. version of this patent [16] appeared in 1970. The precipitation polymerization of several vinyl compounds, including acrylic acid, in liquid and supercritical CO_2, was demonstrated in these patents. In 1986, a Canadian patent [17] described the synthesis of water-soluble PAA in $scCO_2$. The synthesis in $scCO_2$ of thickeners based on cross-linked, water-soluble PAA was reported in 1987 [18]. In 1988, the synthesis of acrylic-acid-type thickeners in $scCO_2$ was discussed in a European patent application [19]. More recently, DeSimone and coworkers [20] studied acrylic acid polymerization in $scCO_2$, and used ethyl mercaptan as a chain transfer agent to control the polymer molecular weight. Finally, Xu et al. [21] explored the effect of cosolvents on the polymerization of acrylic acid in $scCO_2$.

A continuous process has been reported for chain-growth precipitation polymerization of vinylidene fluoride in $scCO_2$, using a continuous stirred tank reactor (CSTR) [8-10]. This process also has been applied to the synthesis of PAA [22]. While batch reactors are useful for the production of small-to-intermediate volume polymers, continuous reactors are more suitable for the production of high-volume, commodity polymers. Compared to batch processes, continuous processes have many advantages, including: (1)

smaller and cheaper reactors; (2) easier recycle of CO_2 and unreacted monomer, and; (3) time-invariant reaction conditions, and hence more uniform polymer properties. In addition, the polymer produced in $scCO_2$ with a CSTR may have properties that are different and advantageous relative to polymer produced in conventional processes [8,9].

The present paper describes detailed studies of the continuous precipitation polymerization of acrylic acid in $scCO_2$ in a CSTR. The reactor temperature was between 50 and 90 °C, the pressure was 207 bar, and the average residence time in the reactor was between 12 and 40 minutes. The product polymer was a white, dry, and fine powder that dissolved in water. A wide range of polymer molecular weights (5 to 200 kg/mol) could be obtained. The effect of the operating variables on polymerization behavior and polymer properties was evaluated. Finally, the measured polymerization kinetics was compared to those for a homogeneous solution polymerization to help in understanding the nature of polymerization processes in $scCO_2$.

3.2 Experimental

Materials. Carbon dioxide (SFC grade, 99.998%) was purchased from National Specialty Gases. The initiator, 2,2'–azobis(2,4-dimethyl-valeronitrile) (V-65B) (high purity), was donated by Wako Chemicals USA. Acrylic acid (99.5%), Toluene (HPLC grade, 99.5%), 1,1,2-trichloro-1,2,2-trifluoroethane (Freon 113) (HPLC grade, 99.8%), and 4-methoxyphenol (MEHQ) (99%) were purchased from the Fisher Scientific. All chemicals were used as received.

Apparatus. Figure 3-1 is a schematic of the polymerization system, which has been described in detail elsewhere [9]. The reactor (G) is an 800 ml, high-pressure autoclave with

a magnetically driven agitator (E). A jacket through which a heating/cooling fluid is circulated is used to control the reaction temperature (H). A previous investigation showed that this reactor behaves as an ideal CSTR [23]. For a typical polymerization experiment, steady state is reached about five average residence times after the startup. Three high-pressure filters (F1, F2, and F3) are used to collect polymer particles. A heated control valve (K) functions as a backpressure regulator to keep the system pressure at the set point.

Polymerization. In a typical experiment, three streams: CO_2, acrylic acid, and V-65B/Freon 113 solution, were fed continuously into the reactor from individual syringe pumps. The concentration of V-65B in Freon 113 varied from 0.08 moles/L to 0.32 moles/L, depending on the inlet initiator concentration. Polymerization took place continuously. Because PAA is not soluble in $scCO_2$, the polymer precipitated and formed particles in the reactor. The product stream, which consisted of a continuous, CO_2-rich phase and a dispersed, polymer-rich phase, was withdrawn from the bottom of the reactor. This stream passed through a heat exchanger to cool it to approximately room temperature. Inhibitor solution, 5wt% MEHQ in toluene, then was introduced into the stream with the inhibitor pump to stop polymerization. Since the presence of oxygen can dramatically increase the inhibition effect of MEHQ [24], the MEHQ solution was kept exposed to air. The product stream then went into a filter where the polymer particles were collected. The CO_2-rich phase passed through the filter and was released through the pressure control valve into a fume hood. During the period that the reactor was not at steady-state, the product stream was passed into one of two "unsteady-state" filters (F1 or F2). Both unsteady-state filters were connected to an atmospheric bag filter. After one unsteady-state filter was full, the stream leaving the reactor was switched to the other, and the first filter was cleaned and refilled with

high-pressure CO_2. In this way, the system ran continuously. After the reactor had reached steady state, the "steady state" filter (F3) was used to collect polymer for evaluation. Once the steady-state filter was full, the product stream was switched back to one of the unsteady-state filters.

In order to remove unreacted monomer, initiator, Freon 113, toluene, and MEHQ from the polymer in the steady-state filter, the filter was filled with liquid CO_2 and then the CO_2 was slowly released from the bottom of the filter. This process was repeated four times. The product polymer was a white, dry, fine powder that dissolved easily in water.

Measurements. The monomer conversion was measured using a gravimetric method, i.e., by weighing the amount of polymer collected during a measured time period. The fractional conversion of monomer (x) was calculated from:

$$x = \frac{\text{mass of polymer collected (g)}}{\text{inlet flowrate of monomer (L/s)} \times \text{momomer density (g/L)} \times \text{collection time (s)}}$$

The monomer concentration in the feed to the reactor was calculated from:

$$[M]_{in} = \frac{\text{inlet flowrate of monomer (L/s)} \times \text{monomer density (g/L)}}{\text{monomer molecular weight (g/mol)} \times \text{total inlet volumetric flowrate (L/s)}}$$

In this equation, the total inlet flowrate is the sum of the flowrates of the monomer, CO_2, and initiator solution. The outlet monomer concentration is given by:

$$[M]_{out} = [M]_{in}(1-x)$$

Finally, the rate of polymerization (R_p) is given by:

$$R_p = [M]_{in}x/\tau$$

The viscosity average molecular weight of polymer was measured by a Rheotek™ TCB-7 automatic viscometer using water containing 0.2 mol/L HCl at 14 °C. The Mark-

Houwink-Sakurada relationship was used to determine the viscosity average molecular weight from the measured intrinsic viscosity [25]:

$$[\eta] = 0.1062\overline{M}_v^{0.5} ml/g$$

Calculation of Outlet Initiator Concentration. The initiator concentration in the stream leaving the reactor was calculated from the equation for the first-order decomposition of a reactant in a CSTR:

$$[I]_{out} = [I]_{in}/(1 + k_d\tau)$$

The value of k_d for V-65B was assumed to be the same in the acrylic acid-CO_2 mixture as in toluene, and was obtained from information provided by the supplier [26].

3.3 Results and Discussion

Inhibitors. Oxygen is a very strong inhibitor for the polymerization of acrylic acid [27]. To remove O_2, the acrylic acid and the V-65B/Freon solution were deoxygenated with high-purity Ar for 60 and 15 minutes, respectively, before they were charged into their respective pumps. The reactor was purged by SFC grade CO_2 before use. The SFC grade CO_2 contained less than 1 ppm O_2. To completely remove O_2 from the CO_2, traps (Alltech High Pressure Oxy-Trap^{TM}) were installed between the CO_2 tanks and CO_2 pumps. Table 3-1 shows the influence of the oxygen traps on acrylic acid polymerization at 50 °C and 207 bar. The rate of polymerization with one O_2 trap was about 13% lower than the rate with three traps in series. Additional traps had no detectable effect on the rate of polymerization. The difference between the molecular weights in Table 3-1 is within the error range of measurement. These observations show that the effect of O_2 on polymerization was reduced to a negligible level by employing three O_2 traps in series.

Commercial monomer-grade acrylic acid typically contains about 200 ppm MEHQ, and storage under an air atmosphere is recommended. It has been found that MEHQ has no detectable effect on the polymerization of acrylic acid in the absence of oxygen [28]. However, MEHQ serves to reduce the rate of oxygen consumption [24]. The acrylic acid used in the first experiment in Table 3-2 contained 210 ppm MEHQ. In the second experiment, the MEHQ concentration was increased to 993 ppm while the other experimental variables were kept unchanged. The rate of polymerization and polymer molecular weight in the two experiments were almost the same. This showed that the effect of MEHQ on polymerization was negligible, and confirmed that the removal of O_2 was complete.

Residence Time: The average residence time (τ) in a CSTR is the volume of the reactor divided by the volumetric flow rate into the reactor. Table 3-3 shows the effect of average residence time on polymerization behavior. As the residence time increased, the monomer conversion increased and the rate of polymerization decreased. The polymer molecular weight was essentially constant over a range of average residence times from 12 to 40 minutes.

The experiments in Table 3-3 were run with the same inlet monomer and initiator concentrations. Therefore, the monomer and initiator concentrations in the reactor at steady-state both decreased as the residence time increased. The polymer concentration (mass/volume) in the reactor effluent ($[P]_{out}$) increased by about a factor of 3 as τ increased from 12 to 40 min. The volume fraction of polymer (ϕ) in the reactor was calculated using a density of 1386 g/L [29]. The results are shown in the last column of Table 3-3. Although this volume fraction is small, it increases by about a factor of 3 as the average residence time increases from 12 to 40 min.

The data in Table 3-3 are tested against the predictions of the classical model for homogeneous solution polymerization in Figures 3-2a and 3-2b. For a solution polymerization of a chain-growth monomer, M, initiated by decomposition of a free-radical initiator, I:

$$R_P = k_p (fk_d / k_t)^{1/2} [M][I]^{1/2} \qquad (3\text{-}1)$$

For a CSTR, the concentration in the reactor is the same as the concentration in the outlet stream, so that:

$$R_p / \left\{ [M]_{out} [I]_{out}^{1/2} \right\} = k_p (fk_d / k_t)^{1/2} \qquad (3\text{-}2)$$

If the polymerization followed this classical model, the value of $R_p / \left\{ [M]_{out} [I]_{out}^{1/2} \right\}$ should be the same for all of the experiments in Table 3-3, since the temperature was the same for all experiments. Figure 3-2a shows that Equation 3-2 does not describe the data in Table 3-3. The value of $R_p / \left\{ [M]_{out} [I]_{out}^{1/2} \right\}$ increases by about 20% as the average residence time increases from 12 to 40 min. This increase coincides with the increase in ϕ shown in Table 3-3, and suggests that the increase in $R_p / \left\{ [M]_{out} [I]_{out}^{1/2} \right\}$ with increasing τ may be the result of polymerization in the polymer particles.

The classical solution polymerization model also predicts the kinetic chain length, ν. For a CSTR,

$$\nu \propto (k_p^2 / fk_d k_t)^{1/2} [M]_{out} / [I]_{out}^{1/2} \qquad (3\text{-}3)$$

If the viscosity-average molecular weight, $\overline{M}_v$ is proportional to ν, then the parameter $\overline{M}_v / \{ [M]_{out} / [I]_{out}^{1/2} \}$ should be the same for all polymerizations at a fixed temperature.

Figure 3-2b shows that this parameter increases by about 40% over the range of residence times in Table 3-3. This behavior again is consistent with the increasing volume

fraction of polymer in the reactor, and with the hypothesis that some polymerization takes place in the polymer particles. As discussed earlier, the molecular weight of polymer formed in the particles should be higher than that formed in the fluid phase.

Initiator Concentration: Table 3-4 shows the effect of inlet initiator concentration at 70 °C and 207 bar, for a constant inlet monomer concentration of 0.5 mol/L and an average residence time of 25 min. The monomer conversion, the rate of polymerization, and the volume fraction of polymer increased as the inlet initiator concentration increased. However, the polymer molecular weight decreased.

Figure 3-3a, a plot of $R_p / \{[M]_{out}[I]_{out}^{1/2}\}$ versus the outlet initiator concentration, shows again that the behavior of this polymerization deviates significantly from that of an ideal, free-radical, solution polymerization. Once again, the increase of $R_p / \{[M]_{out}[I]_{out}^{1/2}\}$ coincides with the increasing volume fraction of polymer in the reactor.

Figure 3-3b shows that $\overline{M}_v / \{[M]_{out} / [I]_{out}^{1/2}\}$ is not constant for the data in Table 3-4. As with Figure 3-2b, this parameter increases with the polymer volume fraction in the reactor.

Monomer Concentration: Table 3-5 shows the effect of monomer concentration on polymerization at 70 °C and 207 bar, with a constant inlet initiator concentration of 0.004 mol/L and a constant residence time of 25 min. The monomer conversion, the rate of polymerization, and the polymer molecular weight all increased with increasing inlet monomer concentration. Figure 3-4a shows $R_p / \{[M]_{out}[I]_{out}^{1/2}\}$ versus the outlet monomer concentration. As the outlet monomer concentration increases, both $R_p / \{[M]_{out}[I]_{out}^{1/2}\}$ and the polymer volume fraction increase. Figure 3-4a and the data in Table 3-5 show that the

effective order of the polymerization with respect to the concentration of acrylic acid monomer is significantly greater than 1.

Figure 3-4b shows $\overline{M}_v / \{[M]_{out} / [I]_{out}^{1/2}\}$ for the data in Table 3-5. Once again, this parameter increases with polymer volume fraction.

Molecular Weight: The molecular weight of PAA defines its end-use applications. For example, PAAs having molecular weights of 5,000 to 20,000 are used as dispersants. Thickeners are derived from the 300,000 to 500,000 range, and flocculants usually have molecular weights of greater than 1 million [30]. Table 3-6 shows that the molecular weight of the product can be changed by varying the reaction conditions. Viscosity average molecular weights from 6.9 kg/mol to 202 kg/mol were produced.

Figure 3-5 is a scanning electron micrograph of the polymer produced in an experiment at 70 °C. The particles generally are spherical, with diameters of approximately 10 to 100 μm.

3.4 Conclusions

The continuous precipitation polymerization of acrylic acid in supercritical carbon dioxide was successfully carried out in a CSTR. The product polymer was a white, dry, fine powder that was easily dissolved in water. A wide range of polymer molecular weights was obtained. The effect of some important operating variables on polymerization behavior was evaluated. The experimental results showed distinct characteristics of precipitation polymerization. The behavior of acrylic acid polymerization in $scCO_2$ is different from what DeSimone, Roberts and co-workers [8-10] found in their studies of the continuous polymerization of vinylidene fluoride in $scCO_2$. In that system, many features of the

polymerization rate and the molecular weight could be described by a model based on the assumption that polymerization took place primarily in the supercritical fluid. Polymerization inside the polymer particles appears to be more important with PAA than with PVDF.

3.5 Acknowledgements

This research was supported by Kenan Center for the Utilization of CO_2 in Manufacturing at North Carolina State University and by the STC Program of the National Science Foundation under Agreement No. CHE-9876674.

3.6 References

1. DeSimone, J. M.; Maury, E. E.; Menceloglu, Y. Z.; McClain, J. B.; Romack, T. J.; Combes, J. R. Science 1994, 265, 356-359.
2. Kendall, J. L.; Canelas, D. A.; Young, J. L.; DeSimone, J. M. Chemical Review 1999, 99, 543-563.
3. (a) McCoy, M. Chemical and Engineering News 1999, 77, 10;
   (b)"DuPont Introduces First Fluoropolymers Made with Supercritical CO_2 Technology",
   "http://www1.dupont.com/NASApp/dupontglobal/corp/index.jsp?page=/news/products_today.html&type=Product_News&year=2002"
4. Lacroix-Desmazes, P.; Andre, P.; DeSimone, J. M.; Ruzette, A-V.; Boutevin, B. J Polym Sci Part A: Polym Chem 2004, 42, 3537-3552.
5. Ma, Z.; Lacroix-Desmazes, P. J Polym Sci Part A: Polym Chem 2004, 42, 2405-2415.

6. Galia, A.; Giaconia, A.; Iaia, V.; Filardo, G. J Polym Sci Part A: Polym Chem 2004, 42, 173-185.
7. Barrett, K. E. J.; Thomas, H. R. in Dispersion Polymerization in Organic Media; Barrett, K. E. J., Ed.; Wiley-Interscience: New York, 1974; Chapter 4, 116-118.
8. Charpentier, P. A.; DeSimone, J. M.; Roberts, G. W. Ind Eng Chem Res 2000, 39, 4588-4596.
9. Saraf, M. K.; Gerard, S.; Wojcinski, L. W. II; Charpentier, P. A.; DeSimone, J. M.; Roberts, G. W. Macromolecules 2002, 35, 7976 – 7985.
10. Ahmed, T. S.; DeSimone, J. M.; Roberts, G. W. Chem Engng Sci 2004, 59, 5139-5144.
11. Kennedy, K. A., "Characterization of Phase Equilibrium Associated with Heterogeneous Polymerizations in Supercritical Carbon Dioxide", Ph. D. Thesis, North Carolina State University (2003).
12. Moore, D. E.; Parts, A. G. Die Makromolekulare Chemie 1960, 37, 108-118.
13. Lewis, O. G.; King, R. M. In Addition and Condensation Polymerization Processes: a Symposium; Gould, R. F., Ed.; American Chemical Society: Washington D. C., 1969; pp 25-45.
14. Nemec, J. W.; Bauer, W. in Encyclopedia of Polymer Science and Engineering, 2nd ed.; Mark, H. F., Ed.; Wiley-Interscience: New York, 1988; vol.1, pp 211-231.
15. Fukui, K.; Fujii, K.; Kagiya, T.; Toriuchi, Y.; Yokota, H. (Sumitomo Chemical Company, Ltd. and Sumitomo Atomic Energy Industries, Ltd.). French Patent 1,524,533, April 1, 1968.

16. Fukui, K.; Fujii, K.; Kagiya, T.; Toriuchi, Y.; Yokota, H. (Sumitomo Chemical Company, Ltd. and Sumitomo Atomic Energy Industries, Ltd.). U. S. Patent 3,522,228, July 28, 1970.
17. Sertage, W. G. J.; Davis, P.; Schenck, H. U.; Denzinger, W.; Hartmann, H. (BASF Corporation). Canadian Patent 1,274,942, October 2, 1990.
18. Hartmann, H.; Denzinger, W. (BASF Corporation). U. S. Patent 4,748,220, May 31, 1988.
19. Herbert, M. W.; Huvard, G. S. (B.F. Goodrich Company). European Patent 0,301,532 (A2), February 1, 1989.
20. Romack, T. J.; Maury, E. E.; DeSimone, J. M. Macromolecules 1995, 28, 912-915.
21. Xu, Q.; Han, B.; Yan, H. Polymer 2001, 42, 1369-1373.
22. Charpentier, P. A.; Kennedy, K. A.; DeSimone, J. M.; Roberts, G. W. Macromolecules 1999 32, 5973-5975.
23. Charpentier, P. A.; DeSimone, J. M.; Roberts, G. W. Chem Engng Sci 2000, 55, 5341-5349.
24. Kurland, J. J.; J Poly Sci: Poly Chem Ed 1980, 18, 1139-1145.
25. Buchholz F. L. in Industrial Polymers Handbook: Products, Processes, Applications; Buchholz, F. L., Ed.; Wiley-VCH: New York, 2000; vol. 1, p 574.
26. Wako Product Information: Azo Polymerization Initiators, Wako Chemicals USA, Inc., Richmond, VA.
27. Blauer, G. Trans Farad Soc 1960, 56, 606-612.
28. Levy, L. B. J Poly Sci: Poly Chem Ed 1985, 23, 1505-1515.

29. Poerschpanke, H. G.; Avela, A.; Reichert, K. H. Die Angewandte Makromolekulare Chemie 1993, 206, 157-169.

30. Will, R.; Sasano, T. in CEH Marketing Research Report; the Chemical Economics Handbook – SRI International, 2001; pp 582.000A-606.4003J.

Nomenclature

f	initiator efficiency
$[I]_{in}$	inlet initiator concentration (mol/L)
$[I]_{out}$	outlet initiator concentration (mol/L)
k_d	rate constant for initiator decomposition (min^{-1})
k_p	rate constant for chain propagation (L/mol-min)
k_t	rate constant for chain termination (L/mole-min)
[MEHQ]	inlet MEHQ concentration in acrylic acid (ppm)
$[M]_{in}$	inlet monomer concentration (mol/L)
$[M]_{out}$	outlet monomer concentration (mol/L)
$\overline{M}_v$	viscosity average molecular weight (kg/mol)
P	pressure (Bar)
$[P]_{out}$	outlet polymer concentration (g/L)
R_p	rate of polymerization (mol/L-s)
T	temperature (°C)
x	fractional monomer conversion
τ	average residence time (min)
$[\eta]$	intrinsic viscosity (ml/g)
ϕ	volume fraction of polymer
ν	kinetic chain length

Table 3-1. The effect of oxygen traps on polymerization

Number of oxygen traps	x (%)	R_p (10^{-4}mol/L/s)	$\overline{M}_v$ (kg/mol)
1	13.7	2.38	173
3	15.5	2.69	160
5	15.6	2.72	184

$[M]_{in}$ = 1.25 mol/L; $[I]_{in}$ = 0.004 mol/L; τ = 12 min; T = 50 °C; P = 207 bar.

Table 3-2. The effect of MEHQ on polymerization

[MEHQ] (ppm)	x (%)	R_p (10^{-4}mol/L/s)	$\overline{M}_v$ (kg/mol)
210	30.8	2.58	175
993	30.2	2.52	173

$[M]_{in}$ = 1.25 mol/L; $[I]_{in}$ = 0.004 mol/L; τ = 25 min; T = 50 °C; P = 207 bar.

Table 3-3. The effect of average residence time, τ

τ min	x (%)	R_p (10^{-4}mol/L/s)	$\overline{M}_v$ (kg/mol)	$[M]_{out}$ (mol/L)	$[P]_{out}$ (g/L)	ϕ
12	15.6	2.72	184	1.05	14.1	0.0101
20	25.5	2.66	171	0.932	23.0	0.0166
25	30.8	2.58	175	0.865	27.8	0.0200
30	34.0	2.35	169	0.825	30.6	0.0221
40	41.9	2.18	174	0.726	37.8	0.0272

$[M]_{in}$ = 1.25 mol/L; $[I]_{in}$ = 0.004 mol/L; T = 50°C; P = 207 bar.

Table 3-4. The effect of inlet initiator concentration, $[I]_{in}$

$[I]_{in}$ (mol/L)	x (%)	R_p (10^{-4}mol/L/s)	$\overline{M}_v$ (kg/mol)	$[M]_{out}$ (mol/L)	$[P]_{out}$ (g/L)	ϕ
0.001	43.7	1.46	73.7	0.282	15.7	0.0114
0.002	55.1	1.84	59.2	0.225	19.9	0.0143
0.003	61.0	2.04	37.7	0.196	22.0	0.0159
0.004	64.9	2.17	34.2	0.176	23.4	0.0169
0.005	68.5	2.29	33.2	0.158	24.7	0.0178

$[M]_{in}$ = 0.5 mol/L; τ = 25 min; T = 70 °C; P = 207 bar.

Table 3-5. The effect of inlet monomer concentration, $[M]_{in}$

$[M]_{in}$ (mol/L)	x (%)	R_p (10^{-4}mol/L/s)	$\overline{M}_v$ (kg/mol)	$[M]_{out}$ (mol/L)	$[P]_{out}$ (g/L)	ϕ
0.25	64.3	1.07	17.1	0.0895	11.6	0.00836
0.5	64.9	2.17	34.2	0.176	23.4	0.0169
0.75	66.6	3.34	60.0	0.251	36.0	0.0260
1.0	70.9	4.74	84.5	0.292	51.1	0.0369
1.25	72.3	6.04	103	0.348	65.1	0.0470

$[I]_{in}$ = 0.004 mol/L; τ = 25 min; T = 70 °C; P = 207 bar.

Table 3-6. Range of molecular weights produced

T (°C)	$[M]_{in}$ (mol/L)	$[I]_{in}$ (mol/L)	$\overline{M}_v$ (kg/mol)
50	2.5	0.002	202
70	1.25	0.004	103
70	0.50	0.004	34.2
90	0.25	0.006	6.85

τ = 25 min; P = 207 bar.

Figure Captions

Figure 3-1. CSTR polymerization system (A and J - CO_2 tanks; B – Acrylic acid; C – Initiator; D – Inhibitor; E – Agitator drive; G – CSTR; H – Heating system; I – Heat exchanger; K – Pressure control valve; F1 and F2 – Unsteady-state filters; F3 – Steady-state filter; P1, P2, P3, P4 and P5 – Syringe pumps; V1, V2, V3, V4, V5 and V6 – Valves; L – Atmospheric bag filter)

Figure 3-2a. The effect of average residence time (τ) on the rate of polymerization (R_p) (T = 50 °C, P = 207 bar, $[M]_{in}$ = 1.25 mol/L, $[I]_{in}$ = 0.004 mol/L)

Figure 3-2b. The effect of average residence time (τ) on the molecular weight ($\overline{M}_v$) (T = 50 °C, P = 207 bar, $[M]_{in}$ = 1.25 mol/L, $[I]_{in}$ = 0.004 mol/L)

Figure 3-3a. The effect of outlet initiator concentration ($[I]_{out}$) on the rate of polymerization (R_p) (T = 70 °C, P = 207 bar, τ = 25 min, $[M]_{in}$ = 0.5 mol/L)

Figure 3-3b. The effect of outlet initiator concentration ($[I]_{out}$) on the molecular weight ($\overline{M}_v$) (T = 70 °C, P = 207 bar, τ = 25 min, $[M]_{in}$ = 0.5 mol/L)

Figure 3-4a. The effect of outlet monomer concentration ($[M]_{out}$) on the rate of polymerization (R_p) (T = 70 °C, P = 207 bar, τ = 25 min, $[I]_{in}$ = 0.004 mol/L)

Figure 3-4b. The effect of outlet monomer concentration ($[M]_{out}$) on the molecular weight ($\overline{M}_v$) (T = 70 °C, P = 207 bar, τ = 25 min, $[I]_{in}$ = 0.004 mol/L)

Figure 3-5. Scanning electron micrograph of PAA particles produced in a CSTR (T = 70 °C; P = 207 bar; τ = 25 min; $[M]_{in}$ = 0.50 mol/L; $[I]_{in}$ = 0.006 mol/L).

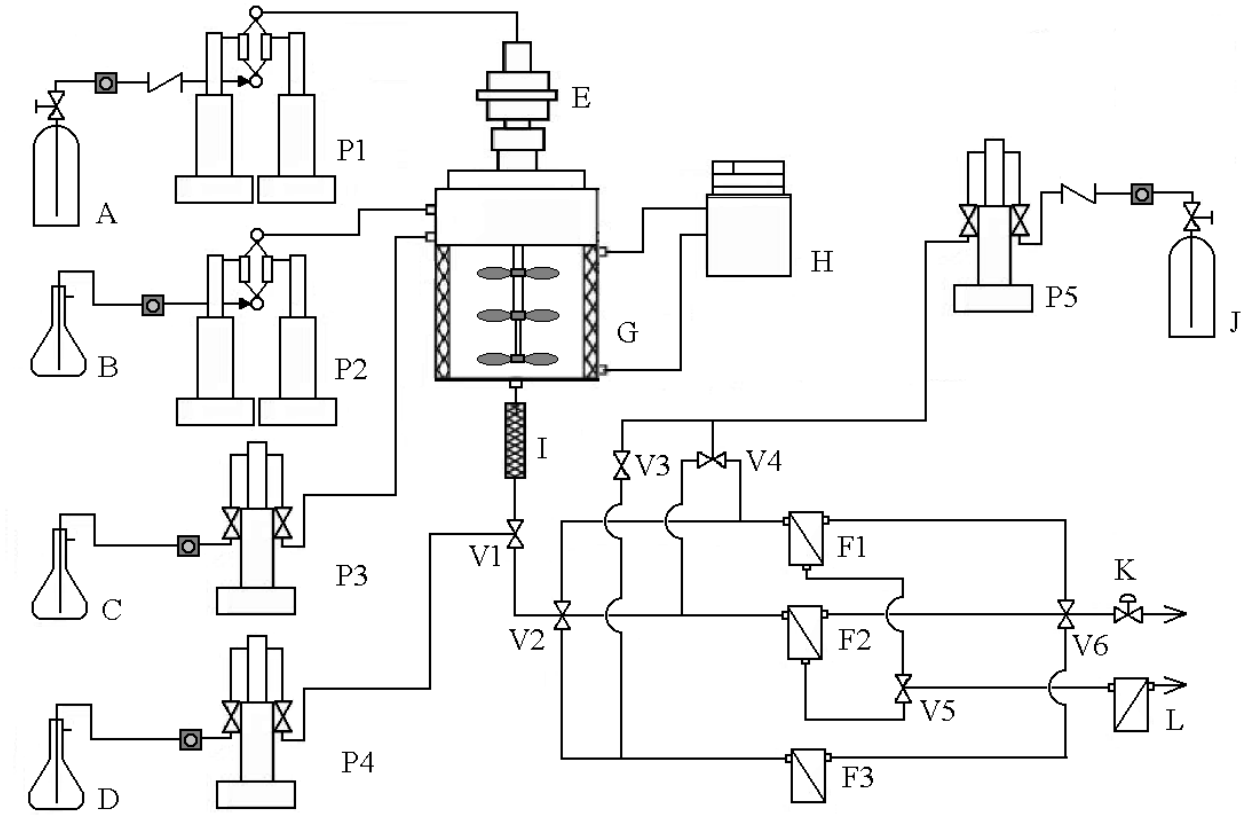

Figure 3-1. CSTR polymerization system (A and J - CO_2 tanks; B – Acrylic acid; C – Initiator; D – Inhibitor; E – Agitator drive; G – CSTR; H – Heating system; I – Heat exchanger; K – Pressure control valve; F1 and F2 – Unsteady-state filters; F3 – Steady-state filter; P1, P2, P3, P4 and P5 – Syringe pumps; V1, V2, V3, V4, V5 and V6 – Valves; L – Atmospheric bag filter)

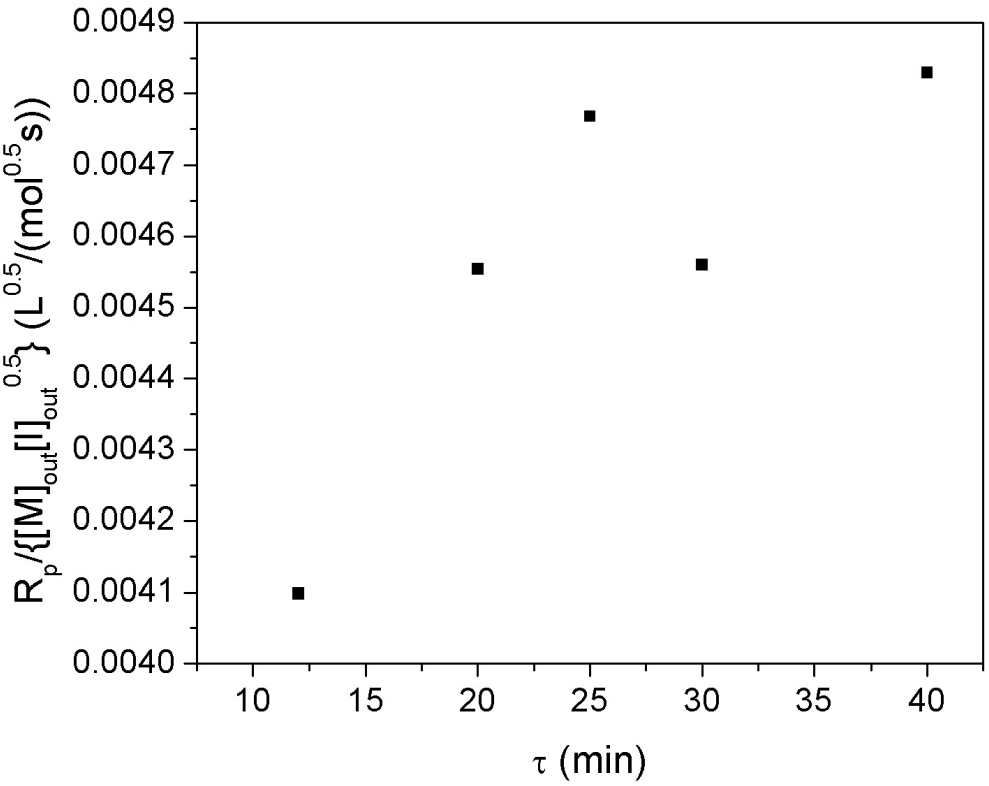

Figure 3-2a. The effect of average residence time (τ) on the rate of polymerization (R_p) (T = 50 °C, P = 207 bar, $[M]_{in}$ = 1.25 mol/L, $[I]_{in}$ = 0.004 mol/L)

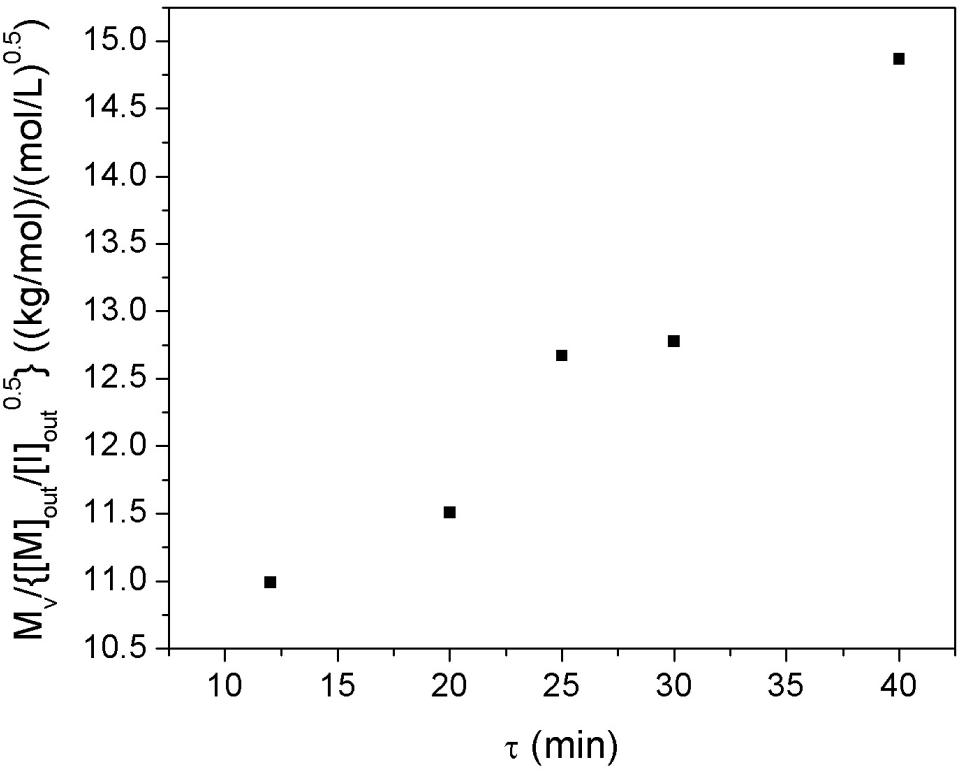

Figure 3-2b. The effect of average residence time (τ) on the molecular weight ($\overline{M}_v$) (T = 50 °C, P = 207 bar, $[M]_{in}$ = 1.25 mol/L, $[I]_{in}$ = 0.004 mol/L)

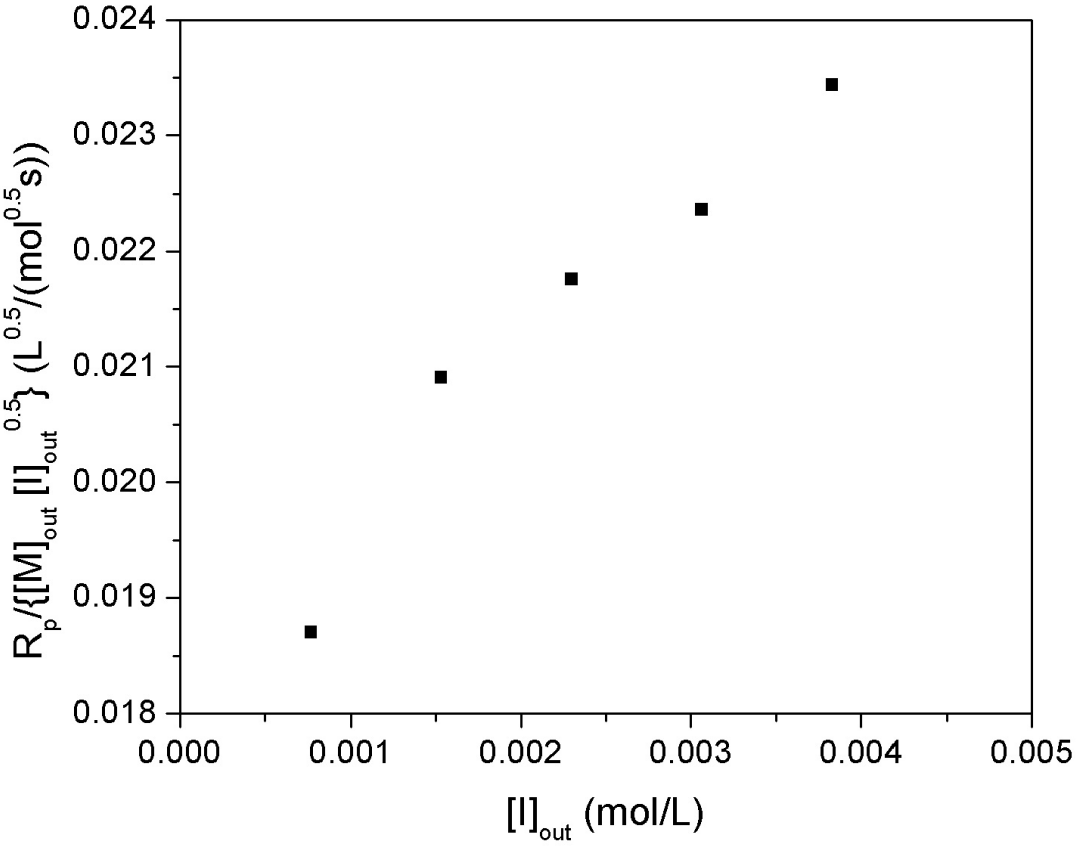

Figure 3-3a. The effect of outlet initiator concentration ($[I]_{out}$) on the rate of polymerization (R_p) (T = 70 °C, P = 207 bar, τ = 25 min, $[M]_{in}$ = 0.5 mol/L)

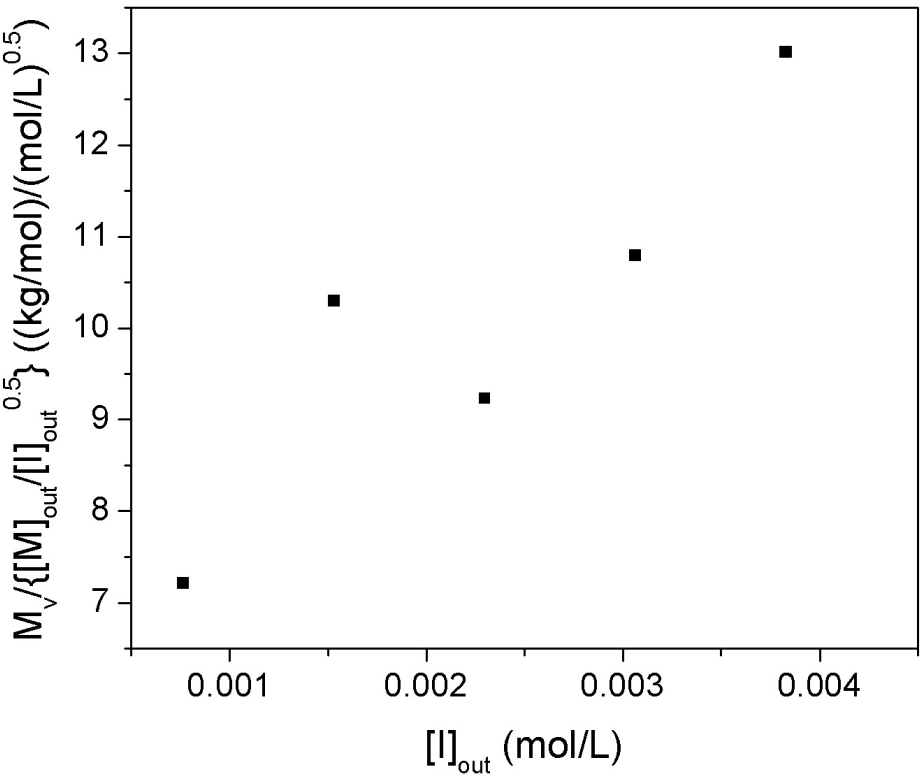

Figure 3-3b. The effect of outlet initiator concentration ($[I]_{out}$) on the molecular weight ($\overline{M}_v$)

(T = 70 °C, P = 207 bar, τ = 25min, $[M]_{in}$ = 0.5 mol/L)

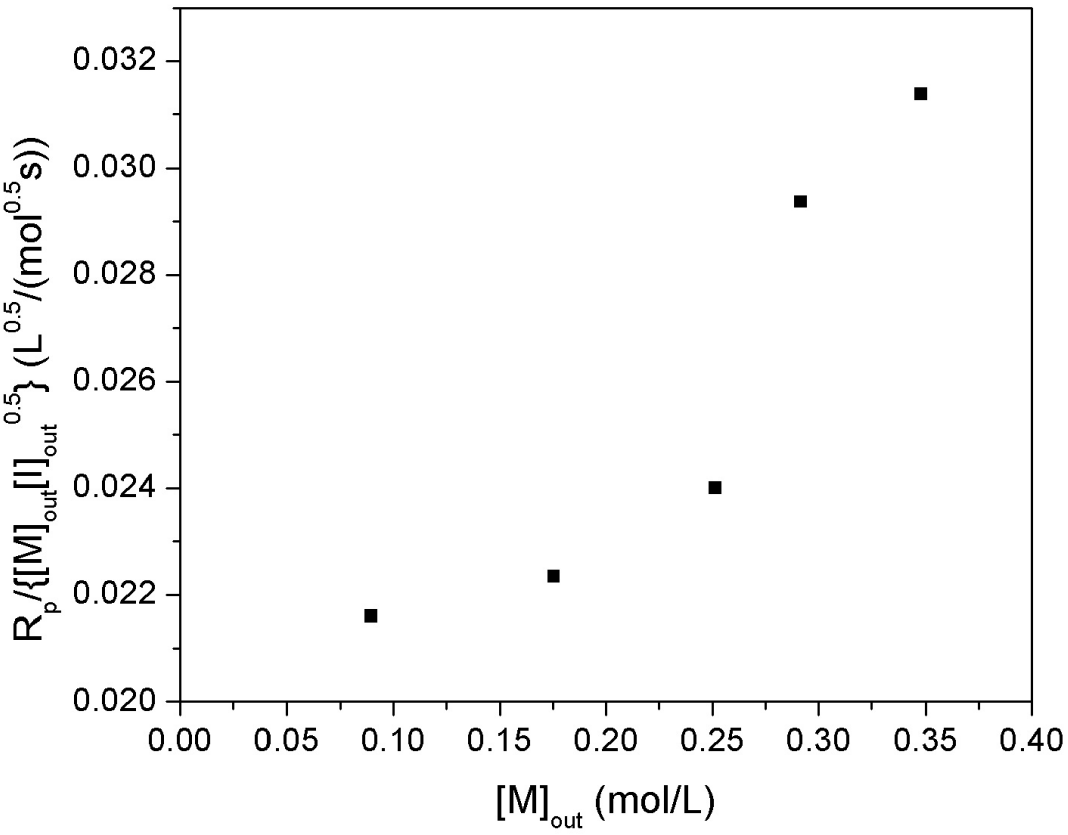

Figure 3-4a. The effect of outlet monomer concentration ($[M]_{out}$) on the rate of polymerization (R_p) (T = 70 °C, P = 207 bar, τ = 25 min, $[I]_{in}$ = 0.004 mol/L)

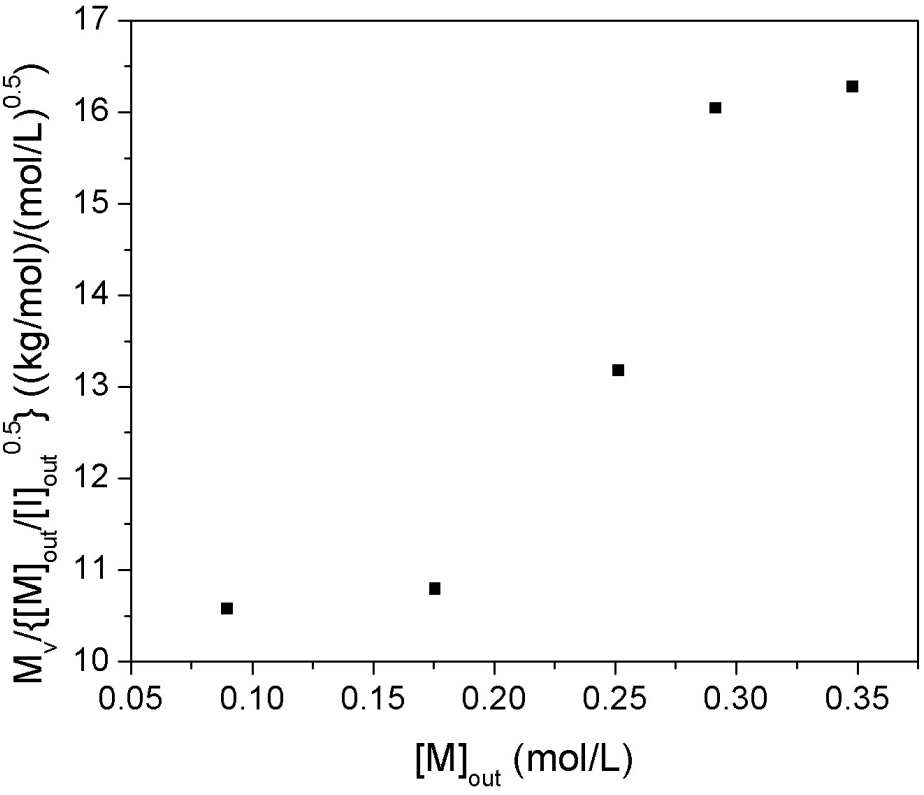

Figure 3-4b. The effect of outlet monomer concentration ($[M]_{out}$) on the molecular weight ($\overline{M}_v$) (T = 70 °C, P = 207 bar, τ = 25 min, $[I]_{in}$ = 0.004 mol/L)

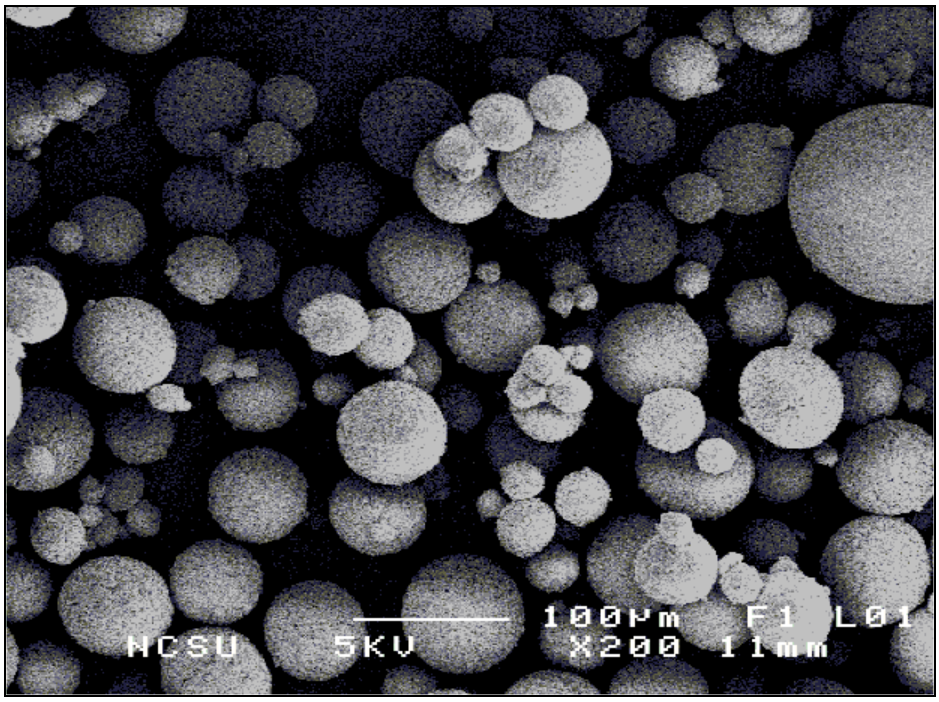

Figure 3-5. Scanning electron micrograph of PAA particles produced in a CSTR (T = 70 °C; P = 207 bar; τ = 25 min; $[M]_{in}$ = 0.50 mol/L; $[I]_{in}$ = 0.006 mol/L).

CHAPTER 4

KINETICS OF PRECIPITATION POLYMERIZATION OF ACRYLIC ACID IN SUPERCRITICAL CARBON DIOXIDE

Tao Liu[1], Joseph M. DeSimone[1, 2], and George W. Roberts[1,*]

[1]Department of Chemical Engineering, Campus Box 7905, North Carolina State University, Raleigh, North Carolina 27695-7905

[2]Department of Chemistry, CB 3290, Venable and Kenan Laboratories, University of North Carolina at Chapel Hill, North Carolina 27599-3290

This is a manuscript to be submitted for publication in

Chemical Engineering Science

February 2004

Abstract

The precipitation polymerization of acrylic acid has been carried out at 50 and 70 °C in $scCO_2$, using a continuous stirred-tank reactor (CSTR) and a batch reaction calorimeter. Three simple kinetic models have been developed to describe this polymerization, and the models have been compared with the experimental results for rate of polymerization and viscosity-average molecular weight. The first model, the "solution polymerization model", is based on the assumption that all of the polymerization reactions take place in the fluid phase, and that no reaction takes place in the polymer phase. In the second model, the "surface polymerization model", chain initiation is assumed to occur in the fluid phase, but chain propagation and chain termination occur in a thin zone on the surface of the polymer particles. The third model, the "particle polymerization model", is similar to the "surface polymerization model", except that chain propagation and chain termination take place uniformly throughout the polymer particle. The surface polymerization model and the particle polymerization model both provided a much better fit of the data from the CSTR than the solution polymerization model. However, the particle polymerization model provided the best description of the data from the batch reaction calorimeter.

Keywords:

Acrylic acid, Kinetics, Modeling, Multiphase reactions, Polymerization, Supercritical fluid

4.1 Introduction

Understanding of the mechanism and kinetics of a polymerization is important to the optimization and control of a commercial process. A model of the polymerization can predict how the reaction conditions will affect both the rate of polymerization and the molecular weight distribution (MWD) of polymer. The rate is important, because most polymerizations are highly exothermic. An improperly-controlled reaction can give rise to operation difficulty and safety problems, and can lead to out-of-specification product. The average molecular weights and the MWD determine the applications of polymer.

The precipitation polymerization of acrylic acid in supercritical carbon dioxide ($scCO_2$) has been known for many years (Canelas and DeSimone, 1997). We recently reported a study of the continuous precipitation polymerization of acrylic acid in $scCO_2$ using a continuous stirred-tank reactor (CSTR) (Liu et al. 2005), and showed that the data were not well described by a homogeneous, free radical, solution polymerization model. This paper extends this earlier work to consider two models that are based on the assumption that chain propagation and termination take place in the precipitated polymer particles.

Precipitation polymerization is a heterogeneous process during which polymer particles continuously form and precipitate from the continuous phase. In precipitation polymerization, the polymer particles are slightly swelled or non-swelled by monomer and/or medium (Arshady, 1992). A typical batch precipitation polymerization begins slowly and gradually accelerates to a maximum rate followed by a diminution in rate as monomer is consumed.

Three polymerization loci exist during precipitation polymerization. These are: the solution phase, the surface of the polymer particles, and the interior of the polymer particles,

as depicted in Figure 4-1. Accordingly, three types of polymerization are named: solution polymerization, surface polymerization, and interior polymerization (Peebles, 1964). The solution polymerization takes place in the same way as in a usual homogeneous solution polymerization. The surface polymerization depends on the surface absorption of monomer. The interior polymerization is affected by solubility and diffusivity of monomer in the polymer phase.

For some polymers, the rigid structure of the polymer can hinder accretion of oligomer radicals (Barrett and Thomas, 1974). Moreover, the solubility of monomer in the polymer particles may be low under reaction conditions. Under these circumstances, most radicals will polymerize in solution until they terminate. Aggregation with other polymer chains then can occur, forming new particles that may agglomerate with existing polymer particles. Under such circumstances, the rate of polymerization within the particles can be negligible.

The precipitation polymerization of vinylidene fluoride in $scCO_2$ appears to behave kinetically like a homogeneous solution polymerization (Charpentier et al. 2000; Saraf et al. 2002; Ahmed et al. 2004). DeSimone, Roberts and coworkers have developed a model based on the assumption that initiation, propagation, and termination all take place homogeneously in the continuous phase, and that no reaction takes place in the polymer phase. This model is able to describe all of the important factors of the polymerization including the kinetics and the existence of a bimodal molecular weight distribution at some experimental conditions. They speculate that the lifetime of a radical in the continuous phase may be much smaller than the time scale for polymer precipitation. If so, the concentration of radicals trapped in

polymer particles would be small, and their contribution to polymerization would not be significant.

However, if the kinetics of polymerization is much slower than the kinetics of precipitation, polymer radicals will precipitate during an early stage of their growth, and the polymerization will continue in the dispersed polymer phase. In this case, the polymerization in the polymer phase can be important, especially if the monomer is highly soluble in the polymer. In the precipitation polymerization of acrylonitrile in water, the rate of polymerization is lowered by removal of the polymer particles during the reaction (Moore and Parts, 1960). It was hypothesized that growing polyacrylonitrile radicals become insoluble in the continuous phase at some stage (5-10 units) in their growth. Upon precipitation, the active end of the radical will be shielded by coiling of the molecule. Coalescence of polymer particles would be expected to greatly enhance the degree of shielding and it is the major factor in the occlusion of radicals. The main effect of occlusion is to reduce the termination coefficient. This will naturally lead to a progressive increase in the rate of reaction and a higher initiator order than normal (Bamford and Jenkins, 1953).

It is believed that the number of particles gets constant in the very early stage of a polymerization. Lewis and King (1969) have found that no new particles are formed beyond about 0.4% conversion in bulk acrylonitrile polymerization. The aggregates of precipitated polymer particles are highly porous, which can be seen by electron micrography. Their studies also show that particles from polymerization in benzene are more compact and denser in appearance than those from bulk polymerization. Lewis and King have established a kinetic model that described the precipitation polymerization of bulk acrylonitrile and acrylonitrile in benzene. They assumed that the surface is the only locus of polymerization

that needs to be considered because the average lifetime of a radical in the solution phase is such that only one to 10 acrylonitrile units can add before the radical collides with a polymer particle. The studies on precipitation polymerization of arylonitrile in aqueous solution also suggest the location of polymerization is the particle surface (McCarthy et al. 1986; Nishida et al. 1995).

Interior polymerization should become more important as the temperature increases. At high temperature, the loosening of coalesced polymer particles will make diffusion of small molecules into polymer particles easier. This may allow and increase the amount of propagation before appreciable bimolecular termination is possible. Bamford and Jenkins (1953) studied the dependence of molecular weight on temperature in the bulk polymerization of acrylonitrile. A number of polymers were prepared using the same initiator concentration at different temperatures. Polymer thus obtained at 55 °C and above showed a smooth decrease of molecular weight with rise in temperature, as would be expected. However, polymer prepared below 55 °C showed an increase in molecular weight with increase in temperature, indicating the increase of propagation with temperature is faster than termination.

Fortini et al. (2004) have used a Mettler-Toledo RC1e reaction calorimeter to study the dispersion polymerization of methyl methacrylate in $scCO_2$. The reaction calorimeter instantaneously measures the temperature of the reactants and the temperature of the reactor inner surface in contact with the reactants over the course of a reaction as a function of time. On the basis of those temperatures, the time evolutions of the heat of polymerization, the rate of polymerization, and the reactant conversion are determined.

In the present paper, kinetics analysis was carried out for the precipitation polymerization of acrylic acid in $scCO_2$. Three different kinetic models were derived and compared with the results of continuous polymerization in a CSTR, as reported in a previous paper (Liu et al. 2005). In addition, the isothermal precipitation polymerization of acrylic acid in $scCO_2$ was carried out in a Mettler-Toledo RC1e reaction calorimeter, similar to that used by Fortini et al. (2004). The data from the calorimeter were compared with the predictions of the three kinetic models.

4.2 Experimental

Materials: Carbon dioxide (SFC grade, 99.998%) was purchased from National Specialty Gases. The initiator, high purity 2,2'–azobis(2,4-dimethyl-valeronitrile) (V-65B), was donated by Wako Chemicals USA. Acrylic acid (99.5%), Toluene (HPLC grade, 99.5%), 1,1,2-trichloro-1,2,2-trifluoroethane (Freon 113) (HPLC grade, 99.8%), and 4-methoxyphenol (MEHQ) (99%) were purchased from the Fisher Scientific. All chemicals were used as received.

Continuous Polymerization: Continuous precipitation polymerization of acrylic acid in $scCO_2$ was carried out in an 800ml CSTR using V-65B as the free-radical initiator. The reactor temperature was between 50 to 70 °C, the pressure was 207 bar, and the average residence time was in the range of 12 to 40 minutes. Additional details of the equipment and the experimental procedures are available elsewhere (Liu et al. 2005).

Reaction Calorimeter: Figure 4-2 is a schematic of the Mettler Toledo RC1e Reaction Calorimeter that was used in this study. The principal component is a 1.2-liter reactor that can be pressurized up to 350 bar and heated to 300 °C. The reactor has a magnetically-driven agitator, a 25 W calibration heater, a pressure sensor and a temperature

sensor. The reactor jacket temperature and the reactor cover temperature were both controlled by a personal computer.

In a typical experiment, the reactor was pressurized to 800 psi with CO_2 and then depressurized to atmospheric pressure 5 times at room temperature before use. Acrylic acid, which had been deoxygenated by high purity argon for 1 hour, then was introduced into the reactor. Some liquid CO_2 was added. The reactor was heated to a temperature that was 1.5°C lower than the desired polymerization temperature and the pressure was increased to the desired level by adding CO_2. Then the measurements of the overall heat transfer coefficient and overall heat capacity of the reactants were carried out. The temperature and pressure were increased to their required points. The initiator/Freon113 solution (0.32 mol/L) was added with a high-pressure pump. The polymerization began shortly thereafter, as indicated by an increase of the temperature and the pressure. The reaction was essentially isothermal; the maximum reaction temperature increase was less than 1 °C. After a few hours, the temperature and pressure became constant. The system was allowed to operate for another few hours to make sure that the polymerization was completed. Then the determinations of overall heat transfer coefficient and overall heat capacity were repeated. Finally, the reactor was quenched by quickly cooling the reactor to 5 °C, and the CO_2 was slowly released.

4.3 Results and Discussion

The product polymer was a white, dry, fine powder that dissolved in water. A wide range of polymer molecular weights (5 to 200 kg/mol) was obtained. The effect of the operating variables on the polymerization rate and on the polymer molecular weight was evaluated, with most experiments carried out in the CSTR.

Kinetic Modeling

Precipitation polymerization of acrylic acid in $scCO_2$ can occur at three different loci: the solution phase, the surface of polymer particles, and the interior of polymer particles. Their importance to the overall polymerization may depend on the experimental conditions. To understand the mechanism and kinetics of this system, the characteristic models corresponding to the three polymerization loci were developed.

Solution Polymerization Model. Poly (acrylic acid) is essentially insoluble in $scCO_2$ (Rindfleisch et al. 1996). A polymer chain should become insoluble at an early stage of growth. If the kinetics of polymerization is much faster than the kinetics of precipitation, most polymer chains will grow and terminate in the solution phase. The question of whether polymerization can takes place in the polymer particles then depends on whether and how rapid monomer and undecomposed initiator can partition into the polymer phase. Partitioning will depend on many factors including solubilities of the various species, hydrodynamic conditions in the reactor, and the size of the polymer particles. The "solution polymerization model" is a limiting case of reactor behavior, in which the concentration of free radicals inside the polymer particles is negligible, and no polymerization takes place in the polymer phase.

Equation 4-1 can be derived for polymerization in a CSTR that obeys the solution polymerization model (see Appendix).

$$R_P = k_p \left(\frac{f k_d}{k_t} \right)^{1/2} [M]_{out} [I]_{out}^{1/2} \frac{(1 - v_p)^{1/2}}{1 + (\alpha - 1) v_p} \qquad (4\text{-}1)$$

The concentrations $[M]_{out}$ and $[I]_{out}$ are the overall concentrations of monomer and initiator, respectively, in the product stream from the CSTR. $[M]_{out}$ can be obtained from the

measured rate of polymer formation, and $[I]_{out}$ can be estimated using the decomposition rate constant for the initiator.

As the volume fraction of the polymer phase (v_p) approaches zero, Equation 4-1 reduces to:

$$R_P = k_p \left(\frac{f k_d}{k_t} \right)^{1/2} [M]_{out} [I]_{out}^{1/2} \qquad (4\text{-}2)$$

which is the classical rate expression for a homogeneous solution polymerization, where the ratio $R_P / \{[M]_{out} [I]_{out}^{1/2}\}$ is only a function of temperature.

In a previous study of the precipitation polymerization of acrylic acid in $scCO_2$ in a CSTR (Liu et al. 2005), it was noted that the value of $R_P / \{[M]_{out} [I]_{out}^{1/2}\}$ increased at constant temperature for experiments where: (1) the inlet monomer concentration was increased at constant residence time and constant inlet initiator concentration, 2) the inlet initiator concentration was increased at constant residence time and constant inlet monomer concentration, and 3) the residence time was increased at constant inlet monomer and initiator concentrations.

According to Equation 4-1, if the partition coefficient α is greater than 1 and v_p is non-zero, the concentration of the monomer in the fluid is less than $[M]_{out}$ because some monomer is "stored" in the polymer particles, where it cannot react according to the solution model. In this case, the precipitation of polymer particles can decrease the monomer concentration in the continuous phase. Therefore, the value of $R_P / \{[M]_{out} [I]_{out}^{1/2}\}$ will decrease as v_p increases.

The data showed that at constant temperature v_p increased as 1) the inlet monomer concentration was increased at constant residence time and constant inlet initiator

concentration, 2) the inlet initiator concentration was increased at constant residence time and constant monomer concentration, and 3) the residence time was increased at constant inlet monomer and initiator concentrations. According to Equation 4-1, an increase in v_p will have the maximum positive effect on $R_P/\{[M]_{out}[I]_{out}^{1/2}\}$ when $\alpha = 0$. In this case, Equation 4-1 becomes:

$$\frac{R_P}{[M]_{out}[I]_{out}^{1/2}} = k_p\left(\frac{fk_d}{k_t}\right)^{1/2}\frac{1}{(1-v_p)^{1/2}} \tag{4-3}$$

This equation predicts that $\{R_P(1-v_p)^{1/2}\}/\{[M]_{out}[I]_{out}^{1/2}\}$ should be constant at constant temperature, provided that $\alpha = 0$. Since α should be greater than 0, $\{R_P(1-v_p)^{1/2}\}/\{[M]_{out}[I]_{out}^{1/2}\}$ will decrease as v_p increases.

Figure 4-3 shows the variation of $\{R_P(1-v_p)^{1/2}\}/\{[M]_{out}[I]_{out}^{1/2}\}$ with v_p. The 70°C data shows a clear increase of $\{R_P(1-v_p)^{1/2}\}/\{[M]_{out}[I]_{out}^{1/2}\}$ with v_p. Due to the large scale of $\{R_P(1-v_p)^{1/2}\}/\{[M]_{out}[I]_{out}^{1/2}\}$ in this figure, the change of the 50°C data are not clear in Figure 4-3. However, when the data are plotted on a scale of 0.004 to 0.005 $(L/mol)^{0.5}/s$ a steady increase at 50°C can be observed. Therefore, the solution polymerization model cannot account for the rate of precipitation polymerization of acrylic acid in $scCO_2$. Polymerization in the polymer phase must be taken into consideration.

Surface Polymerization Model. If most polymer chains precipitate early in their growth, the rate of solution polymerization will be negligible compared with the rate of polymerization in the polymer particles. If the polymer phase is dense, diffusion of monomer into polymer particles will be slow and polymerization will take place primarily in a thin layer on the particle surface. In this model, chain initiation is assumed to take place

exclusively in the solution phase, but chain propagation and chain termination are assumed to take place exclusively on the polymer particle surface. With these assumptions, the rate of polymerization and the kinetic chain length are described by Equations 4-4 and 4-5 for polymerization in an ideal CSTR.

$$R_P = K_1[M]_{in}^{\frac{4}{3}}(1-x)x^{\frac{1}{3}}\left(\frac{[I]_{in}}{k_d\tau+1}\right)^{\frac{1}{2}} \tag{4-4}$$

$$\upsilon = K_2[M]_{in}^{\frac{4}{3}}(1-x)x^{\frac{1}{3}}\left(\frac{[I]_{in}}{k_d\tau+1}\right)^{-\frac{1}{2}} \tag{4-5}$$

where

$$K_1 = 2.2N^{\frac{1}{6}}k_p\left(\frac{fk_d}{k_t}\right)^{\frac{1}{2}}\delta^{1/2}\alpha\left(\frac{M_m}{\rho_p}\right)^{\frac{1}{3}} \tag{4-6}$$

$$K_2 = \frac{K_1}{2fk_d} \tag{4-7}$$

If the viscosity average molecular weight, $\overline{M}_v$, is proportional to the kinetic chain length, Equation 4-8 can be derived from Equation 4-5.

$$\frac{\overline{M}_v}{M_m} = \psi K_2[M]_{in}^{\frac{4}{3}}(1-x)x^{\frac{1}{3}}\left(\frac{[I]_{in}}{k_d\tau+1}\right)^{-\frac{1}{2}} \tag{4-8}$$

The values of K_1 and ψK_2 shown in Table 4-1 were determined by fitting Equations 4-4 and 4-8 to the experimental data. The fits of these equations to the data are shown in Figures 4-4 and 4-5 in the form of parity plots. The surface polymerization model predicts most of the experimental results quite well.

The ratio $\psi K_2/K_1$ can be calculated from K_1 and ψK_2, as given in Table 4-1. According to Equation 4-7, the ratio K_2/K_1 is given by $1/(2fk_d)$. Therefore, the value of ψ can

be calculated if f and k_d are known. Since ψ is the constant of proportionality between $\{\overline{M}_v / M_m\}$ and the kinetic chain length, ν, the value of ψ provides a test of the physical reality of the model. As a first approximation, the rate constant for the decomposition of V-65B in $scCO_2$/acrylic acid was assumed to be the same as the rate constant for V-65B decomposition in toluene (Wako Chemicals USA). The value of f was assumed to be the same as that of 2,2'-azobis(isobutyronitrile) (AIBN) in $scCO_2$ (Guan et al. 1993). At 70 °C, the value of ψ is 2.40. This seems reasonable, because the viscosity-average molecular weight ($\overline{M}_v$) usually is higher than the number-average molecular weight ($\overline{M}_n$), and $\overline{M}_n$ should be higher than the kinetic chain length by a factor of up to 2. The estimated value of ψ at 50 °C, 0.90, is too low. Some of the discrepancy may result from error in estimating the initiator decomposition rate constant and the initiator efficiency. It is also possible that the discrepancy is caused by the model assumptions. Nevertheless, the magnitude of these estimates of ψ is reasonable, and lends some support to the physical basis of the surface polymerization model.

Particle Polymerization Model. If diffusion of monomer into polymer particles is rapid compared to the rate of polymerization, reaction will take place almost homogeneously throughout the whole particle. If initiation takes place in the fluid phase, and the propagation and termination reactions take place uniformly in the polymer particles, Equations 4-9 and 4-10 can be derived (see Appendix)

$$R_P = \frac{[M]_{in}^{\frac{3}{2}}(1-x)x^{\frac{1}{2}}}{a[M]_{in}x+b}\left(\frac{[I]_{in}}{k_d\tau+1}\right)^{\frac{1}{2}} \tag{4-9}$$

$$\upsilon = \frac{[M]_{in}^{\frac{3}{2}}(1-x)x^{\frac{1}{2}}}{c[M]_{in}x+d}\left(\frac{[I]_{in}}{k_d\tau+1}\right)^{-\frac{1}{2}} \tag{4-10}$$

where

$$a = \frac{1}{k_p}\left(\frac{k_t}{fk_d}\right)^{\frac{1}{2}}\left(\frac{M_m}{\rho_p}\right)^{\frac{1}{2}}\left(\frac{\alpha-1}{\alpha}\right) \tag{4-11}$$

$$b = \frac{1}{k_p}\left(\frac{k_t}{fk_d}\right)^{\frac{1}{2}}\left(\frac{\rho_p}{M_m}\right)^{\frac{1}{2}}\left(\frac{1}{\alpha}\right) \tag{4-12}$$

$$c = 2fk_d a \tag{4-13}$$

$$d = 2fk_d b \tag{4-14}$$

$$\frac{a}{b} = \frac{c}{d} = \frac{M_m}{\rho_p}(\alpha - 1) \tag{4-15}$$

If the viscosity-average molecular weight is proportional to the kinetic chain length, Equation 4-16 can be derived from Equation 4-10.

$$\frac{\overline{M}_v}{M_m} = \psi\frac{[M]_{in}^{\frac{3}{2}}(1-x)x^{\frac{1}{2}}}{c[M]_{in}x + d}\left(\frac{[I]_{in}}{k_d\tau + 1}\right)^{-\frac{1}{2}} \tag{4-16}$$

By fitting Equations 4-9 and 4-16 to the experimental results, the four parameters, a, b, c/ψ, and d/ψ, are determined. These values are given in Table 4-2. Figure 4-6 and Figure 4-7 shows that the particle polymerization model also describes most of experimental results quite well.

Using the values of a, b, c/ψ, and d/ψ, the values of ψ and α can be calculated. These values are shown in Table 4-2. It should be noted that, in the calculation of α the density of polymer phase was assumed to be the same as the density of pure poly(acrylic acid) at room temperature and atmospheric pressure. Actually, the former should be lower than the later because of the absorption of CO_2 and monomer into polymer. Therefore, α was

overestimated. All values of ψ and α are in reasonable range. This is quite surprising considering the estimates of initiator decomposition and the density of polymer phase.

Both the surface polymerization model and the particle polymerization model fit the experimental results better than the solution polymerization model. Their performance suggests that polymerization in the polymer phase is much more important than polymerization in the solution phase. However, the data taken in the CSTR do not allow these two models to be discriminated.

Reaction Calorimetry. Figure 4-8 presents the results of an experiment in the calorimeter at 50°C. The pressure increased with monomer conversion, similar to other heterogeneous polymerizations in $scCO_2$ (Lepilleur and Beckman, 1997). Phase separation and the non-ideal behavior of the fluid phase appear to be responsible for this behavior (Lepilleur and Beckman, 1997). The reaction began slowly and gradually accelerated. The rate of polymerization reached a maximum when the monomer conversion was 31.9%. The rate then decreased to essentially zero. This result confirmed the conclusion that this polymerization did not behave like a conventional solution polymerization. If the polymerization took place predominantly in the fluid phase, the rate of polymerization would decrease monotonically with time.

Equations 4-17 and 4-18 were derived for batch precipitation polymerization, based on the assumptions of the surface polymerization model and the particle polymerization model, respectively (see Appendix):

$$R_P = [M]_0 \frac{dx}{dt} = K[M]_0^{4/3}(1-x)x^{1/3}[I]_0^{1/2}\exp\left(-\frac{k_d t}{2}\right) \tag{4-17}$$

$$R_P = [M]_0 \frac{dx}{dt} = \frac{[M]_0^{3/2}(1-x)x^{1/2}}{a[M]_0 x + b}[I]_0^{1/2}\exp\left(-\frac{k_d t}{2}\right) \tag{4-18}$$

Both models predict the existence of a maximum rate of polymerization. In the experiment shown in Figure 4-8, R_P reached its maximum in less than 1 hour, which is much shorter than the half-life time of V-65B at 50 °C, $t_{1/2}$ = 13.4hour. Therefore, the exponential terms in Equations 4-17 and 4-18 are negligible, so

$$R_P = K[M]_0^{4/3}(1-x)x^{1/3}[I]_0^{1/2} \tag{4-19}$$

$$R_P = \frac{[M]_0^{3/2}(1-x)x^{1/2}[I]_0^{1/2}}{a[M]_0 x + b} \tag{4-20}$$

The surface polymerization model, Equation 4-19, predicts that the monomer conversion is 25% when the rate of polymerization reaches its maximum, and this conversion, x_m, does not change with experimental conditions.

The particle polymerization, Equation 4-20, gives:

$$\frac{1-3x_m}{x_m^2 + x_m} = \frac{a}{b}[M]_0 \tag{4-21}$$

Equation 4-15 has shown that $a/b=(M_m/\rho_p)(\alpha-1)$. Therefore, the particle polymerization model predicts that x_m is a function of the initial monomer concentration ($[M]_0$), the density of polymer phase (ρ_p), and the partition coefficient of monomer (α).

In Figure 8, x_m is 31.9% and $[M]_0$ is 1.0mol/L. Therefore, a/b equals 0.102 L/mol. The monomer partition coefficient (α) is then determined as 3.0 by Equation 4-15. This value is of the same order of magnitude as those listed in Table 2. The value calculated by Equation 4-21 may be more reliable, because it does not depend on the assumed initiator decomposition rate constant (k_d) and initiation efficiency (f).

On the basis of our calorimetric study, we believe the particle polymerization model provides a better description of acrylic acid polymerization in $scCO_2$ compared with the surface polymerization model.

4.4 Conclusions

The kinetics of precipitation polymerization is analyzed and three kinetic models are derived. The first model assumes that the polymerization takes place only in the solution phase, with no reactions in the polymer phase. The second model assumes that chain initiation takes place in the solution phase, but chain propagation and termination take place in a thin layer on particle surface. The third one also assumes that chain initiation take place only in the fluid phase, but it assumes chain propagation and chain termination occur homogeneously throughout the polymer particle. The model predictions were compared with the experimental results of the continuous precipitation polymerization of acrylic acid in $scCO_2$ in a CSTR. The solution polymerization model didn't agree with the experimental results well. The other two models both predicted the experimental results well. However, the calorimetry experimental results showed that the particle polymerization model described the polymerization behavior better than the surface polymerization model.

4.5 Acknowledgements

This research is supported by Kenan Center for the Utilization of CO_2 in Manufacturing at North Carolina State University and the STC Program of the National Science Foundation under Agreement No. CHE-9876674.

4.6 References

Ahmed, T.S., DeSimone, J.M., Roberts, G.W., 2004. Continuous precipitation polymerization of vinylidene fluoride in supercritical carbon dioxide: Modeling the molecular weight distribution. Chemical Engineering Science, 59, 5139-5144.

Arshady, R., 1992. Suspension, emulsion, and dispersion polymerization – a methodological survey. Colloid & Polymer Science, 270, 717-732.

Bamford, C.H., Jenkins, A.D., 1953. Studies in polymerization. VI. Acrylonitrile – the behaviour of free radicals in heterogeneous systems. Proceedings of the Royal Society of London, Series A, Methematical and Physical Science, 216, 515-539.

Barrett, K.E.J., Thomas, H.R., 1974. Kinetics and mechanism of dispersion polymerization, in: Barrett, K.E.J. (Ed.), Dispersion Polymerization in Organic Media, Wiley-Interscience, New York, p. 115.

Canelas, D.A., DeSimone, J.M., 1997. Polymerization in liquid and supercritical carbon dioxide. Advances in Polymer Science, 133, 103-140.

Charpentier, P.A., DeSimone, J.M., Roberts, G.W., 2000. Continuous precipitation polymerization of vinylidene fluoride in supercritical carbon dioxide: Modeling the rate of polymerization. Industrial & Engineering Chemistry Research, 39, 4588-4596.

Fortini, S., Lavanchy, F., Nising, P., Meyer, T., 2004. A new tool for the study of polymerization under supercritical conditions - Preliminary results. Macromolecular Symposia, 206, 79-92.

Guan, Z.B., Combes, J.R., Menceloglu, Y.Z., DeSimone, J.M., 1993. Homogeneous free-radical polymerizations in supercritical carbon dioxide: 2. Thermal decomposition of 2,2'-azobis(isobutyronitrile). Macromolecules, 26, 2663-2669.

Lepilleur, C., Beckman, E., 1997. Dispersion polymerization of methyl methacrylate in supercritical CO_2. Macromolecules, 30, 745-756.

Lewis, O.G., King, R.M., 1969. Free radical polymerization kinetics of immobilized chains, in: Gould, R.F. (Ed.), Addition and Condensation Polymerization Processes: a Symposium. American Chemical Society, Washington D. C., p. 25.

Liu, T., DeSimone, J.M., Roberts, G.W., 2005. Continuous precipitation polymerization of acrylic acid in supercritical carbon dioxide: polymerization rate and polymer molecular weight. Journal of Polymer Science Part A – Polymer Chemistry, in press.

McCarthy, S.J., Elbing, E.E., Wilson, I.R., Gilbert, R.G., Napper, D.H., Sangster, D.F.,1986. Seeded heterogeneous polymerization of acrylonitrile. Macromolecules, 19, 2440-2448.

Moore, D.E., Parts, A.G., 1960. Kinetics of the polymerization of acrylonitrile. Die Makromolekulare Chemie, 37, 108-118.

Nishida, R., Poehlein, G.W., Schork, F.J., 1995. Polymerization of acrylonitrile in continuous stirred tank reactors. Polymer Reaction Engineering, 3, 397-420.

Peebles, L.H.J. 1964. Copolymerizations involving acrylonitrile as a principal component, in: Ham, G.E. (Ed.), Copolymerization, Interscience Publishers, New York, p. 546.

Poersch-Panke, H.G., Avela, A., Reichert, K.H., 1993. Precipitation polymerization of acrylic acid – kinetics, viscosity and heat transfer. Die Angewandte Makromolekulare Chemie, 206, 157-169.

Rindfleisch, F., DiNoia, T.P., McHugh, M.A., 1996. Solubility of polymers and copolymers in supercritical CO_2. Journal of Physical Chemistry, 100, 15581-15587.

Saraf, M.K., Gerard, S., Wojcinski, L.M., Charpentier, P.A., DeSimone, J.M., Roberts, G.W., 2002. Continuous precipitation polymerization of vinylidene fluoride in supercritical

carbon dioxide: Formation of polymers with bimodal molecular weight distributions. Macromolecules, 35, 7976 – 7985.

Wako Product Information: Azo Polymerization Initiators. Wako Chemicals USA, Inc. Richmond, VA.

Xu, Q., Han, B., Yan, H., 2001. Effect of cosolvents on the precipitation polymerization of acrylic acid in supercritical carbon dioxide. Polymer, 42, 1369-1373.

Nomenclature:

a	parameter of the particle polymerization model, (s)
b	parameter of the particle polymerization model, (mol·s/L)
c	parameter of the particle polymerization model
d	parameter of the particle polymerization model, (mol/L)
f	initiation efficiency
$[I]_0$	initial initiator concentration, (mol/L)
$[I]_c$	initiator concentration in the continuous phase, (mol/L)
$[I]_p$	initiator concentration in the polymer phase, (mol/L)
$[I]_s$	initiator concentration on the polymer particle surface, (mol/L)
$[I]_{in}$	inlet initiator concentration, (mol/L)
$[I]_{out}$	outlet initiator concentration, (mol/L)
K_1	parameter of the surface polymerization model, $(mol/L)^{5/6}/s$
K_2	parameter of the surface polymerization model, $(mol/L)^{5/6}$
k_d	rate constant of the decomposition of initiator, (s^{-1})
k_p	rate constant of chain propagation, (L/(mol·s))
k_t	rate constant of chain termination, (L/(mol·s))
M_m	monomer molecular weight, (g/mol)
$\overline{M}_n$	number-average molecular weight (g/mol)
$\overline{M}_v$	viscosity-average molecular weight (g/mol)
$[M]_0$	initial monomer concentration, (mol/L)
$[M]_c$	monomer concentration in the continuous phase, (mol/L)

$[M]_p$ monomer concentration in the polymer phase, (mol/L)

$[M]_s$ monomer concentration on the particle surface, (mol/L)

$[M]_{in}$ inlet monomer concentration, (mol/L)

$[M]_{out}$ outlet monomer concentration, (mol/L)

N number of polymer particles in a unit volume, (m^{-3})

$[P\cdot]_c$ radical concentration in the continuous phase, (mol/L)

$[P\cdot]_p$ radical concentration in the polymer phase, (mol/L)

$[P\cdot]_s$ radical concentration on the particle surface, (mol/L)

R_i rate of initiation, (mol/(L·s))

R_I overall rate of initiation, (mol/(L·s))

R_p rate of polymerization, (mol/(L·s))

R_P overall rate of polymerization, (mol/(L·s))

$R_{P,max}$ the maximum rate of polymerization, (mol/(L·s))

R_t rate of termination, (mol/(L·s))

R_T overall rate of termination, (mol/(L·s))

S total particle surface area in a unit volume, (m^{-1})

t reaction time (s)

x monomer fractional conversion

x_m monomer fractional conversion corresponding to the maximum rate of polymerization

v_c volume fraction of the continuous phase

v_p volume fraction of the polymer phase

α monomer partition coefficient

β initiator partition coefficient

δ active thickness on the polymer particle surface (m)

ρ_p density of polymer phase (g/L)

τ residence time, (s)

υ kinetic chain length

ψ constant of proportionality between $\{\overline{M}_v / M_m\}$ and υ

Table 4-1. The parameters of the surface polymerization model

T(°C)	K_1 $(mol/L)^{5/6}/s$	ψK_2 $(mol/L)^{5/6}$	$\psi K_2/K_1$ (s)	f	k_d (s^{-1})	ψ
70	3.22×10^{-2}	228	7.08×10^{3}	0.83	2.04×10^{-4}	2.40
50	6.46×10^{-3}	246	3.81×10^{4}	0.83	1.44×10^{-5}	0.90

Table 4-2. The parameters of the particle polymerization model

T (°C)	a (s)	b (mol·s /L)	c/ψ	d/ψ (mol/L)	f	k_d (s^{-1})	$\psi = \frac{2ak_d}{c/\psi} f$	$\psi = \frac{2bk_d}{d/\psi} f$	$\alpha = 1 + \left(\frac{a}{b}\right)\frac{\rho_p}{M_m}$ *	$\alpha = 1 + \left(\frac{c}{d}\right)\frac{\rho_p}{M_m}$ *
70	8.45	23.0	0.0009	0.0034	0.83	2.04×10^{-4}	3.18	2.29	8.07	6.09
50	102	179	0.002	0.0027	0.83	1.44×10^{-5}	1.20	1.56	12.0	15.2

*- $M_m / \rho_p = 0.052 L/mol$ (Poersch-Panke et al. 1993).

Figures

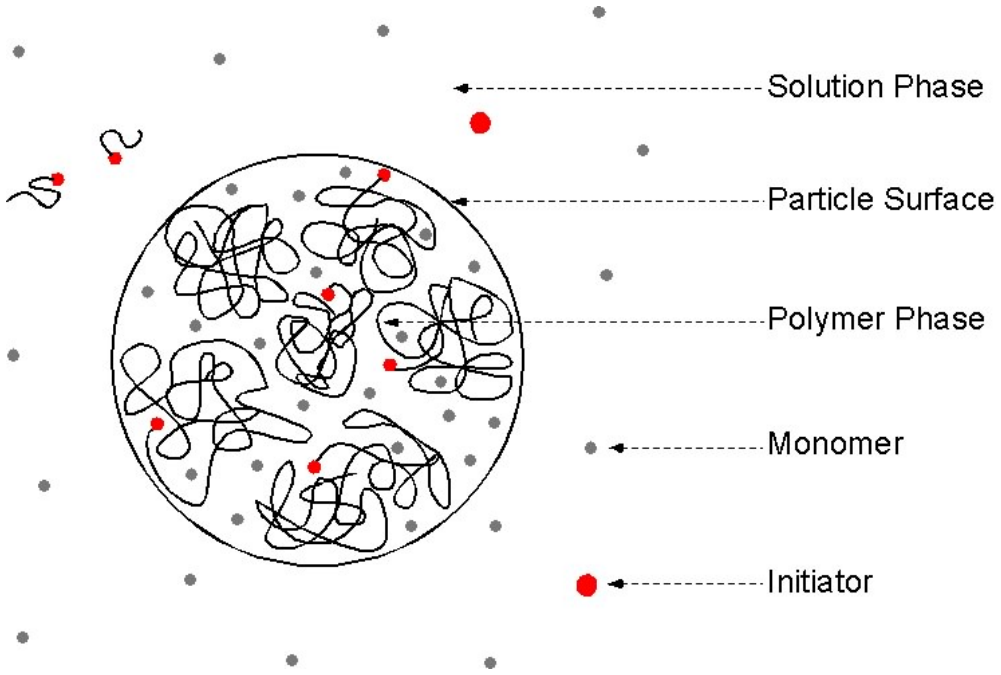

Figure 4-1. Three polymerization loci in a precipitation polymerization system

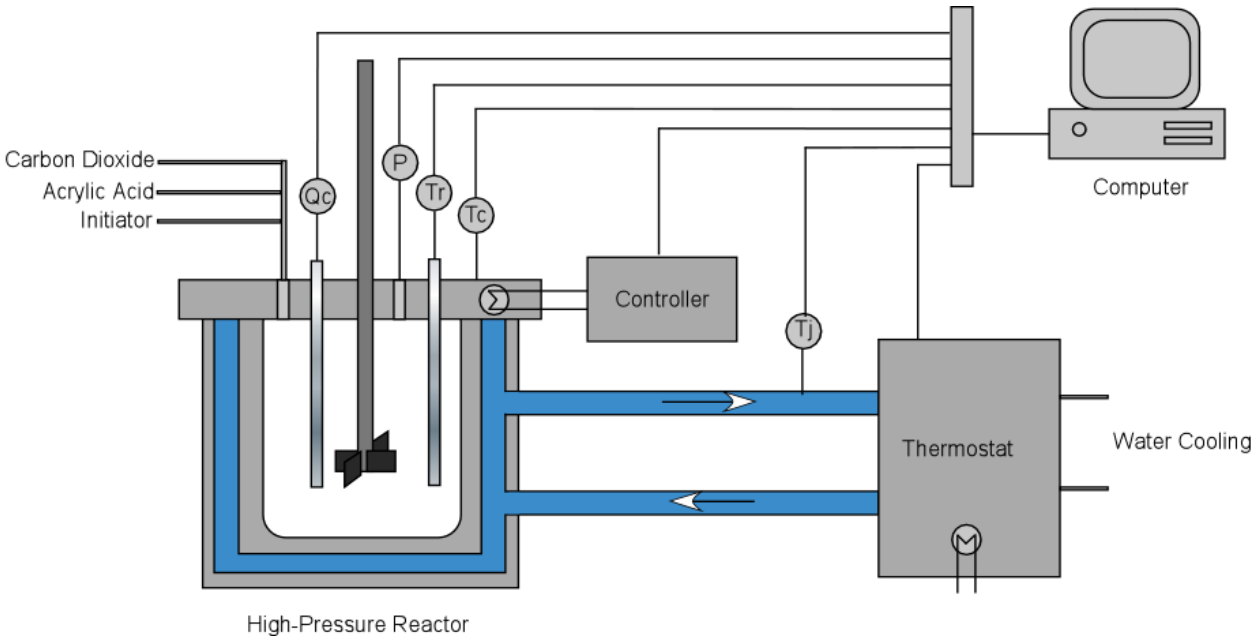

Figure 4-2. A schematic of the Mettler-Toledo RC1e reaction calorimeter

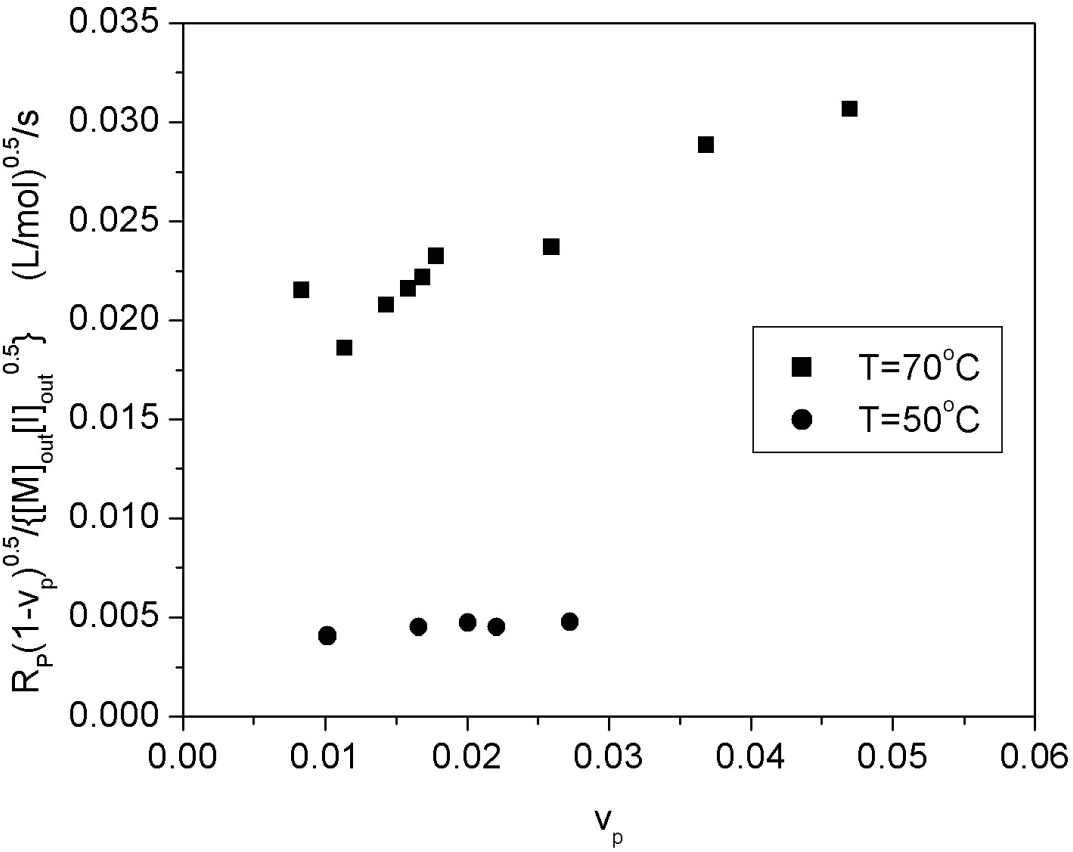

Figure 4-3. Comparison of the solution polymerization model with the experimental data from the CSTR (P = 207 bar)

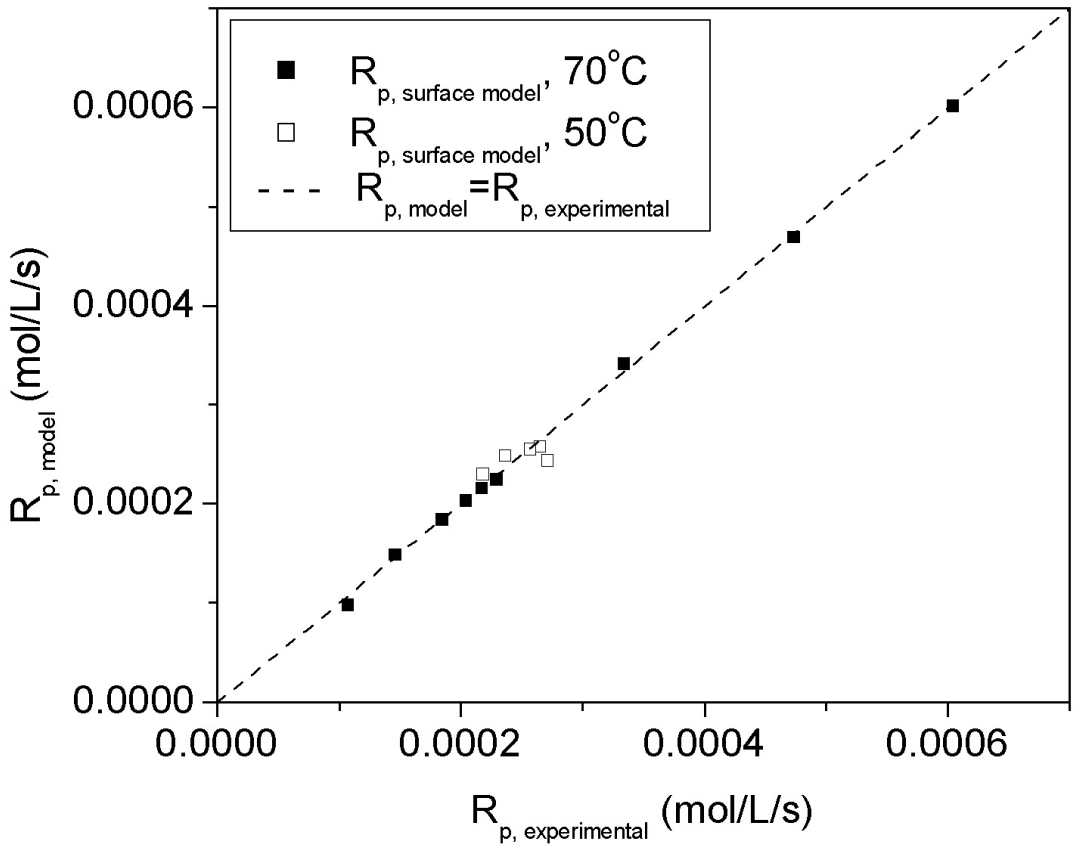

Figure 4-4. Comparison of the rate of polymerization calculated by the surface polymerization model with the experimental results ($K_1 = 3.22\times10^{-2}$ $(mol/L)^{5/6}/s$ at 70 °C and 207 bar; $K_1 = 6.46\times10^{-3}$ $(mol/L)^{5/6}/s$ at 50 °C and 207 bar)

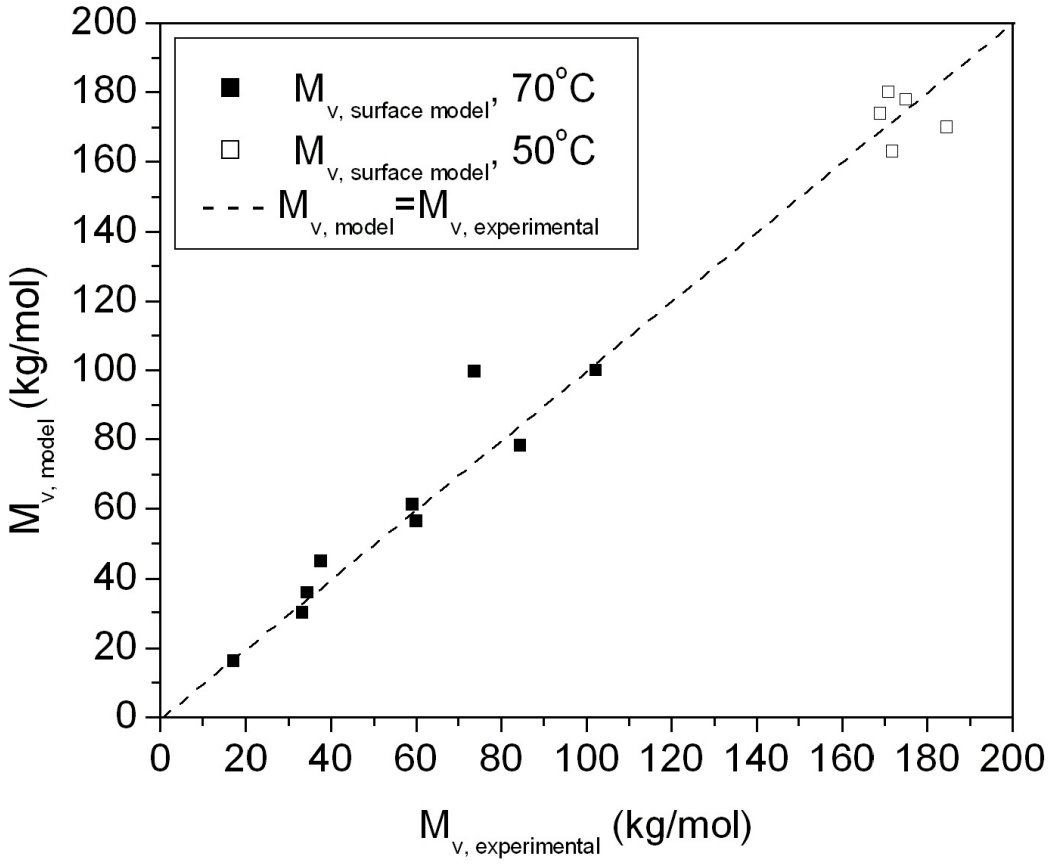

Figure 4-5. Comparison of the viscosity-average molecular weight calculated by the surface polymerization model with the experimental results (ψK_2 = 228 $(mol/L)^{5/6}$ at 70 °C and 207 bar; ψK_2 = 246$(mol/L)^{5/6}$ at 50 °C and 207 bar)

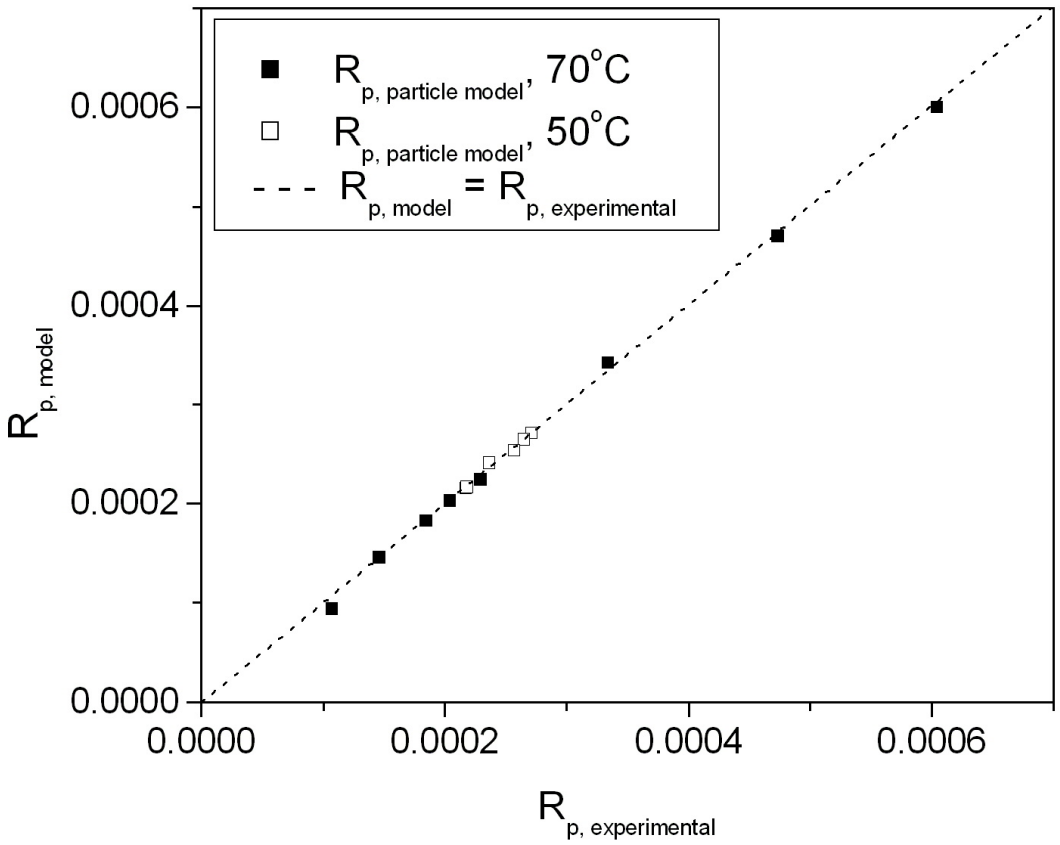

Figure 4-6. Comparison of the rate of polymerization calculated by the particle polymerization model with the experimental results (a = 8.45 s, b = 23.0 mol·s/L, at 70 °C and 207 bar; a = 102 s, b = 179 mol·s/L, at 50 °C and 207 bar)

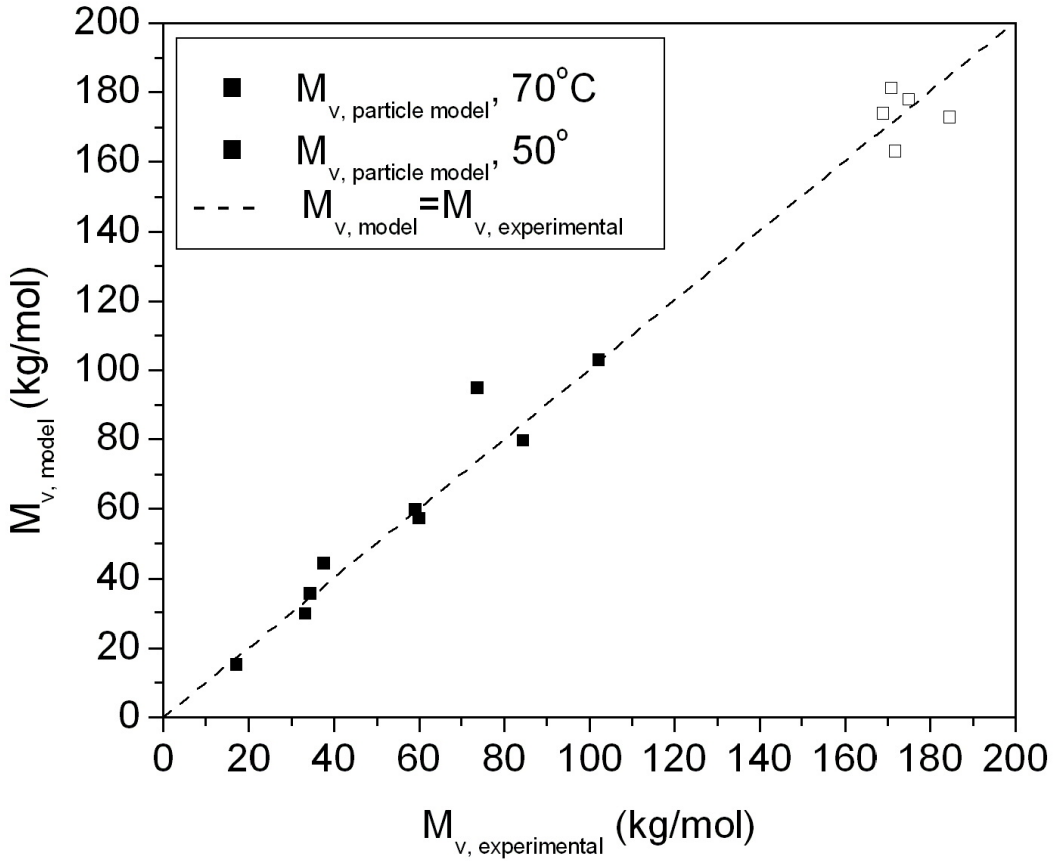

Figure 4-7. Comparison of the viscosity-average molecular weight calculated by the particle polymerization model with the experimental results (c/ψ = 0.0009, d/ψ = 0.0034 mol/L, at 70 °C and 207 bar; c/ψ = 0.002, d/ψ = 0.0027 mol/L, at 50 °C and 207 bar)

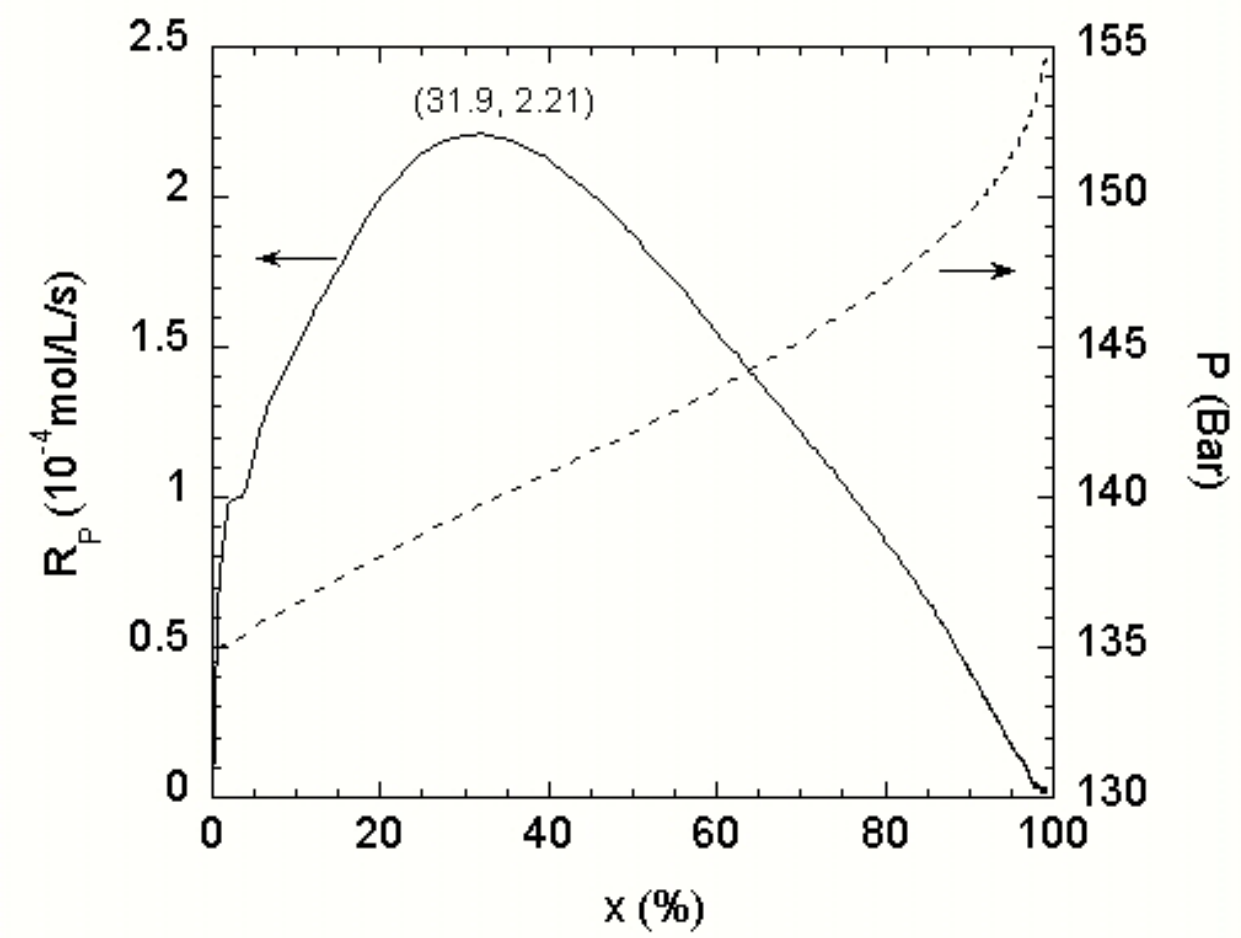

Figure 4-8. An isothermal polymerization experiment in the Mettler-Toledo RC1e reaction calorimeter (T = 50 °C, $[M]_0$ = 1.0 mol/L, $[I]_0$ = 0.002 mol/L, Reaction time = 8 hour)

4.7 Appendix: Model Developments

Equations A0-1 through A0-3 are true for a polymerization in CSTR, with the assumptions that 1) the reactor runs at its steady state, 2) no volume change due to the polymerization, and 3) the rate of initiator decomposition is only a function of temperature.

$$R_P = \frac{[M]_{in} x}{\tau} \quad \text{A0-1}$$

$$[I]_{out} = \frac{[I]_{in}}{k_d \tau + 1} \quad \text{A0-2}$$

$$[M]_{out} = [M]_{in}(1-x) \quad \text{A0-3}$$

Let v_c and v_p represent the volume fractions of the continuous phase and the polymer phase, respectively. Then,

$$v_c + v_p = 1 \quad \text{A0-4}$$

The volume fraction of the polymer phase can be calculated with Equation A0-5:

$$v_p = \frac{[M]_{in} x M_m}{\rho_p} \quad \text{A0-5}$$

For a batch polymerization, Equations A0-6 to A0-9 are true:

$$R_P = [M]_0 \frac{dx}{dt} \quad \text{A0-6}$$

$$[M] = [M]_0(1-x) \quad \text{A0-7}$$

$$[I] = [I]_0 \exp(-k_d t) \quad \text{A0-8}$$

$$v_p = \frac{[M]_0 x M_m}{\rho_p} \quad \text{A0-9}$$

4.7.1 Solution Polymerization Model

This model assumes that chain initiation, propagation, and termination all take place in the continuous phase, and there is no reaction in the polymer phase. Therefore,

$$R_i = 2fk_d[I]_c \qquad \text{A1-1}$$

$$R_p = k_p[P\cdot]_c[M]_c \qquad \text{A1-2}$$

$$R_t = 2k_t[P\cdot]_c^2 \qquad \text{A1-3}$$

Assuming the two phases keep concentration equilibrium:

$$\alpha = \frac{[M]_p}{[M]_c} \qquad \text{A1-4}$$

$$\beta = \frac{[I]_p}{[I]_c} \qquad \text{A1-5}$$

By using the steady state assumption of free radical polymerization, which says that the rate of initiation is equal to the rate of termination, the radical concentration in the continuous phase can be determined:

$$[P\cdot]_c = \left\{ \frac{fk_d}{k_t}[I]_c \right\}^{1/2} \qquad \text{A1-6}$$

The outlet monomer concentration is the average of the monomer concentration in the continuous phase and that in the polymer phase:

$$[M]_c v_c + [M]_p v_p = [M]_{out} \qquad \text{A1-7}$$

By combing Equations A0-4, A1-4, and A1-7, the monomer concentration in the continuous phase is given by:

$$[M]_c = \frac{[M]_{out}}{1+(\alpha-1)v_p} \qquad \text{A1-8}$$

Similarly,

$$[I]_c = \frac{[I]_{out}}{1+(\beta-1)v_p} \qquad \text{A1-9}$$

Since the model assumes no reaction in the polymer phase, there should no initiator in the polymer phase, i.e. β = 0. Equation A1-9 reduces to

$$[I]_c = \frac{[I]_{out}}{1-v_p} \qquad \text{A1-10}$$

Substitute A1-6, A1-8, and A1-10 into A1-2, the rate of polymerization in the continuous phase is obtained:

$$R_p = k_p\left(\frac{fk_d}{k_t}\right)^{\frac{1}{2}} \frac{[M]_{out}}{1+(\alpha-1)v_p}\left\{\frac{[I]_{out}}{1-v_p}\right\}^{\frac{1}{2}} \qquad \text{A1-11}$$

The overall rate of polymerization can be expressed as:

$$R_P = R_p v_c = k_p\left(\frac{fk_d}{k_t}\right)^{1/2}[M]_{out}[I]_{out}^{1/2}\frac{(1-v_p)^{1/2}}{1+(\alpha-1)v_p} \qquad \text{A1-12}$$

4.7.2 Surface Polymerization Model

This model assumes that the chain initiation takes place in the continuous phase, but the chain propagation and chain termination take place in a thin layer on the particle surface. In the continuous phase:

$$R_I = R_i v_c = 2fk_d[I]_c v_c \qquad \text{A2-1}$$

On the particle surface:

$$R_P = R_p(\delta S) = k_p[P\cdot]_s[M]_s(\delta S) \qquad \text{A2-2}$$

$$R_T = R_t(\delta S) = 2k_t[P\cdot]_s^2(\delta S) \qquad \text{A2-3}$$

where δ is the active thickness on the particle surface in which chain propagation and termination take place homogeneously.

It is also assumed that the monomer concentration and the initiator concentration are at their equilibriums:

$$\alpha = \frac{[M]_s}{[M]_c} \qquad \text{A2-4}$$

$$\beta = \frac{[I]_s}{[I]_c} \qquad \text{A2-5}$$

Let A2-1 equal A2-3, we get the free radical concentration on the particle surface:

$$[P\cdot]_s = \left(\frac{fk_d}{\delta k_t}\right)^{\frac{1}{2}} \left(\frac{v_c}{S}\right)^{\frac{1}{2}} [I]_c^{\frac{1}{2}} \qquad \text{A2-6}$$

Following the same procedure used by the solution polymerization model, the monomer concentration and the initiator concentration in the continuous phase are obtained:

$$[M]_c = \frac{[M]_{out}}{\alpha\delta S + v_c} \qquad \text{A2-7}$$

$$[I]_c = \frac{[I]_{out}}{\beta\delta S + v_c} \qquad \text{A2-8}$$

If $\delta S << v_p << v_c \approx 1$ the monomer concentration and initiator concentration in the continuous phase are close to the outlet monomer concentration and initiator concentration:

$$[M]_c \approx [M]_{out} \qquad \text{A2-9}$$

$$[I]_c \approx [I]_{out} \qquad \text{A2-10}$$

From A2-4 and A2-9, we get:

$$[M]_s = \alpha[M]_{out} \qquad \text{A2-11}$$

Substitute Equation A2-10 into Equation A2-6 and let v_c equal 1, we obtain

$$[P\cdot]_s = \left(\frac{fk_d}{\delta k_t}\right)^{\frac{1}{2}}\left(\frac{1}{S}\right)^{\frac{1}{2}}[I]_{out}^{\frac{1}{2}} \qquad \text{A2-12}$$

Substitute Equations A2-11 and A2-12 into A2-2, we get

$$R_P = k_p\left(\frac{fk_d}{k_t}\right)^{\frac{1}{2}}\alpha\delta^{\frac{1}{2}}S^{\frac{1}{2}}[I]_{out}^{\frac{1}{2}}[M]_{out} \qquad \text{A2-13}$$

Assume there are N particles in a unit volume, then

$$S = N\cdot 4\pi r^2 = 4.836N^{\frac{1}{3}}v_P^{\frac{2}{3}} \qquad \text{A2-14}$$

Substitute the above Equation into A2-13, we get

$$R_P = 2.20N^{\frac{1}{6}}k_p\left(\frac{fk_d}{k_t}\right)^{\frac{1}{2}}\alpha\delta^{\frac{1}{2}}[I]_{out}^{\frac{1}{2}}[M]_{out}v_p^{\frac{1}{3}} \qquad \text{A2-15}$$

Substitute A0-2, A0-3, and A0-5 into the above equation, we obtain

$$R_P = K_1[M]_{in}^{\frac{4}{3}}(1-x)x^{\frac{1}{3}}\left(\frac{[I]_{in}}{k_d\tau+1}\right)^{\frac{1}{2}} \qquad \text{A2-16}$$

where

$$K_1 = 2.2N^{\frac{1}{6}}k_p\left(\frac{fk_d}{k_t}\right)^{\frac{1}{2}}\delta^{\frac{1}{2}}\alpha\left(\frac{M_A}{\rho_p}\right) \qquad \text{A2-17}$$

If the residence time is very short in comparison with the half-time of the initiator, we can assume the initiator concentration is constant. Then Equation A2-16 will become

$$R_P = K_1[M]_{in}^{\frac{4}{3}}(1-x)x^{\frac{1}{3}}[I]_{in}^{\frac{1}{2}} \qquad \text{A2-18}$$

Let $dR_P/dx = 0$, we will get x_m = 0.25, which indicates at constant inlet monomer and initiator concentration the rate of polymerization reaches its maximum ($R_{p,max}$) when the monomer conversion gets to 25%. Since initiator concentration decrease as residence time

increases, $R_{p,max}$ will appear when the monomer conversion is less than, but very close to, 25%.

The polymerization kinetic chain length is defined as

$$\upsilon = \frac{R_P}{R_I} \tag{A2-19}$$

Assume v_c=1 and substitute A2-10 into A2-1,

$$R_I = 2fk_d[I]_{out} \tag{A2-20}$$

Substitute A2-16 and A2-20 into A2-19,

$$\upsilon = \frac{K_1}{2fk_d}[M]_{in}^{\frac{4}{3}}(1-x)x^{\frac{1}{3}}\left(\frac{[I]_{in}}{k_d\tau+1}\right)^{-\frac{1}{2}} \tag{A2-21}$$

Let

$$K_2 = \frac{K_1}{2fk_d} \tag{A2-22}$$

We have

$$\upsilon = K_2[M]_{in}^{\frac{4}{3}}(1-x)x^{\frac{1}{3}}\left(\frac{[I]_{in}}{k_d\tau+1}\right)^{-\frac{1}{2}} \tag{A2-23}$$

For a batch process, following the same procedure, we have

$$R_P = K_1[M]_0^{\frac{4}{3}}(1-x)x^{\frac{1}{3}}[I]_0^{\frac{1}{2}}\exp\left(-\frac{k_dt}{2}\right) \tag{A2-24}$$

$$\upsilon = K_2[M]_0^{\frac{4}{3}}(1-x)x^{\frac{1}{3}}[I]_0^{-\frac{1}{2}}\exp\left(\frac{k_dt}{2}\right) \tag{A2-25}$$

Substitute A2-24 into A0-6, we get

$$\frac{dx}{dt} = K_1[M]_0^{\frac{1}{3}}(1-x)x^{\frac{1}{3}}[I]_0^{\frac{1}{2}}\exp\left(-\frac{k_dt}{2}\right) \tag{A2-26}$$

This equation can be solved to get a function describing the increase of monomer conversion with reaction time.

Equation A2-24 predicts the existence of a maximum rate of polymerization, $R_{p,max}$. If the reaction time before $R_{p,max}$ is much shorter than the half-life of the initiator, Equation A2-24 reduces to

$$R_P = K_1[M]_0^{\frac{4}{3}}(1-x)x^{\frac{1}{3}}[I]_0^{\frac{1}{2}} \qquad \text{A2-27}$$

Let $dR_P / dx = 0$, we get $x_m = 0.25$, which indicates the rate of batch polymerization reaches its maximum when the monomer conversion gets to 25%. Since initiator concentration decreases as monomer conversion increases, $R_{p,max}$ will appear when monomer conversion is less than, but very close to, 25%.

4.7.3 Particle Polymerization Model

This model assumes the chain initiation takes place only in the continuous phase while the chain propagation and chain termination take place homogeneously throughout the polymer particles.

In the continuous phase:

$$R_I = 2fk_d[I]_c v_c \qquad \text{A3-1}$$

In the polymer phase:

$$R_P = k_p[P\cdot]_p[M]_p v_p \qquad \text{A3-2}$$

$$R_T = 2k_t[P\cdot]_p^2 v_p \qquad \text{A3-3}$$

Assume the two phases keep concentration equilibriums,

$$\alpha = \frac{[M]_p}{[M]_c} \qquad \text{A3-4}$$

$$\beta = \frac{[I]_p}{[I]_c} \qquad \text{A3-5}$$

Follow the same procedure of the solution polymerization model, we get

$$[M]_c = \frac{[M]_{out}}{1+(\alpha-1)v_p} \qquad \text{A3-6}$$

$$[I]_c = \frac{[I]_{out}}{1+(\beta-1)v_p} \qquad \text{A3-7}$$

Substitute A3-4 into A3-6,

$$[M]_p = \frac{\alpha[M]_{out}}{1+(\alpha-1)v_p} \qquad \text{A3-8}$$

We can also assume that the initiator absorbed by the polymer phase is negligible. Then,

$$[I]_c = \frac{[I]_{out}}{v_c} \qquad \text{A3-9}$$

Substitute A3-9 into A3-1, we get

$$R_I = 2fk_d[I]_{out} \qquad \text{A3-10}$$

Let A3-10 equal A3-3, we get the radical concentration in the polymer phase.

$$[P\cdot] = \left(\frac{fk_d}{k_t}\right)^{\frac{1}{2}}\left(\frac{[I]_{out}}{v_p}\right)^{\frac{1}{2}} \qquad \text{A3-11}$$

Substitute A3-8 and A3-11 into A3-2, we get

$$R_P = k_p\left(\frac{fk_d}{k_t}\right)^{\frac{1}{2}}\frac{\alpha[M]_{out}}{1+(\alpha-1)v_p}[I]_{out}^{\frac{1}{2}}v_p^{\frac{1}{2}} \qquad \text{A3-12}$$

Substitute A0-2, A0-3, and A0-5 into A3-12,

$$R_P = \frac{[M]_{in}^{\frac{3}{2}}(1-x)x^{\frac{1}{2}}}{a[M]_{in}x+b}\left(\frac{[I]_{in}}{k_d\tau+1}\right)^{\frac{1}{2}} \qquad \text{A3-13}$$

where

$$a = \frac{1}{k_p}\left(\frac{k_t}{fk_d}\right)^{\frac{1}{2}}\left(\frac{M_m}{\rho_p}\right)^{\frac{1}{2}}\left(\frac{\alpha-1}{\alpha}\right) \quad \text{A3-14}$$

$$b = \frac{1}{k_p}\left(\frac{k_t}{fk_d}\right)^{\frac{1}{2}}\left(\frac{\rho_p}{M_m}\right)^{\frac{1}{2}}\left(\frac{1}{\alpha}\right) \quad \text{A3-15}$$

$$\frac{a}{b} = \frac{M_m}{\rho_p}(\alpha-1) \quad \text{A3-16}$$

We can get the kinetic chain length by dividing A3-13 with A3-10

$$\upsilon = \frac{[M]_{in}^{\frac{3}{2}}(1-x)x^{\frac{1}{2}}}{c[M]_{in}x+d}\left(\frac{[I]_{in}}{k_d\tau+1}\right)^{-\frac{1}{2}} \quad \text{A3-17}$$

where

$$c = 2fk_d a \quad \text{A3-18}$$

$$d = 2fk_d b \quad \text{A3-19}$$

If the initiator half-life is much longer than the residence time, we can assume the initiator concentration is constant in the reaction. Then Equation A3-13 becomes

$$R_P = \frac{[M]_{in}^{\frac{3}{2}}(1-x)x^{\frac{1}{2}}}{a[M]_{in}x+b}[I]_{in}^{\frac{1}{2}} \quad \text{A3-20}$$

Let $dR_P / dx = 0$, we get:

$$\frac{1-3x_m}{x_m^2+x_m} = \frac{a}{b}[M]_{in} \quad \text{A3-21}$$

Therefore, the rate of polymerization can reach its maximum at a certain monomer conversion, x_m, which is a function of the inlet monomer concentration and the ratio of a/b.

For a batch polymerization, following the same procedure, we get:

$$R_P = \frac{[M]_0^{\frac{3}{2}}(1-x)x^{\frac{1}{2}}}{a[M]_0 x + b}[I]_0^{\frac{1}{2}} \exp\left(-\frac{k_d t}{2}\right) \quad \text{A3-22}$$

$$\upsilon = \frac{[M]_0^{\frac{3}{2}}(1-x)x^{\frac{1}{2}}}{c[M]_0 x + d}[I]_0^{-\frac{1}{2}} \exp\left(\frac{k_d t}{2}\right) \quad \text{A3-23}$$

$$\frac{dx}{dt} = \frac{[M]_0^{\frac{1}{2}}(1-x)x^{\frac{1}{2}}}{a[M]_0 x + b}[I]_0^{\frac{1}{2}} \exp\left(-\frac{k_d t}{2}\right) \quad \text{A3-24}$$

Equation A3-24 can be solved to get a function describing the increase of monomer conversion with reaction time. If the reaction time before the rate of polymerization reaches its maximum ($R_{P,max}$) is much shorter than the half-life of the initiator, the initiator concentration will not decrease much during that period of time. In this case, Equation 3-22 reduces to

$$R_P = \frac{[M]_0^{\frac{3}{2}}(1-x)x^{\frac{1}{2}}}{a[M]_0 x + b}[I]_0^{\frac{1}{2}} \quad \text{A-3-25}$$

Let $dR_P / dx = 0$, we get:

$$\frac{1-3x_m}{x_m^2 + x_m} = \frac{a}{b}[M]_0 \quad \text{A3-26}$$

Therefore, the rate of polymerization can reach $R_{P,max}$ at a certain monomer conversion, x_m, which is a function of the initial monomer concentration and the ratio of a/b. From Equation A3-16 we know a/b is a function of monomer partition coefficient (α). If we know α, we can calculate x_m; or if we get x_m, for example, using reaction calorimeter, we can determine α:

$$\alpha = 1 + \frac{a}{b}\Big/\frac{M_m}{\rho_P} \quad \text{A3-27}$$

CHAPTER 5

PARTICLE FORMATION IN CONTINUOUS POLYMERIZATION OF ACRYLIC ACID IN SUPERCRITICAL CARBON DIOXIDE

Tao Liu[1], Joseph M. DeSimone[1, 2], and George W. Roberts[1, *]

[1]Department of Chemical Engineering, Campus Box 7905, North Carolina State University, Raleigh, North Carolina 27695-7905

[2]Department of Chemistry, CB 3290, Venable and Kenan Laboratories, University of North Carolina at Chapel Hill, North Carolina 27599-3290

Abstract

The continuous precipitation polymerization of acrylic acid in supercritical carbon dioxide ($scCO_2$) was carried out in a continuous stirred tank reactor (CSTR) using 2, 2'-azobis (2, 4-dimethyl-valeronitrile) as the free-radical initiator. The product polymer was white, dry, fine powder. Scanning electron micrographs showed that at different conditions three types of particles were obtained: coagulum of primary particles of about 100 nanometers in size, irregular particles of 5-20 micrometers, and spherical particles of 10 – 100 micrometers. It is believed that the glass transition temperature of polymer in $scCO_2$, T_g, was much lower than the glass transition temperature of the pure polymer, T_{g0}, due to the plasticization effect of $scCO_2$. It is speculated that the polymer coagulum was produced when the polymerization temperature, T_P, was below T_g, the irregular particles were produced when T_P was in the glass transition region, and the spherical particles were produced when T_P was above T_g. The CO_2 absorption into poly(acrylic acid) was measured with a quartz crystal microbalance. The T_g depression by $scCO_2$ was calculated with the Chow's equation. The calculated results lent strong support to the proposed particle formation mechanism.

Keywords

acrylic acid, continuous polymerization, supercritical CO_2, morphology, plasticization, glass transition temperature.

5.1 Introduction

Acrylic acid polymers are widely used as dispersants, thickeners, flocculants and superabsorbent polymers (SAP) [1]. They commonly are prepared by aqueous solution polymerization, although heterogeneous polymerizations in organic media also are used [1]. As people's interest of using supercritical carbon dioxide ($scCO_2$) as polymerization media grows, precipitation polymerization of acrylic acid in supercritical carbon dioxide ($scCO_2$) is getting more attention [2].

Precipitation polymerization of acrylic acid in carbon dioxide (CO_2) was first reported in a French patent in 1968 [3]. The U. S. version of this patent was granted in 1970 [4]. The precipitation polymerization of several vinyl compounds, including acrylic acid, in liquid and supercritical CO_2, was demonstrated in these patents. In 1986, a Canadian patent application described the synthesis of water-soluble poly(acrylic acid) (PAA) in $scCO_2$ [5]. In 1987, the synthesis in $scCO_2$ of thickeners based on cross-linked, water-soluble PAA was reported in a U.S. patent application [6]. A similar study was also reported in a European patent [7] filed in 1988. More recently, DeSimone and coworkers [8] studied acrylic acid polymerization in $scCO_2$, and used ethyl mercaptan as a chain transfer agent to control the polymer molecular weight. Finally, Xu et al. [9, 10] explored the effect of cosolvents on the polymerization of acrylic acid in $scCO_2$.

The polymers prepared in the previous studies were white, fluffy, fine powders. The polymer particles were agglomerates of primary particles of about 100nm in size [8-10]. In this paper, we report the production of PAA particles with completely different morphologies, by precipitation polymerization of acrylic acid in $scCO_2$ using a continuous stirred-tank reactor (CSTR). For the first time PAA spheres of 10 to 100 μm were prepared.

The major factors that affect the polymer morphology are discussed, and a particle formation mechanism is proposed.

5.2 Experimental

Continuous Polymerization. The continuous precipitation polymerization of acrylic acid in $scCO_2$ was carried out in a CSTR. The reactor is an 800 ml, high-pressure autoclave with a magnetically driven agitator. A jacket through which a heating/cooling fluid is circulated is used to control the reaction temperature. Three high-pressure filters are used to collect polymer particles. A heated control valve functions as a backpressure regulator to keep the system pressure at the set point. 2,2'–azobis(2,4-dimethyl-valeronitrile) (V-65B, high purity, Wako Chemicals) was used as the initiator. The reactor temperature was between 50 and 90 °C, the pressure was 20.7MPa, and the average residence time was between 12 and 40 minutes. Detailed descriptions of the polymerization apparatus and polymerization procedure are available elsewhere [11].

The viscosity average molecular weight of polymer ($\overline{M}_v$) was measured by an automatic viscometer (Rheotek^{TM} TCB-7) [11]. The polymer particle morphology was determined by scanning electron micrography (SEM, JEOL 6400F Field Emission). The polymer glass transition temperature (T_g) was measured by differential scanning calorimetry (DSC, TA Q-100).

Quartz Crystal Microbalance (QCM) Measurement: QCM has been a powerful tool for the study of CO_2 absorption into polymers [12-17], due to its good accuracy and easy operation. The QCM is composed of a thin quartz crystal with metal electrodes on both sides. When an alternating electric field is applied between the electrodes, the crystal vibrates at its

resonant frequency, due to the piezoelectric effect. For a QCM coated with a thin polymer film, at a certain temperature, the frequency of the quartz crystal changes with: (1) mass change on the crystal surface (Δm), (2) pressure (P), and (3) density (ρ_f) and viscosity (μ_f) of the surrounding fluid. The resonant frequency difference (ΔF) between the initial frequency (F_0) and that measured at a certain pressure (F) can be calculated by the following equation [12, 16]:

$$\Delta F = \Delta F_m + \Delta F_P + \Delta F_f \tag{5-1}$$

In this equation, the three terms on the right hand side represent the effects of mass (ΔF_m), pressure (ΔF_P), and density and viscosity of the fluid (ΔF_f). The theoretical expressions for these terms are listed below:

$$\Delta F_m = -C_m \Delta m \tag{5-2}$$

$$\Delta F_P = C_P P \tag{5-3}$$

$$\Delta F_f = -\left(\frac{C_m}{2}\right)\left(\frac{\rho_f \mu_f}{\pi F_0}\right)^{1/2} \tag{5-4}$$

where

$$C_m = \frac{2F_0^2}{\left(\mu_q \rho_q\right)^{1/2}} \tag{5-5}$$

$$C_P = \alpha F_0 \tag{5-6}$$

In these equations, C_m and C_P are the mass and pressure sensitivity of QCM, respectively; μ_q is the shear modulus of quartz, ρ_q is the density of the crystal, and α is the pressure proportionality constant. According to Park et al.[15], α can be calculated by the following equation:

$$\alpha(MPa^{-1}) = 1.095 \times 10^{-5} - 2 \times 10^{-8} T(^{\circ}C) \quad (5\text{-}7)$$

The QCM apparatus used in this research is composed of a quartz crystal mounted in a high-pressure cell, a temperature-controlled water-bath, an oscillator, and a data-acquisition system. The cell can stand pressure up to about 50 MPa. The temperature can be controlled in a range from room temperature to 90 °C, with accuracy of ±0.1 °C. The oscillator (PLO-10, Maxtek Inc.) can be operated in the 3-6 MHz frequency range. The quartz crystal used in this work is 5MHz AT-cut Si with gold electrodes (model # 131223, International Crystal Manufacturing). For this crystal, $\mu_q = 2.947 \times 10^{11}$ g cm^{-1} s^{-2}, $\rho_q = 2.648$ g cm^{-3}.

A 1.0% PAA solution was prepared by dissolving 0.15 g polymer ($\overline{M}_v$=175 kg/mol, Table 5-1) in 15 g methanol (99.9%, HPLC grade, Fisher). Prior to coating a polymer film on the crystal, the blank crystal was mounted in the QCM apparatus to determine the fundamental frequency in vacuum at the experimental temperature. After that, the crystal was dipped vertically into the PAA solution for several minutes. Then it was slowly withdrawn from the solution. The coated crystal was mounted in the pressure cell and dried at the experimental temperature under vacuum until the frequency became constant. This indicated the complete removal of the solvent. The stabilized frequency was used to calculate the polymer mass deposited on the crystal.

After measuring the mass of the coated polymer, CO_2 (99.99%, National Specialty Gases) was added into the high-pressure cell to increase the pressure to the desired value. The sorption equilibrium was achieved in a short period of time. After one hour, the pressure was increased to another desired value by introducing more CO_2 into the cell, and another sorption equilibrium was obtained. At the completion of an isotherm, the CO_2 was released

and vacuum was utilized to degas the film, allowing the measurement at a different temperature.

5.3 Results and Discussion

Some typical polymerization experiments are listed in Table 5-1. All product polymers were white, dry powder. The corresponding SEM pictures can be found in Figures 5-1 to 5-4. The first experiment was carried out at 50 °C. Figures 5-1 shows the polymer particles were agglomerates of primary particles of about 100nm in size. The second experiment was carried out at 70 °C. Figure 5-2 shows the polymer particles were irregular, with diameters in the range of 5 – 20 micrometers. The third experiment was also carried out at 70 °C, but with lower inlet monomer concentration ($[M]_{in}$) and higher inlet initiator concentration ($[I]_{in}$). Accordingly, a much lower molecular weight was produced. Figure 5-3 shows the polymer particles produced by this experiment were spheres of 10 – 100 micrometers in diameter. The fourth experiment was carried out at 90 °C. The lowest molecular weight was obtained due to the highest temperature, the highest initiator concentration, and the lowest monomer concentration. Figure 5-4 shows the polymer particles were spheres of 10-100 micrometers in diameter, similar to those of the third experiment.

The bulk densities of the polymers are different. Among the four samples listed in Table 5-1, the spherical particles have the highest density, while the coagulum has the lowest density. Also, the flowabilities of the polymer powders were different. The spherical particles have the highest flowability, while the polymer agglomerates have the lowest flowability. Finally, the textures of these polymers are different too. If one twists the polymer

agglomerates with his fingers, he cannot feel the existence of any polymer particles, due to the small size of the primary particles. However, when he tried with the other three polymers the existence of hard particles cam be clearly felt.

The polymer morphologies reported in the literature, such as those by DeSimone et al. [8] and Xu et al. [9, 10], are all agglomerates, similar to the one shown in Figure 5-1. The present work is the first time that much larger PAA particles are prepared by precipitation polymerization of acrylic acid in $scCO_2$.

It is speculated that the polymerization temperature and the agitation intensity are the major factors that affect the polymer morphology. Both DeSimone et al. [8]and Xu et al. [9, 10] carried out their polymerizations in batch reactors at 62 °C. The batch reactors are small view cells that use magnetic stir bar for agitation. In contrast, the CSTR used in this work is an 800ml high-pressure autoclave that has a magnetically driven high-speed agitator. The dimensions of the CSTR and the agitator are shown in Figure 5-5. The agitator has three downward propellers installed along its shaft. It is operated at 1800rpm. It is believed that this agitator can disperse the polymer particles much more efficiently than the stir bar used by view cell.

Figure 5-6 shows a hypothesized particle formation mechanism. The polymerization temperature in this work is from 50 to 90 °C. The literature value of the glass transition temperature of PAA is between 106 and 126 °C, depending on the concentration of residue solvent in polymer [18]. $ScCO_2$ has strong a plasticization effect on polymers [12, 13, 19-39]. It can greatly depress the polymer glass transition temperature. In the continuous precipitation polymerization of acrylic acid in $scCO_2$, polymer particles formed and precipitated from the CO_2 phase. They absorbed certain amounts of CO_2. Therefore, the glass

transition temperature of polymers in the CSTR, T_g, should be lower than that of the pure polymer, T_{g0}. When the polymerization temperature, T_P, was below T_g, the polymer was in its glassy state. Solid primary particles formed and precipitated from the CO_2 phase. They could agglomerate with each other to form a loosely combined coagulum. When T_P was above T_g, the polymer was in its fluid state, and could be dispersed into polymer spheres by high-speed agitation. When T_P was in the polymer glass transition region, the chain flexibility was higher than that of the polymer glass, but lower than that of the polymer fluid. Then irregular particles were formed. After the product stream left the reactor, it was cooled down to approximately room temperature, which is much lower than T_g. Therefore polymer particles could keep their original shape.

Both irregular particles and spherical particles could be formed at 70 °C. This probably is due to increased T_g with a higher polymer molecular weight. Under the same polymerization temperature and pressure (70 °C, 20.7 MPa), the low molecular weight polymer had lower T_g. 70 °C might be higher than its T_g. Therefore, polymer spheres were obtained. The high molecular weight polymer had higher T_g. 70 °C might be in its glass transition region. Accordingly, irregular particles were produced.

If the proposed particle formation mechanism is true, the T_g of PAA under the polymerization conditions (50 – 90 °C, 20.7 MPa) should be between 50 and 90 °C, and very close to 70 °C.

CO_2 absorption into PAA was measured by QCM. The isotherms at 50 °C, 70 °C and 90 °C are shown in Figure 5-7. The CO_2 solubility in PAA is much lower than that in poly(methyl methacrylate) (PMMA) or polystyrene (PS) [14].

Table 5-2 lists the solubility parameters of PMMA, PS, and PAA calculated by group contribution methods on the basis of the group constants of Small [40]. In comparison with PMMA and PS, PAA is a much more polar material. Figure 5-8 shows the solubility parameter of CO_2 calculated by an empirical equation proposed by Giddings et al. in 1968 [41]:

$$\delta = 1.25 P_c^{1/2} \frac{\rho_r}{\rho_{r,l}} \tag{5-8}$$

where δ is the solubility parameter in cal/cm^3, P_c is the critical pressure in atmospheres, ρ_r is the reduced density, and $\rho_{r,l}$, the reduced density of liquids, which is normally about 2.66. The equation gives satisfactory estimation of the CO_2 solubility parameter in comparison with other methods [42, 43]. The solubility parameter of $scCO_2$ is closer to the solubility parameters of PMMA and PS than to that of PAA. This explains the lower CO_2 absorption into PAA.

Chow [44] has proposed a correlation to calculate the T_g depression due to absorbed diluent:

$$\ln\left(\frac{T_g}{T_{g0}}\right) = \beta\left[\theta \ln\theta + (1-\theta)\ln(1-\theta)\right] \tag{5-9}$$

where

$$\theta = \frac{M_p}{zM_d}\frac{\omega}{1-\omega} \tag{5-10}$$

$$\beta = \frac{zR}{M_p \Delta C_p} \tag{5-11}$$

In the above equations, T_{g0} is the glass transition temperature of the pure polymer, M_p is the molar mass of the polymer repeat unit, M_d is the molar mass of the diluent, R is the gas

constant, ω is the diluent solubility in the polymer, ΔC_p is the heat capacity change associated with the glass transition of the pure polymer, and z is the lattice coordination number. For polymers with small repeat units, such as PS and PMMA, z = 1 gives a good fit of experimental results, whereas for polymers with larger repeat units, such as polycarbonate and poly(ethylene terephthalate), z = 2 works better [19, 20, 24, 25, 29].

For the PAA prepared in the first experiment in Table 5-1, DSC measurement shows that, T_{g0} = 120.90 °C, ΔC_p = 0.40±0.10 J/(g °C). The T_g depression due to the plasticization effect of $scCO_2$ was calculated by the Chow's equation, and it is shown in Figure 5-9. It shows that $scCO_2$ can dramatically decrease the T_g of PAA.

On the basis of QCM measurement and the Chow's equation, we determined the T_g of the product polymer under the polymerization conditions. Table 5-3 compared the polymerization temperature (T_P) with the calculated T_g. As the particle formation mechanism predicted, the calculated T_g was between 50 °C and 90 °C and It is close to 70 °C. At 50 °C and 20.7 MPa, T_P is about 12 °C lower than T_g. This coincides with the production of polymer agglomerates. At 90 °C under 20.7 MPa, T_P is about 18 °C higher than T_g. This coincides with the production of polymer spheres. Finally, at 70 °C and 20.7 MPa, T_P is close to T_g. It coincides with the production of both spherical particles, when the polymer molecular weight was low, and irregular particles, when the polymer molecular weight was high. These results lend strong support to the proposed particle formation mechanism.

5.4 Conclusions

The continuous precipitation polymerization of acrylic acid in supercritical carbon dioxide was carried out in a CSTR. Three types of polymer particles were prepared:

agglomerates of primary particle of 100 nanometers in size, irregular particles of 5 to 20 micrometers, and spherical particles of 10 to 100 micrometers. It was believed that the polymer coagulum was produced when the polymerization temperature, T_P, was below T_g, the irregular particles were prepared when T_P was in the glass transition region, and the spherical particles were produced when T_P was above T_g. The CO_2 absorption into PAA was measured by QCM. The T_g depression due to CO_2 absorption was calculated by the Chow's equation. The calculated results lent strong support to the proposed particle formation mechanism.

5.5 Acknowledgments

This research was supported by Kenan Center for the Utilization of CO_2 in Manufacturing at North Carolina State University and by the STC Program of the National Science Foundation under Agreement No. CHE-9876674.

5.6 References

1. Swift, G. in Encyclopedia of Polymer Science and Technology, 2nd ed.; Bailey, J.; Kroschwitz, J. I. Ed.; Wiley-Interscience: New York, 2003; vol.1, pp 79-96.
2. Canelas, D. A.; DeSimone, J. M. Advances in Polymer Science 1997, 133, 103-140.
3. Fukui, K.; Fujii, K.; Kagiya, T.; Toriuchi, Y.; Yokota, H. (Sumitomo Chemical Company, Ltd. and Sumitomo Atomic Energy Industries, Ltd.). French Patent 1,524,533, April 1, 1968.

4. Fukui, K.; Fujii, K.; Kagiya, T.; Toriuchi, Y.; Yokota, H. (Sumitomo Chemical Company, Ltd. and Sumitomo Atomic Energy Industries, Ltd.). U. S. Patent 3,522,228, July 28, 1970.

5. Sertage, W. G. J.; Davis, P.; Schenck, H. U.; Denzinger, W.; Hartmann, H. (BASF Corporation). Canadian Patent 1,274,942, October 2, 1990.

6. Hartmann, H.; Denzinger, W. (BASF Corporation). U. S. Patent 4,748,220, May 31, 1988.

7. Herbert, M. W.; Huvard, G. S. (B.F. Goodrich Company). European Patent 0,301,532 (A2), February 1, 1989.

8. Romack, T. J.; Maury, E. E.; DeSimone, J. M. Macromolecules 1995, 28, 912-915.

9. Xu, Q.; Han, B.; Yan, H. Polymer 2001, 42, 1369-1373.

10. Xu, Q.; Han, B.; Yan, H. Journal of Applied Polymer Science 2003, 88, 1876-1880.

11. Liu, T.; DeSimone, J. M.; Roberts, G. W. Journal of Polymer Science Part A: Polymer Chemistry (in press)

12. Miura, K.; Otake, K.; Kurosawa, S.; Sako, T.; Sugeta, T.; Nakane, T.; Sato, M.; Tsuji, T.; Hiaki, T.Hongo, M. Fluid Phase Equilibria 1998, 144, 181-189.

13. Zhang, C.; Cappleman, B. P.; Defibaugh-Chavez, M.; Weinkauf, D. H. Journal of Polymer Science Part B-Polymer Physics 2003, 41, 2109-2118.

14. Aubert, J. H. Journal of Supercritical Fluids 1998, 11, 163-172.

15. Park, K. H.; Koh, M. S.; Yoon, C. H.; Kim, H. W.; Kim, H. D. Journal of Supercritical Fluids 2004, 29, 203-212.

16. Wu, Y. T.; Akoto-Ampaw, P. J.; Elbaccouch, M.; Hurrey, M. L.; Wallen, S. L.; Grant, C. S. Langmuir 2004, 20, 3665-3673.

17. Wu, Y. T.; Grant, C. S. in Dekker Encyclopedia of Nanoscience and Nanotechnolgy, Schwarz, J. A.; Contescu, C. I.; Putyera, K., Ed. 2004, Marcel Dekker, Inc.: New York. p. 1977-1990.

18. Buchholz, F.L.; Graham, A.T. in Industrial Polymers Handbook: Products, Processes, Applications, Wilks, E. S., Ed. 2001, Wiley-VCH, Weinheim (Federal Republic of Germany). p. 565-585.

19. Chiou, J. S.; Barlow, J. W.; Paul, D. R. Journal of Applied Polymer Science 1985, 30, 2633-2642.

20. Chiou, J. S.; Paul, D. R. Journal of Applied Polymer Science 1986, 32, 2897-2981.

21. Sanders, E. S.; Jordan, S. M.; Subramanian, R. Journal of Membrane Science 1992, 74, 29-36.

22. Story, B. J.; Koros, W. J. Journal of Membrane Science 1992, 67, 191-210.

23. Goel, S. K.; Beckman, E. J. Polymer 1993, 34, 1410-1417.

24. Handa, Y. P.; Capowski, S.; Oneill, M. Thermochimica Acta 1993, 226, 177-185.

25. Handa, Y. P.; Lampron, S.; O'Neill, M. L. Journal of Polymer Science Part B-Polymer Chemistry 1994, 32, 2549-2553.

26. Ghosal, K.; Chern, R. T.; Freeman, B. D.; Daly, W. H.; Negulescu, I. I. Macromolecules 1996, 29, 4360-4369.

27. Handa, Y. P.; Kruus, P.; Oneill, M. Journal of Polymer Science Part B-Polymer Physics 1996, 34, 2635-2639.

28. Shieh, Y. T.; Su, J. H.; Manivannan, G.; Lee, P. H. C.; Sawan, S. P.; Spall, W. D. Journal of Applied Polymer Science 1996, 59, 707-717.

29. Banerjee, T.; Lipscomb, G. C. Journal of Applied Polymer Science 1998, 68, 1441-1449.

30. Mi, Y. L.; Zheng, S. X. Polymer 1998, 39, 3709-3712.

31. Bos, A.; Punt, I. G. M.; Wessling, M.; Strathmann, H. Journal of Membrane Science 1999, 155, 67-78.

32. Royer, J. R.; DeSimone, J. M.; Khan, S. A. Macromolecules 1999, 32, 8965-8973.

33. Ma, L.; Zhang, L.; Yang, J. C.; Xie, X. M. Journal of Applied Polymer Science 2002, 86, 2272-2278.

34. Sato, Y.; Takikawa, T.; Yamane, M.; Takishima, S.; Masuoka, H. Fluid Phase Equilibria 2002, 194, 847-858.

35. Alessi, P.; Cortesi, A.; Kikic, I.; Vecchione, F. Journal of Applied Polymer Science 2003, 88, 2189-2193.

36. Kikic, I.; Vecchione, F.; Alessi, P.; Cortesi, A.; Eva, F.; Elvassore, N. Industrial & Engineering Chemistry Research 2003, 42, 3022-3029.

37. Shenoy, S. L.; Fujiwara, T.; Wynne, K. J. Macromolecules 2003, 36, 3380-3385.

38. Garcia-Leiner, M.; Lesser, A. J. Journal of Applied Polymer Science 2004, 93, 1501-1511.

39. Tang, M.; Huang, Y. C.; Chen, Y. P. Journal of Applied Polymer Science 2004, 94, 474-482.

40. Grulke, E. A. in Polymer Handbook, Brandrup, J.; Immergut, E. H.; Grulke, E. A., Ed. 1999, John Wiley & Sons, Inc.: New York. p. 675-714.

41. Giddings, J. C.; Myers, M. N.; McLaren, L.; Keller, R. A. Science 1968, 162, 67-73.

42. Allada, S. R.; Industrial & Engineering Chemistry Research 1984, 23, 344-348.

43. Williams, L. L.; Rubin, J. B.; Edwards, H. W. Industrial & Engineering Chemistry Research 2004, 43, 4967-4972.

44. Chow, T. S. Macromolecules 1980, 13, 362-364.

Nomenclature

C_m	mass sensitivity of QCM ($\mu g/cm^2$)
C_P	pressure sensitivity of QCM (μg/MPa)
ΔC_p	polymer heat capacity change at glass transition (J/g-K)
F	frequency of quartz crystal (Hz)
F_0	initial frequency of quartz crystal (Hz)
ΔF_f	quartz crystal frequency change due to fluid density and viscosity change (Hz)
ΔF_m	quartz crystal frequency change due to mass change (Hz)
ΔF_P	quartz crystal frequency change due to pressure change (Hz)
Δm	mass change ($\mu g/cm^2$)
M_d	molecular weight of diluent (g/mol)
M_p	molecular weight of polymer repeat unit (g/mol)
$\overline{M}_v$	viscosity average molecular weight of polymer (g/mol)
P	pressure (MPa)
P_c	critical pressure (atm)
R	gas constant (J/mol-K)
T_P	polymerization temperature (°C)
T_g	glass transition temperature of polymer (°C, or K)
T_{g0}	glass transition temperature of pure polymer (°C, or K)
z	lattice coordination number
α	pressure proportionality constant (MPa^{-1})
δ	solubility parameter ($(cal/cm^3)^{1/2}$, or $MPa^{1/2}$)

μ_q	shear modulus of quartz (g/cm-s^2)
μ_f	viscosity of fluid (Pa s)
ρ_q	density of quartz (g/cm^3)
ρ_f	density of fluid (g/cm^3)
ρ_r	reduced supercritical fluid density
$\rho_{r,l}$	reduced liquid density
ω	CO_2 absorption into polymer (g CO_2 / g Polymer)

Table 5-1. Typical continuous polymerization experiments

T (°C)	$[M]_{in}$ (mol/L)	$[I]_{in}$ (mol/L)	Yield (%)	$\overline{M}_v$ (kg/mol)	Polymer Morphology
50	1.25	0.004	30.8	175	coagulum
70	1.25	0.001	54.5	157	Irregular Particles
70	0.50	0.006	80.8	28.9	Spherical Particles
90	0.25	0.006	46.1	6.9	Spherical Particles

Note: τ = 25 min; P = 20.7 MPa; Agitation speed = 1800rpm.

Table 5-2. The calculated value of polymer solubility parameters (δ)

	δ ($MPa^{1/2}$)*
PMMA	18.87
PS	19.66
PAA	22.35 – 23.16

* - Calculated by group contribution method on the basis of the group constants of Small [40]

Table 5-3. The polymerization temperature and the corresponding glass transition temperature

Temperature (T_P) (°C)	Pressure (MPa)	CO_2 Absorption (g CO_2 / g PAA)	T_g calculated by the Chow's Equation (°C)
50	20.7	0.134	61.6
70	20.7	0.113	66.8
90	20.7	0.100	71.6

Figure Captions

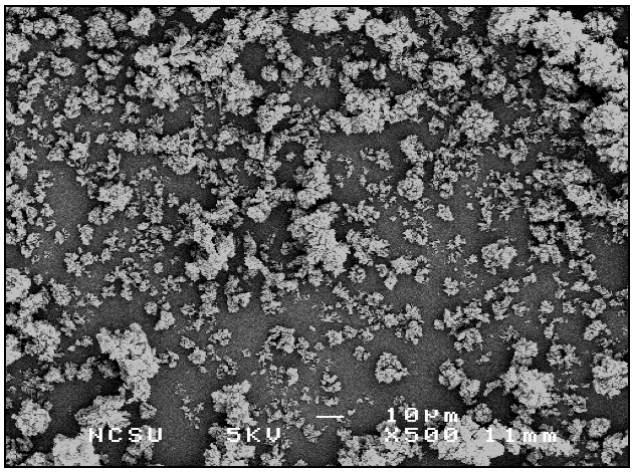

(a)

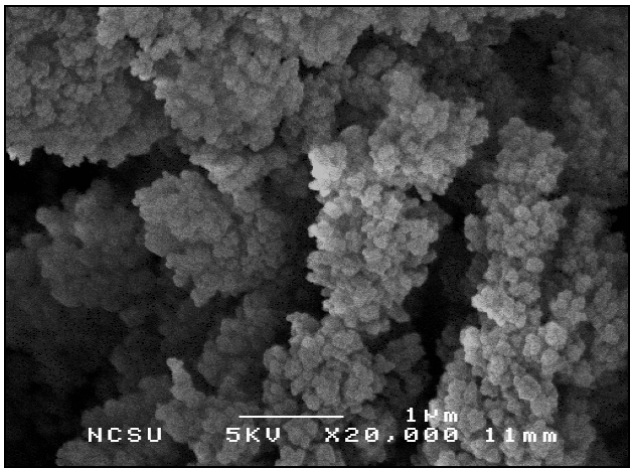

(b)

Figure 5-1. SEM of PAA particles produced in a CSTR polymerization (T = 50 °C; P = 20.7 MPa; τ = 25min; $[M]_{in}$ = 1.25 mol/L; $[I]_{in}$ = 0.00 1mol/L)

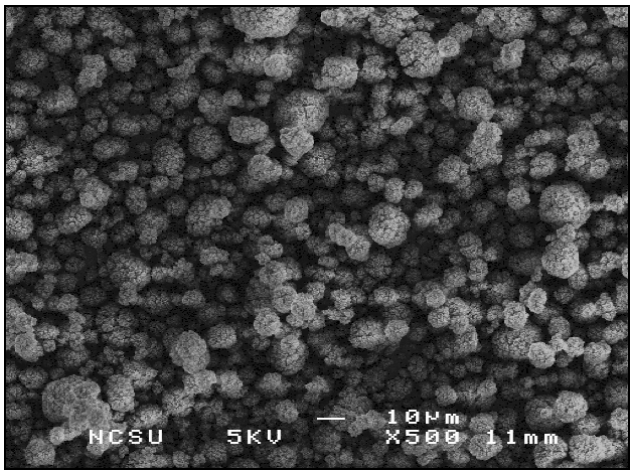

Figure 5-2. SEM of PAA particles produced in a CSTR polymerization (T = 70 °C; P = 20.7 MPa; τ = 25 min; $[M]_{in}$ = 1.25 mol/L; $[I]_{in}$ = 0.001 mol/L)

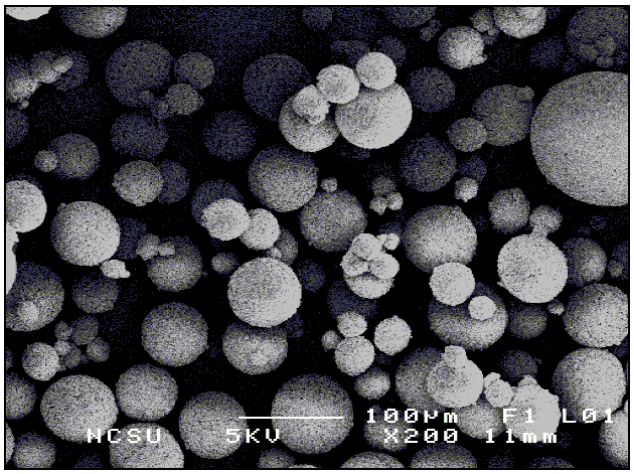

Figure 5-3. SEM of PAA particles produced in a CSTR polymerization (T = 70 °C; P = 20.7 MPa; τ = 25 min; $[M]_{in}$ = 0.50 mol/L; $[I]_{in}$ = 0.006 mol/L)

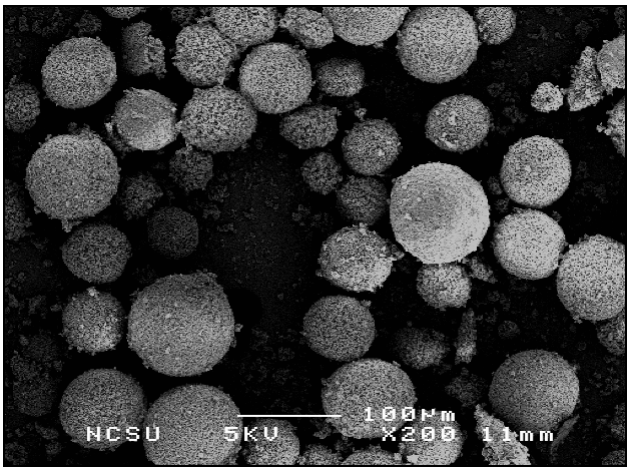

Figure 5-4. SEM of PAA particles produced in a CSTR polymerization (T = 90 °C; P = 20.7 MPa; τ = 25 min; $[M]_{in}$ = 0.25 mol/L; $[I]_{in}$ = 0.006 mol/L)

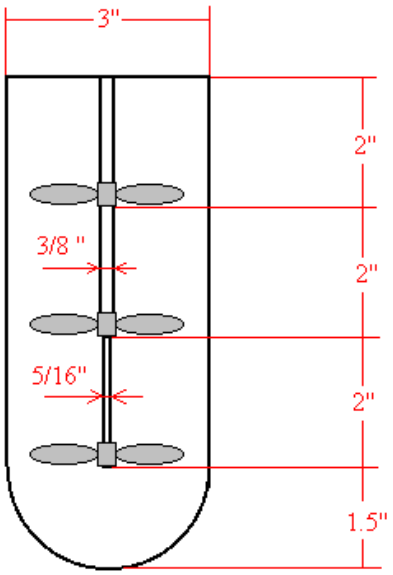

Reactor

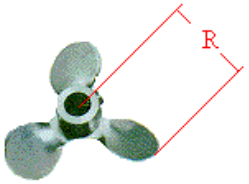

Bore Diameter (inch)	R (inch)
5/16	1
3/8	1

Propeller

Figure 5-5. The dimensions of the CSTR and the agitator

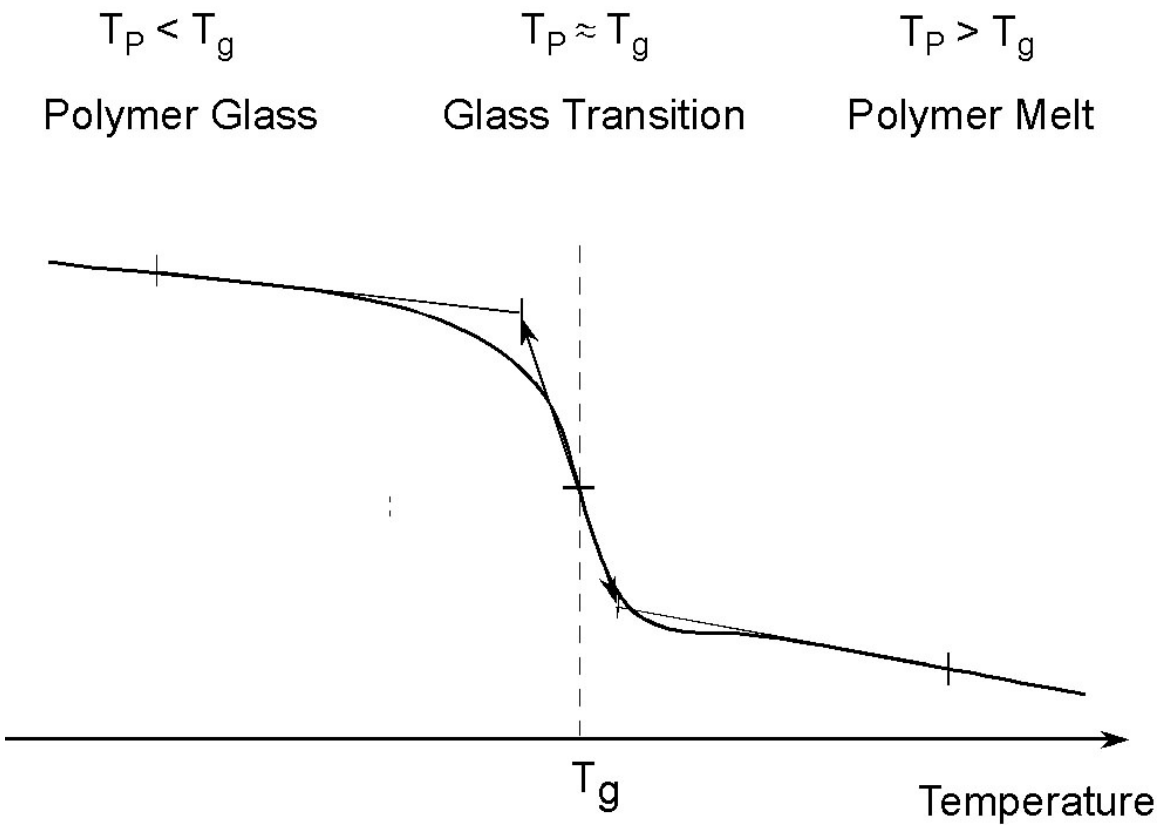

Figure 5-6. A proposed particle formation mechanism

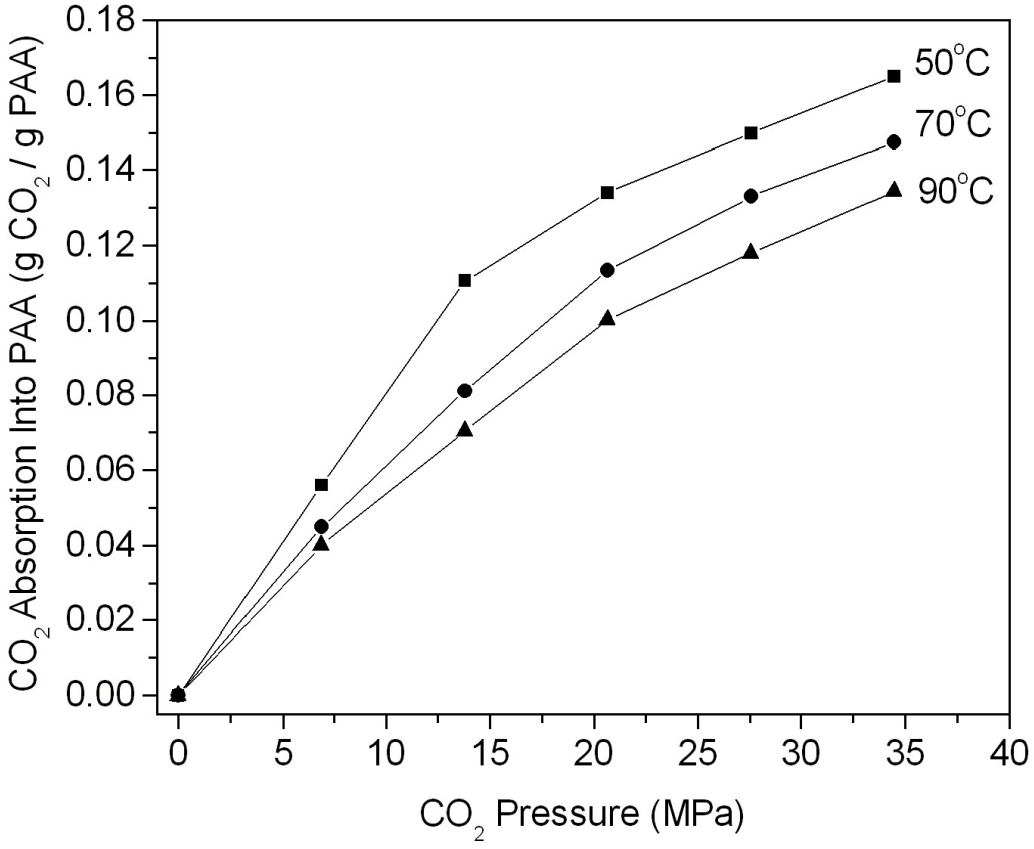

Figure 5-7. CO_2 absorption into PAA measured by QCM

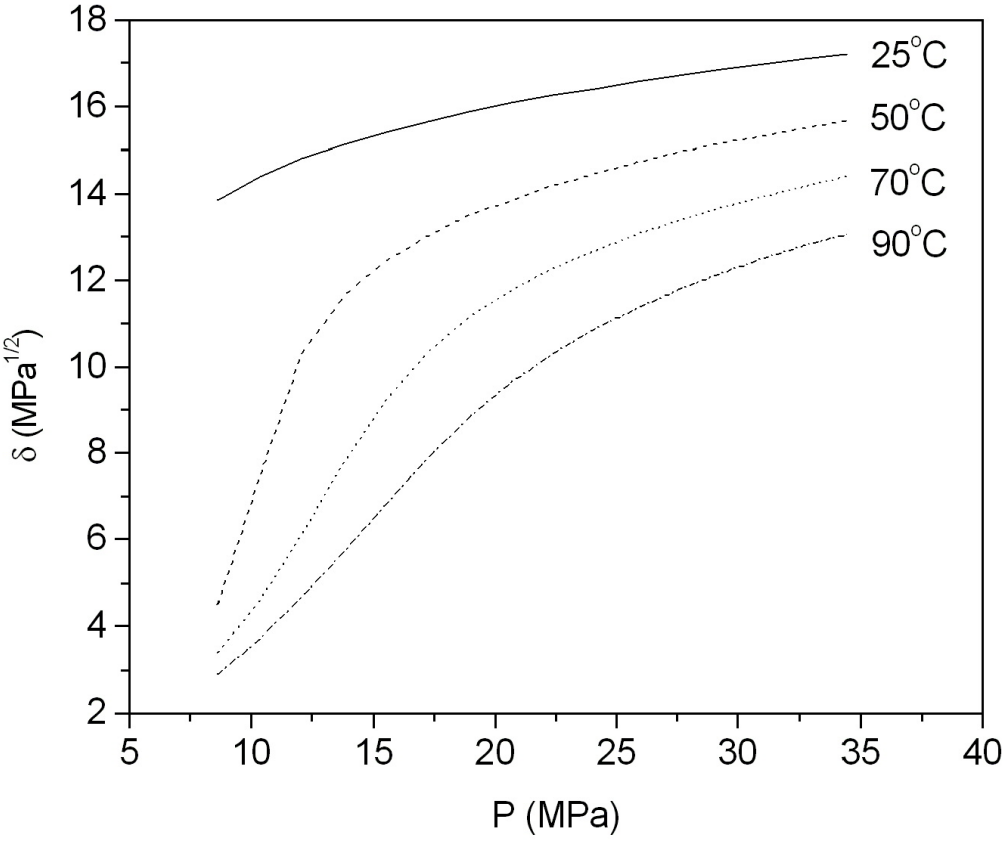

Figure 5-8. The calculated CO_2 solubility parameter

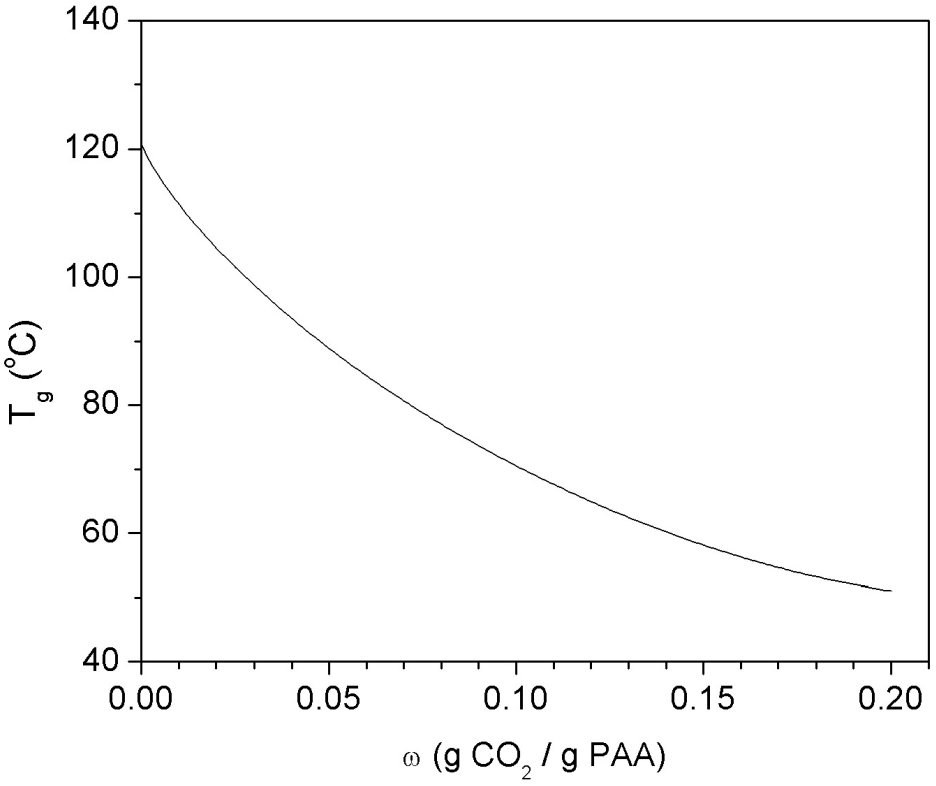

Figure 5-9. The T_g of PAA calculated with the Chow's Equation (z = 1, T_{g0} = 120.90 °C, ΔC_p = 0.40 J/(g °C))

CHAPTER 6

PRECIPITATION CROSS-LINKING POLYMERIZATION OF ACRYLIC ACID IN SUPERCRITICAL CARBON DIOXIDE

Tao Liu[1], Joseph M. DeSimone[1, 2], and George W. Roberts[1,*]

[1]Department of Chemical Engineering, Campus Box 7905, North Carolina State University, Raleigh, North Carolina 27695-7905

[2]Department of Chemistry, CB 3290, Venable and Kenan Laboratories, University of North Carolina at Chapel Hill, North Carolina 27599-3290

Abstract

Cross-linking polymerization of acrylic acid in supercritical carbon dioxide was carried out in a batch reactor at 50 °C and 207 bar with tetraallyl pentaerythritol ether and triallyl pentaerythritol ether as the cross-linkers and 2, 2'-azobis (2, 4-dimethyl-valeronitrile) as the free radical initiator. All polymers were white, dry, fine powder. Scanning electron microscopy showed the polymer morphology was not affected by cross-linking. As the cross-linker concentration in polymerization increased, the polymer glass transition temperature first decreased, then increased. By adjusting the cross-linker concentration, water-soluble and water-insoluble poly(acrylic acid)s were synthesized. The polymer thickening effect was measured with a dynamic stress rheometer, and it strongly depended on the degree of cross-linking.

Keywords:

acrylic acid, cross-linking, precipitation, polymerization, supercritical carbon dioxide, solubility, glass transition temperature.

6.1 Introduction

Cross-linked poly(acrylic acid)s (PAAs) are widely used as thickeners, flocculants and superabsorbent polymers (SAPs). By far, the most prevalent commercial process to make such polymers is solution polymerization of acrylic acid with a cross-linking monomer in water [1]. To get dry polymer, a costly drying process is necessary. Other processes, such as suspension polymerization, emulsion polymerization and precipitation polymerization are carried out in organic media. The use of solvents and/or surfactants inevitably leads to chemical contamination of the polymer. For applications where extremely clean PAA or PAA derivatives are desired (e.g. food and pharmaceutical applications), costly purification processes are necessary. Although contamination can be reduced to very low levels, complete removal cannot be accomplished.

Precipitation polymerization of acrylic acid in CO_2 was first reported in a French patent [2] in 1968. The United States version of this patent [3] appeared in 1970. The precipitation polymerization of several vinyl compounds, including acrylic acid, in liquid and supercritical CO_2 was demonstrated in these patents. In comparison with the conventional methods, the CO_2-based technique has many advantages, including (1) CO_2 is an environmentally benign medium; (2) the products are completely dry after depressurizing to remove the CO_2; and (3) the final polymer is virtually free of contamination. Unreacted monomer and initiator are easily removed by supercritical fluid extraction.

In 1986, a Canadian patent [4] described the synthesis of water-soluble acrylic acid homopolymer in $scCO_2$. In 1987, the synthesis of thickeners based on cross-linked, water-soluble PAA in $scCO_2$ was reported in a U.S. patent application [5]. In 1988, a similar study was discussed in a European patent application [6]. More recently, DeSimone and coworkers

[7] studied acrylic acid polymerization in $scCO_2$, and used ethyl mercaptan as a chain transfer agent to control the polymer molecular weight. Xu et al. [8,9] explored the effect of cosolvents on the polymerization of acrylic acid in $scCO_2$. Finally, we studied the continuous polymerization of acrylic acid in $scCO_2$ by using a continuous stirred tank reactor [10].

The present paper describes the synthesis of cross-linked PAA by polymerization of acrylic acid with a cross-linker in $scCO_2$ in a 20-ml batch reactor at 50 °C and 207 bar. By adjusting the degree of cross-linking, water-soluble and water-insoluble polymers were synthesized. The effect of cross-linking on polymer properties was evaluated.

6.2 Experimental

Materials. CO_2 (SFC grade, 99.998%) was purchased from National Specialty Gases. The initiator, 2,2'–azobis(2,4-dimethyl-valeronitrile) (V-65B) (high purity), was donated by Wako Chemicals USA. Triallyl pentaerythritol ether (APE3) (76.1%) and tetraallyl pentaerythritol ether (APE4) (90.4%) were obtained from Monomer-Polymer & Dajac Laboratories, Inc. Acrylic acid (99.5%), 1,1,2-trichloro-1,2,2-trifluoroethane (Freon 113) (HPLC grade, 99.8%), and deionized water (D.I. Water) were purchased from the Fisher Scientific. All chemicals were used as received.

Polymerization. The polymerization was carried out in a 20-ml, stainless steel high-pressure view cell. A magnetic stir bar was used for agitation. The reactor was purged with SFC grade CO_2 before use. In a typical polymerization, 2.0 ml of acrylic acid containing known amount of cross-linker and 0.1ml V-65B/Freon 113 solution were charged to the reactor. Liquid CO_2 was then added until about 2/3 of the reactor volume was occupied. The reactor was then heated to 50 °C. A small amount of CO_2 was added into the reactor to

increase its pressure to 207 bar. The polymerization started as a homogeneous solution. After a short induction period, polymer particles started to appear in the reactor. The reaction was allowed to run for 10hr. Then the CO_2 was slowly released while the reactor temperature was kept at 50 °C. The reactor was cooled to approximately room temperature, and the product polymer was collected. Yield above 90% was achieved in all experiments.

Characterization. Scanning electron micrography (SEM, JEOL 6400F Field Emission) was used to observe the polymer morphology; differential scanning calorimetry (DSC, TA Q-100) was used to determine the polymer glass transition temperature; and a dynamic stress rheometer (DSR®) was used for viscosity measurement.

6.3 Results and Discussion

In all experiments, the product polymers were fluffy fine powders. Electron micrographs of some products are shown in Figure 6-1. The polymers are aggregates of primary particles of about 100nm in size. There is no obvious morphology change observed, although the cross-linker concentration used in polymerization to make these polymers are different. Therefore, the cross-linking precipitation polymerization can be carried out like normal precipitation polymerization of acrylic aid in $scCO_2$ without concern for viscosity increases, as observed in aqueous solution polymerizations.

The effect of cross-linker concentration on the polymer glass transition temperature is shown in Figure 6-2. When the cross-linker concentration was low, the glass transition temperature decreased as the cross-linker concentration increased. When the cross-linker concentration was high, the glass transition temperature increased with the cross-linker concentration. When the cross-linker concentration was low, the main effect of the small

amount of cross-linker was to make the polymer chains branched. The branch chains increased the free volume of polymer, which decreased the glass transition temperature. However, when the cross-linker concentration was high, the large amount of cross-linker could make polymer chains cross-linked together to become networks. The networks made chain movement more difficult. Therefore, the polymer glass transition temperature increased with the degree of cross-linking. Figure 6-2 shows that APE3 has a weaker effect on the glass transition temperature than APE4. This is because each APE3 molecule has only three double bonds while each APE4 molecule has four double bonds. For the same amount of cross-linker used, APE3 could only make fewer branches or produce less cross-linking.

Cross-linked water-soluble PAA is a good thickener. Water-insoluble PAA is useful for the preparation of SAPs. To check the water-solubility of a polymer, 0.1 g of the polymer was dispersed in 10ml D.I. water. After 24 hour of stirring, some polymer samples were completely dissolved, while the others were not, depending on the degree of cross-linking. The viscosity of the polymer/water mixture was measured by DSR at 25 °C. The plots of viscosity versus shear rate were shown in Figure 6-3a and Figure 6-3b. When the cross-linker concentration was below 0.2% wt, the polymers were soluble in water. For these polymers, the solution viscosity increased dramatically with the cross-linker concentration (Figure 6-3a). When the cross-linker concentration was above 0.2%, the polymers were not completely soluble in water. The increase of cross-linker concentration could only decrease the thickening effect of the polymer (Figure 6-3b), because the polymer became more and more insoluble in water as the cross-linker concentration increased. The polymer/water mixture finally became a system of polymer particles dispersed in water, instead of a polymer solution.

The water-insoluble polymer could be removed from the aqueous phase by filtration or centrifugation. Then the viscosity of the aqueous phase (or, filtrate) could be measured. Figure 6-4 shows that although the 1% cross-linked polymer has a much higher thickening effect than the 5% cross-linked polymer, the viscosities of their filtrates were the same. Both are close to the viscosity of water. Therefore, there was essentially no polymer left in either filtrate. In other words, both polymers were completely insoluble in water. In comparison with the 5% cross-linked polymer, the 1% cross-linked polymer might have more capacity to swell in water [11], and it might have more side chains that could extend into the surrounding water, and these produced a stronger thickening effect than the 5% cross-linked polymer.

Figure 6-5 shows that the two cross-linkers have the same effect on polymer thickening. No obvious difference can be observed between the two polymers cross-linked with different cross-linkers.

The monomer and initiator concentration in the polymerization also had a very strong effect on the thickening effect of the water-soluble polymers. Figure 6-6 shows that when the monomer concentration decreased or the initiator concentration increased, the polymer thickening effect decreased. This is because these concentration changes decreased the polymerization kinetic chain length. Figure 6-6 also shows that the monomer concentration has a stronger effect than the initiator concentration. This is because the kinetic chain length of free radical polymerization depends on the monomer concentration to a higher order than the initiator concentration.

6.4 Conclusions

Cross-linking polymerization of acrylic acid was carried out in $scCO_2$ in a batch reactor at 50 °C and 207 bar with APE3 and APE4 as the cross-linkers and V-65B as the free radical initiator. The product polymers were white, fine, fluffy powder. No effect of cross-linking on polymer morphology was observed. By adjusting the cross-linker concentration, water-soluble polymer and water-insoluble polymer were produced. It was found that the thickening effect of the water-soluble polymer not only depended on the cross-linker concentration, but also depended on the monomer concentration and the initiator concentration. The polymer glass transition temperature was strongly affected by the cross-linker type and the cross-linker concentration.

6.5 References

1. Nemec, J. W.; Bauer, W. in Encyclopedia of Polymer Science and Engineering, 2nd ed.; Mark, H. F., Ed.; Wiley-Interscience: New York, 1988; vol.1, pp 211-231.
2. Fukui, K.; Fujii, K.; Kagiya, T.; Toriuchi, Y.; Yokota, H. (Sumitomo Chemical Company, Ltd. and Sumitomo Atomic Energy Industries, Ltd.). French Patent 1,524,533, April 1,1968.
3. Fukui, K.; Fujii, K.; Kagiya, T.; Toriuchi, Y.; Yokota, H. (Sumitomo Chemical Company, Ltd. and Sumitomo Atomic Energy Industries, Ltd.). U. S. Patent 3,522,228, July 28, 1970.
4. Sertage, W. G. J.; Davis, P.; Schenck, H. U.; Denzinger, W.; Hartmann, H. (BASF Corporation). Canadian Patent 1,274,942, October 2, 1990.

5. Hartmann, H.; Denzinger, W. (BASF Corporation). U. S. Patent 4,748,220, May 31, 1988.

6. Herbert, M. W.; Huvard, G. S. (B.F. Goodrich Company). European Patent 0,301,532 (A2), February 1, 1989.

7. Romack, T. J.; Maury, E. E.; DeSimone, J. M. Macromolecules1995, 28, 912-915.

8. Xu, Q.; Han, B.; Yan, H. Polymer 2001, 42, 1369-1373.

9. Xu, Q.; Han, B.; Yan, H. Journal of Applied Polymer Science 2003, 88, 1876-1880.

10. Liu, T.; DeSimone, J. M.; Roberts, G. W. Journal of Polymer Science Part A – Polymer Chemistry (in press)

11. Brannon-Peppas, L.; Peppas, N. A. Journal of Controlled Release 1991, 16, 319 –330.

Figure Captions

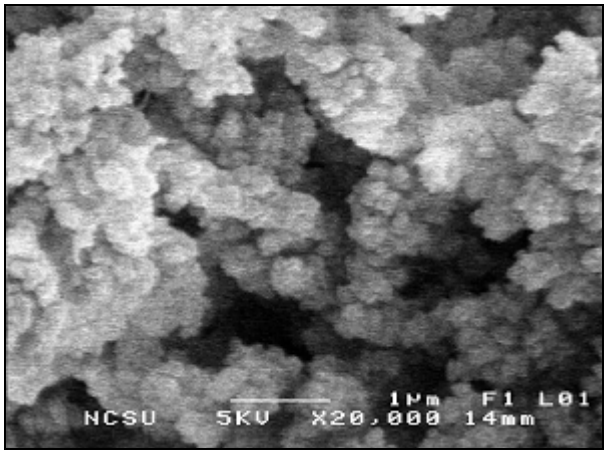

(a)

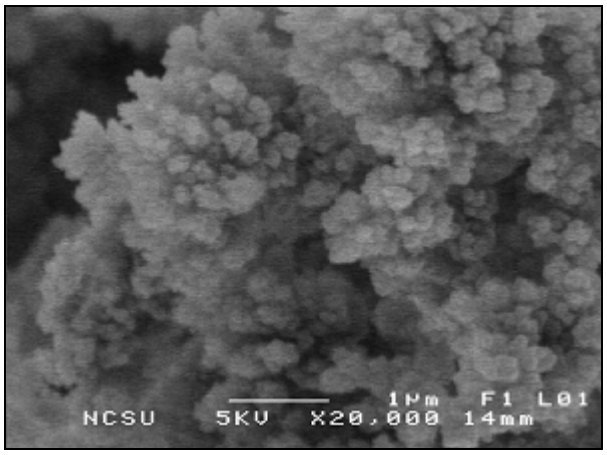

(b)

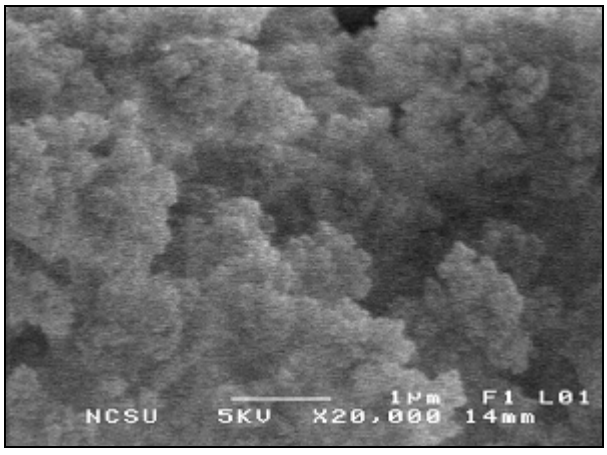

(c)

Figure 6-1. Morphology comparison of the homopolymer with the cross-linked polymers (a - homopolymer, b - polymer with 1% APE4 cross-linker, c – polymer with 5% APE4 cross-linker)

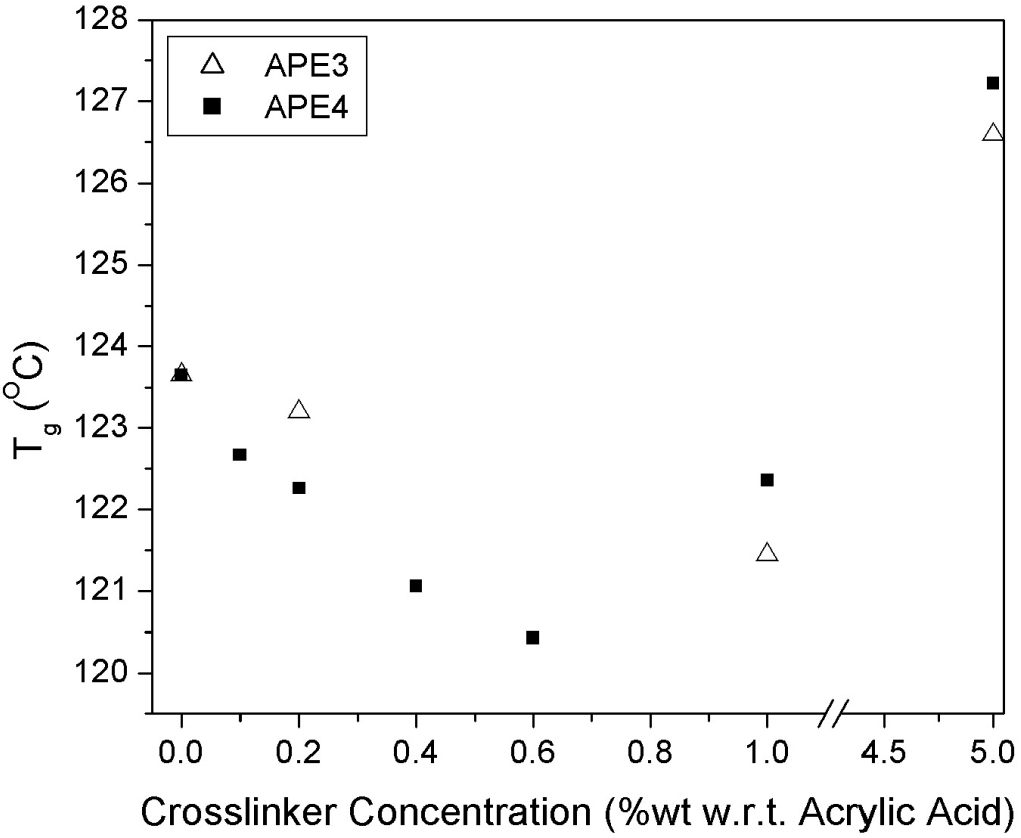

Figure 6-2. The effect of cross-linker concentration on the polymer glass transition temperature (T = 50 °C, P = 207 bar, $[M]_0$ = 1.46 mol/L, $[I]_0$ = 0.0024 mol/L)

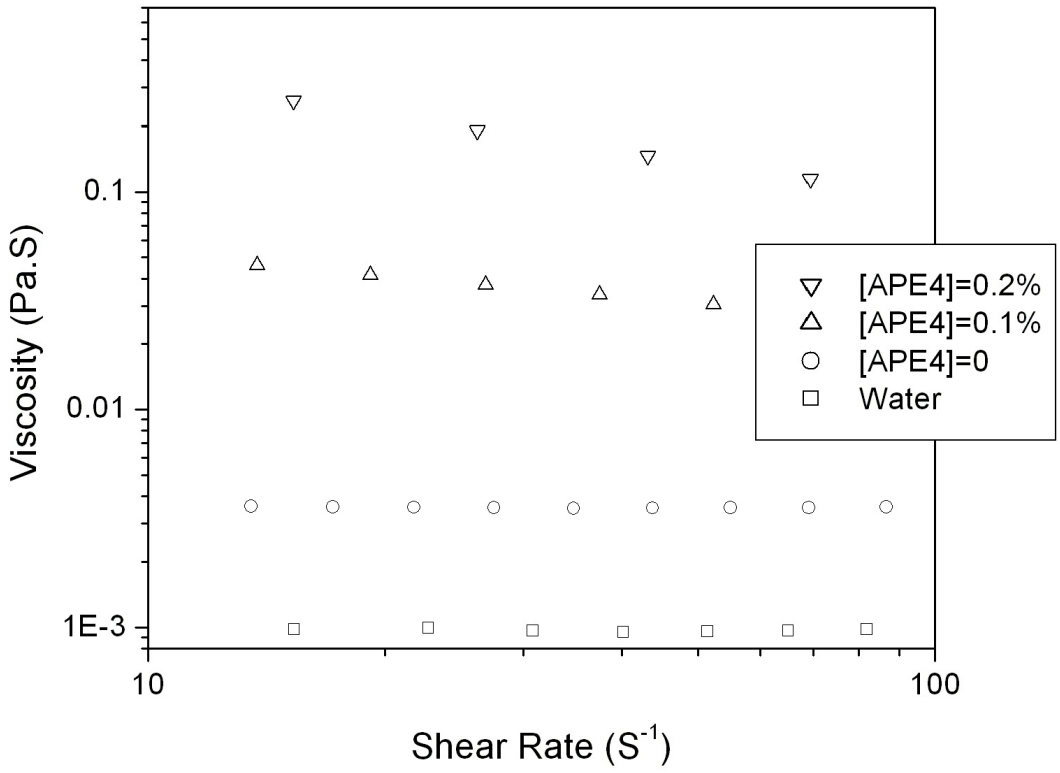

Figure 6-3a. The effect of cross-linker concentration on the polymer thickening effect: low cross-linker concentrations (T = 50 °C, P = 207 bar, $[M]_0$ = 1.46 mol/L, $[I]_0$ = 0.0024 mol/L)

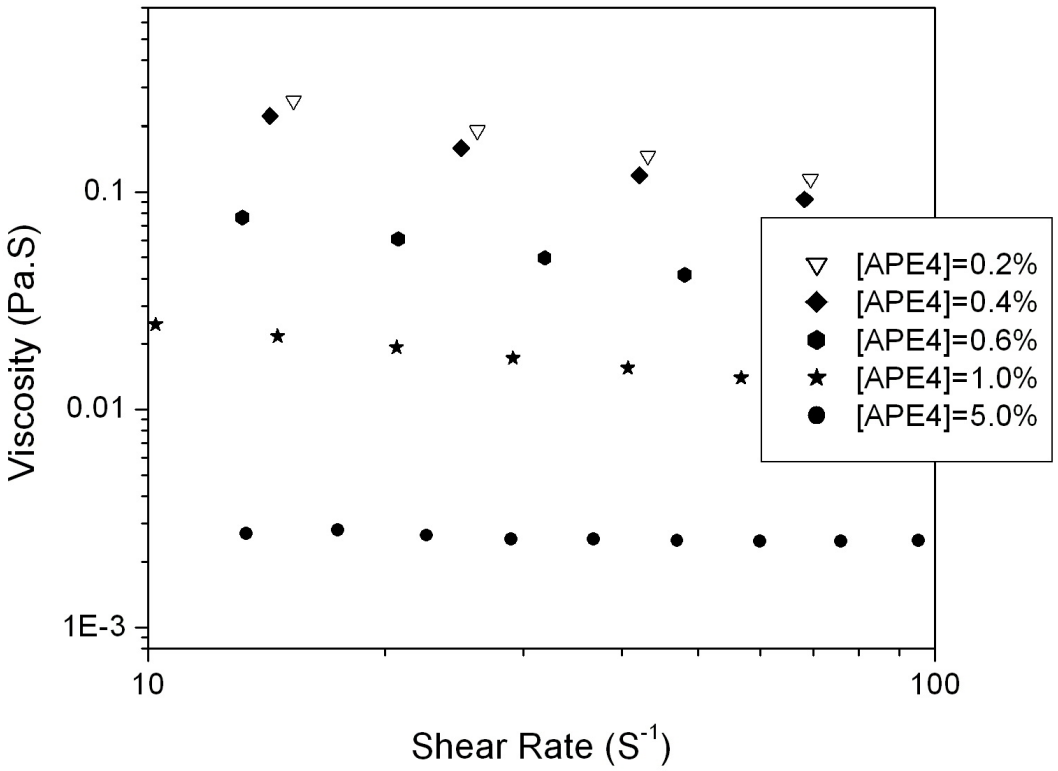

Figure 6-3b. The effect of cross-linker concentration on the polymer thickening effect: high cross-linker concentrations (T = 50 °C, P = 207 bar, $[M]_0$ = 1.46 mol/L, $[I]_0$ = 0.0024 mol/L)

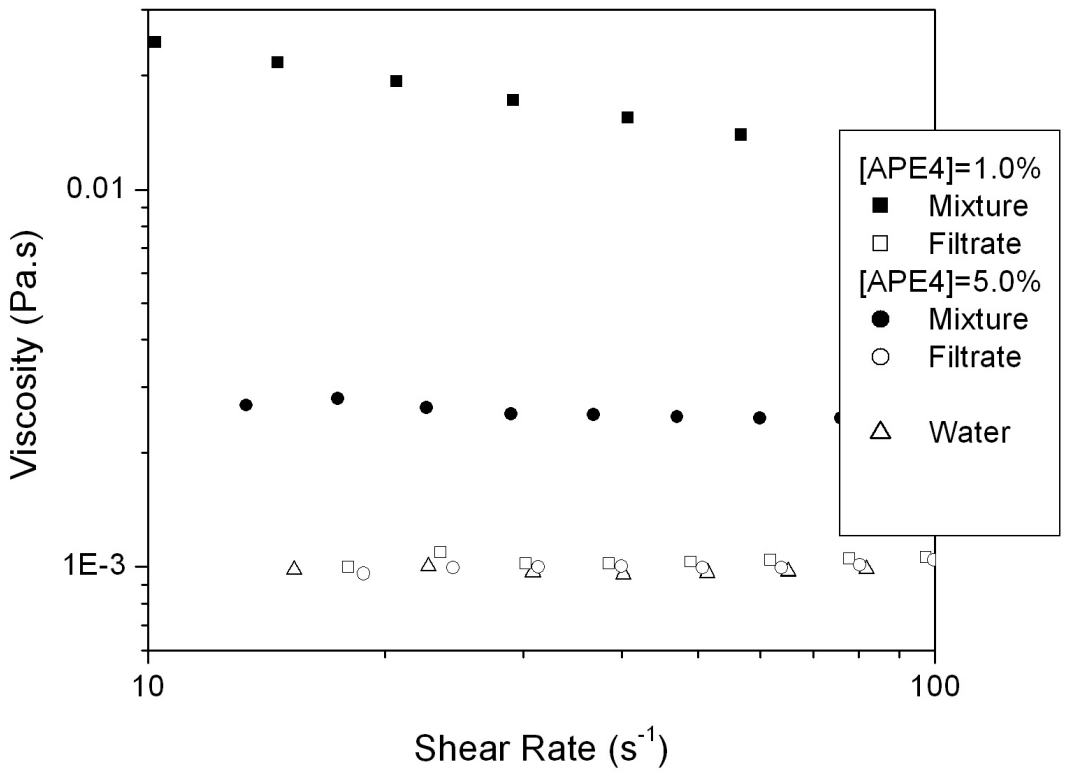

Figure 6-4. The viscosities of the polymer/water mixtures and their filtrates at 25 °C

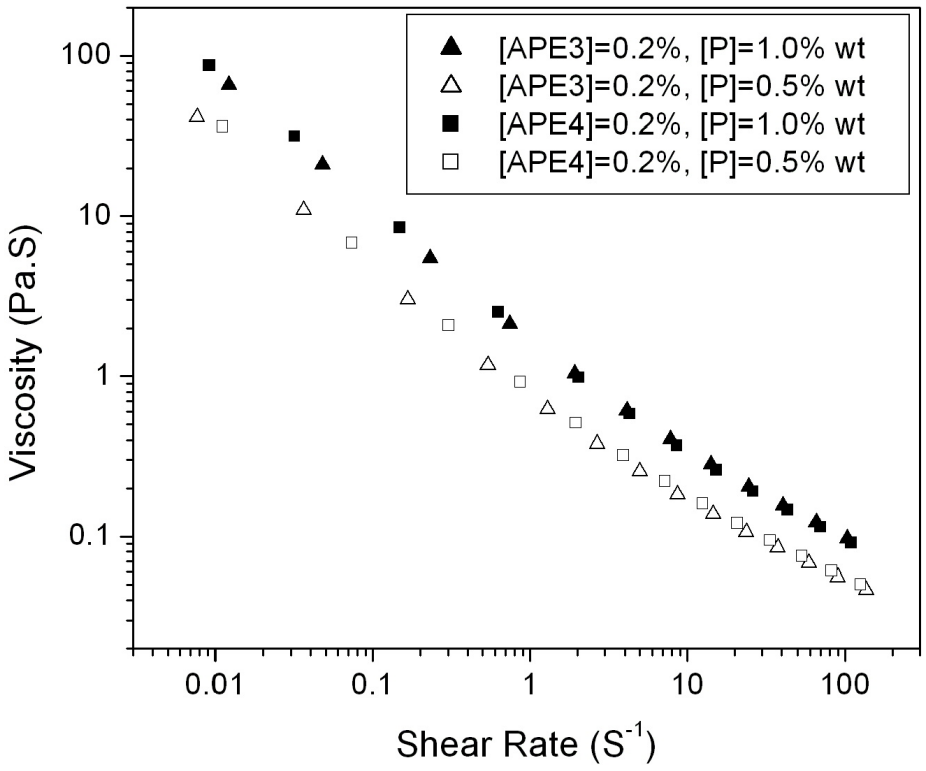

Figure 6-5. The effect of cross-linker structure on the polymer thickening effect

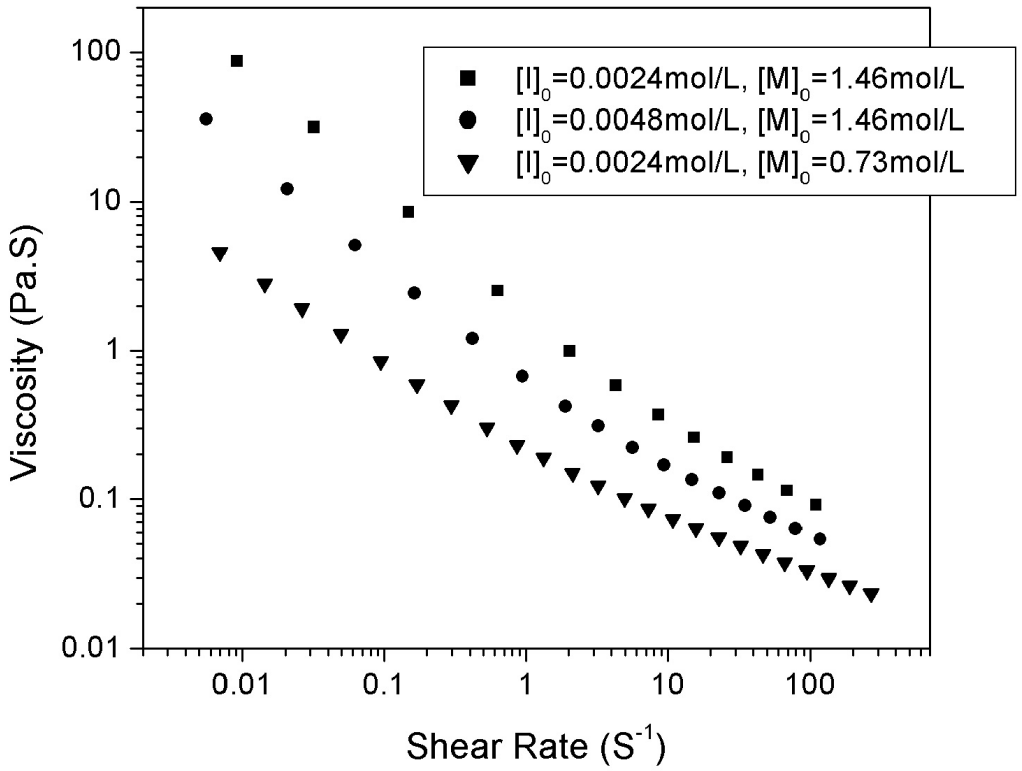

Figure 6-6. The effect of monomer concentration and initiator concentration on the polymer thickening effect

CHAPTER 7

PREPARATION OF SUPERABSORBENT POLYMERS WITH SUPERCRITICAL CARBON DIOXIDE TECHNOLOGY

7.1 Introduction

Superabsorbent polymers (SAPs) are widely used in applications such as disposable infant diapers, adult incontinence pads, female hygiene products, agriculture, electric batteries and wire cables. Most SAPs are cross-linked copolymers of acrylic acid and metal acrylates, such as sodium acrylate and ammonia acrylate. As the largest application of acrylic acid polymers, SAPs account for 73% of PAA consumption in 2000. The U.S. demand for SAPs is estimated at 800 million pounds in 2003, and it is expected to grow at an average annual rate of 5% during 2003 – 2008 [1].

By far the most prevalent commercial process to make SAPs is cross-linking polymerization of acrylic acid in water [2]. The monomer concentration in the polymerization ranges from about 16% to about 43% on a weight basis. The polymerization produces a hydrogel intermediate containing a large amount of water. Commercially, about 2 to 5 kg of water must be removed by evaporation for 1 kg of polymer produced. The moisture concentration at the end of the drying step will be from about 1 to 5%.

Suspension polymerization in organic solvents is also used to make SAPs [2]. Usually high molecular weight aliphatic hydrocarbons (C10 – C14) are used as the continuous phase. Because heat transfer in this process is better than in the aqueous process, a much higher monomer concentration can be used in the polymerization phase. Therefore, the drying cost

is reduced. However, this advantage is negated by the low polymerization phase ratio (ratio of dispersed phase to continuous phase), which is limited to 1:1 or less.

This chapter describes a new process for making SAPs. In this process, water-insoluble PAA is prepared by precipitation cross-linking polymerization of acrylic acid in supercritical carbon dioxide ($scCO_2$). Then the polymer was neutralized to make SAPs using ammonia gas or sodium hydroxide alcohol solution. Since solvent-free PAA is directly produced without costly drying or purification, this process has the potential to decrease the production cost. However, the study is still in its early stages, and only preliminary results are presented here.

7.2 Experimental

Materials. Deionized water (D.I. Water), Methanol (HPLC grade, 99.9%) and Ethyl alcohol (ACS grade, 99.5%) were purchased from the Fisher Scientific. Ammonia (99.99%) and sodium hydroxide (99.998%) were purchased from Aldrich. All chemicals were used as received.

Polymerization. Water-insoluble cross-linked PAAs were prepared by precipitation cross-linking polymerization of acrylic acid in $scCO_2$. The polymerization could be carried out in a continuous stirred tank reactor (CSTR) (see Chapter 3) or a batch reactor (see Chapter 6). In polymerization, the cross-linkers were charged into the reactor together with acrylic acid. The product polymer was a fine fluffy powder. It was dried in a vacuum oven (0.02 bar, 70 °C) for two days before neutralization.

Neutralization. Figure 7-1 shows the batch reactor system that was used to neutralize PAA with ammonia gas. In a typical experiment, 1g cross-linked, water-insoluble PAA was

added into the 20-ml view cell. The system was sealed. Then ammonia gas was charged into the 6-ml view cell and the pressure inside was increased to about 100 psi. Then the valve separating the two view cells was opened to let the ammonia gas get in contact with the polymer. The pressure in the 6-ml view cell quickly decreased to atmospheric. The temperature in the 20-ml view cell first jumped to a temperature higher than room temperature, ~70 °C, then decreased back to room temperature. This process could be repeated a few times to get a higher degree of neutralization. The neutralized polymer was dried in a vacuum oven (40 °C, 2×10^{-5} bar) for 24 hours. Then elementary analysis was carried out to determine the nitrogen weight concentration in polymer, through which the degree of neutralization could be calculated.

When sodium hydroxide alcohol solution was used to neutralize PAA, the experiment was carried out in a 100-ml Pyrex bottle. A magnetic stir bar was used for mixing. In a typical experiment, 80ml ethyl alcohol was charged into the bottle. Then a known amount of sodium hydroxide was dissolved in the ethyl alcohol. Cross-linked, water-insoluble PAA was added into the solution for neutralization. Since the polymer was insoluble in ethyl alcohol, the ethyl alcohol solution became a milky slurry. The slurry was agitated for 2 hours. Then it was filtered to separate the polymer from the solution. The filtration cake was dried in a vacuum oven (70 °C, 0.02 bar) for 2 days to remove the absorbed ethyl alcohol. The polymer was weighed and the degree of neutralization was calculated.

7.3 Results and Discussion

Table 1 shows two neutralization experiments in which ammonia was used as the neutralization agent. In the first experiment, the 6-ml view cell was filled with ammonia gas

three times. About 0.08 gram ammonia gas reacted with the polymer. Elementary analysis showed that 38% of the carboxyl acid groups were neutralized. In the second experiment, the neutralization was repeated until no obvious ammonia consumption could be observed. 73% of the carboxyl acid groups were neutralized.

Figure 7-2 shows the pressure change in the second neutralization experiment. In the beginning of the experiment, the system was at room temperature (25 °C) and atmospheric pressure (0 psi). The 6-ml view cell was filled with ammonia gas and its pressure was increased to 107 psi. The valve between the two view cells was opened and the ammonia gas was released to the 20-ml view cell that contained 1g PAA. The pressure decreased to zero in less than 1 minute. It indicated all ammonia gas had been consumed. If there was no reaction, the pressure could only be decreased to about 26 psi due to volume change. As this process was repeated, the reaction slowed down. During the fourth time, it took about 13 minutes for the pressure to decrease from 20 psi to 12 psi. Theoretically, only 50% of the carboxyl groups had been neutralized by then. At room temperature, PAA is in its glassy state. It is difficult for the ammonia gas to diffuse into the polymer particles to react with the carboxylic acid groups inside. Therefore, the degree of neutralization is low.

Figure 7-3 shows an experiment in which sodium hydroxide ethyl alcohol solution was used as the neutralization agent. 1.11 g sodium hydroxide was dissolved in 80ml ethyl alcohol solution. Then 3g cross-linked PAA was dispersed into the solution by stirring. The pH value of the solution decreased very quickly in the beginning of the reaction, especially in the first 30 minutes. In less than 60 minutes, it had become constant, implying the reaction had been completed.

Table 2 shows three experiments in which NaOH solutions were used to neutralize the same amount of PAA. The experimental degree of neutralization was close to the theoretical predictions which assumed that all NaOH had been consumed. Because ethyl alcohol could swell the polymer particles, It is much easier for OH^- to diffuse into the polymer. Therefore, higher degree of neutralization could be achieved easily.

Water absorption tests showed that a 73% neutralized 5.8% cross-linked polymer (Table 7-2) could quickly absorb more than 20 times its weight in water. In comparison with the commercial SAPs, which can easily absorb forty times their weight in water, the water absorption of our polymer is low. The equilibrium swelling of anionic polyelectrolyte gels depends on many factors, such as the chain length between crosslinks, the kinetic chain length of polymerization, and the neutralization degree, just to mention a few [3-5]. By adjusting the polymerization conditions, the water absorption capacity of the neutralized polymer can likely be improved.

7.4 Conclusions

Water-insoluble PAA was prepared by precipitation cross-linking polymerization of acrylic acid in $scCO_2$. The polymer could be neutralized with ammonia gas or sodium hydroxide alcohol solution. When ammonia gas was the neutralization agent, solvent-free poly(acrylic acid-co-ammonium acrylate) was prepared. Due to the difficulty of diffusion of ammonia into the glassy polymer, the polymer could only be partially neutralized at room temperature. When the polymer was neutralized by sodium hydroxide alcohol solution, filtration and drying processes had to be used to remove the alcohol from the product

polymer. However, since the solvent could swell the polymer to make the diffusion of small molecules into polymer easier, neutralization degree close to 100% could be achieved easily.

7.5 References

1. Will, R.; Sasano, T. in CEH Market Research Reports; Chemical Economics Handbook – SRI International: 2001; p 582.000 A – 582.005 J.
2. Graham, A. T.; Wilson, L. R. in Modern Superabsorbent Polymer Technology; Buchholz, F. L.; Graham, A. T. Ed.; Wiley – VCH: New York, 1998; Chapter 3, p69-118.
3. Brannon-Peppas, L.; Peppas, N. A. Journal of Controlled Release 1991, 16, 319 –330.
4. Jabbari, E.; Nozari, S. European Polymer Journal 2000, 36, 2685-2692.
5. Buchholz, F. L. in Modern Superabsorbent Polymer Technology; Buchholz, F. L.; Graham, A. T. Ed.; Wiley – VCH: New York, 1998; Chapter 5, p167-221.

Table 7-1. Neutralization of PAA with ammonia gas

PAA* (g)	NH_3(g)	N Composition (%)	Degree of Neutralization (%)
1.0	0.08	6.72	38.0
1.0	-	12.0	73.0

*-the cross-linker (APE4) concentration is 1%wt.

Table 7-2. Neutralization of PAA with sodium hydroxide ethyl alcohol solution

PAA*	NaOH	Time	Degree of Neutralization (%)	
(g)	(g)	(hr)	Theoretical	Experimental
4.0	1.46	2	70.0	72.6
4.0	1.46	2	70.0	73.0
4.0	2.08	4	98.5	96.4

*-the cross-linker (APE4) concentration is 5.8%wt.

Figure Captions

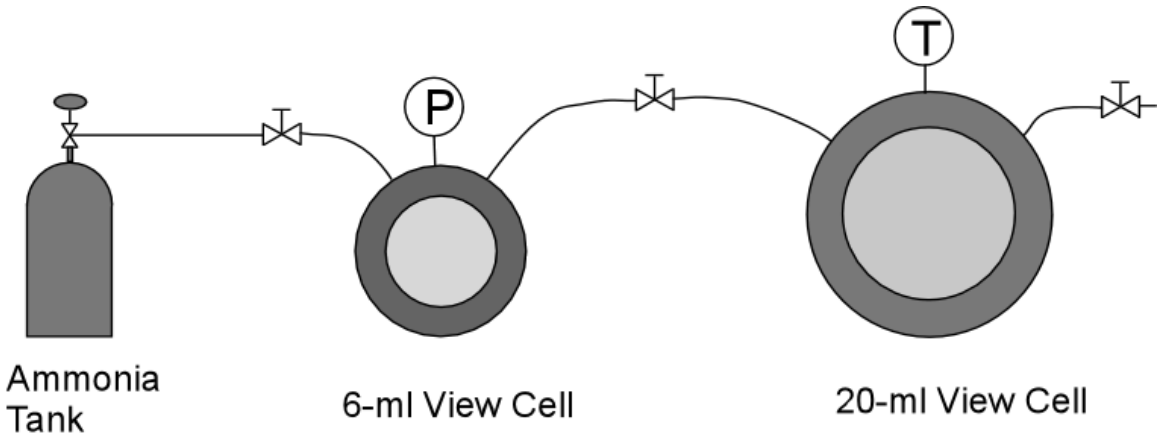

Figure 7-1. Experimental setup for PAA neutralization with ammonia gas

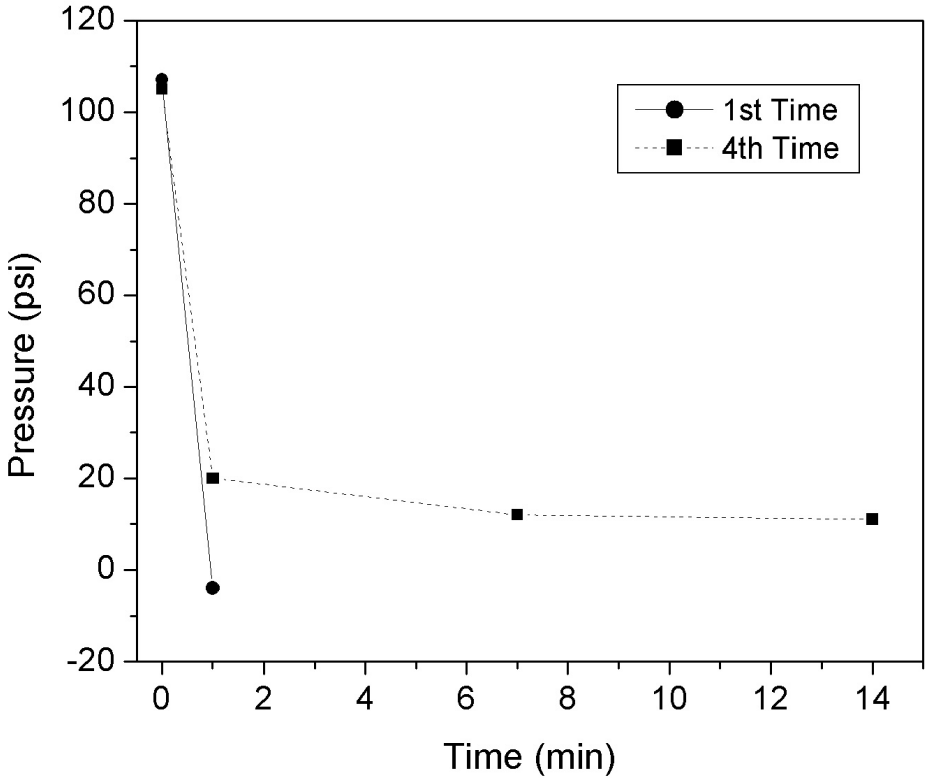

Figure 7-2. PAA neutralization with ammonia gas

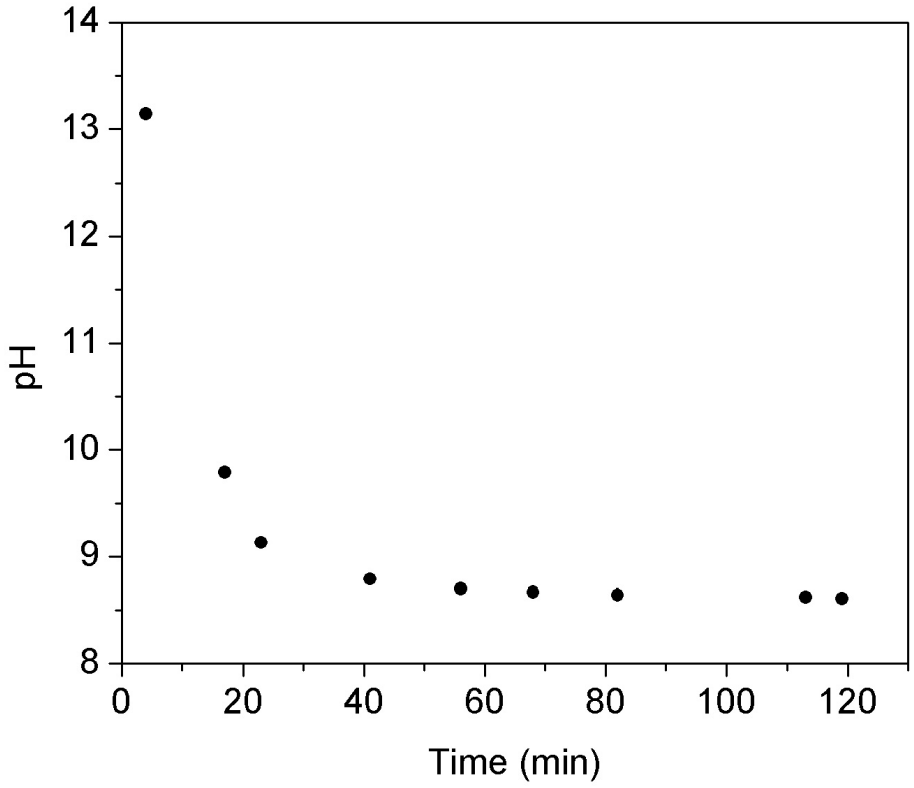

Figure 7-3. The decrease of pH value of a sodium hydroxide ethyl alcohol solution after the addition of cross-linked water-insoluble PAA

CHAPTER 8

CONCLUSIONS AND RECOMMENDATIONS FOR FUTURE WORK

8.1 Conclusions

8.1.1 Continuous Precipitation Polymerization of Acrylic Acid in Supercritical Carbon Dioxide

The precipitation polymerization of acrylic acid in supercritical carbon dioxide ($scCO_2$) was studied in a continuous stirred-tank reactor (CSTR) using 2, 2'-azobis (2, 4-dimethyl-valeronitrile) (V-65B) as the free-radical initiator. The reactor temperature was between 50 and 90 °C, the pressure was 207 bar, and the average residence time was between 12 and 40 minutes. The product polymer was a white, dry, fine powder that dissolved in water. A wide range of polymer molecular weights (5 to 200 kg/mol) could be obtained.

The effects of the operating variables on the polymerization rate and on the polymer molecular weight were evaluated. The experimental results showed distinct characteristics of precipitation polymerization. The behavior of acrylic acid polymerization in $scCO_2$ is different from what DeSimone, Roberts and co-workers [1-3] found in their studies of the continuous polymerization of vinylidene fluoride in $scCO_2$. In that system, many features of the polymerization rate and the molecular weight could be described by a model based on the assumption that polymerization took place primarily in the supercritical fluid. Polymerization inside the polymer particles appears to be more important with poly(acrylic acid) (PAA) than with poly(vinylidene fluoride).

The kinetics of precipitation polymerization was analyzed and three kinetic models were derived. The first model assumes that the polymerization takes place only in the

solution phase, with no reactions in the polymer phase. The second model assumes that chain initiation takes place in the solution phase, but chain propagation and termination take place in a thin layer on particle surface. The third one assumes that chain initiation take place only in the fluid phase, but it assumes chain propagation and chain termination occur homogeneously throughout the polymer particle. The model predictions were compared with the experimental results from the continuous precipitation polymerization of acrylic acid in $scCO_2$ in a CSTR and those from an isothermal reaction calorimeter. The solution polymerization model didn't agree with the experimental results well. The other two models both predicted the experimental results well. However, the calorimetric experimental results showed that the particle polymerization model described the polymerization behavior better.

Scanning electron micrography (SEM) showed that three types of polymer particles were obtained: coagulum of primary particles of about 100 nanometers in size, irregular particles of about 5–20 micrometers, and spherical particles of about 10–100 micrometers. $ScCO_2$ could greatly reduce the polymer glass transition temperature (T_g). It is believed that the polymer coagulum was produced when the polymerization temperature, T_P, was below T_g, the irregular particles were prepared when T_P was in the glass transition region, and the spherical particles were produced when T_P was above T_g. The CO_2 absorption into PAA was measured with a quartz crystal microbalance. The T_g depression due to CO_2 absorption was calculated by the Chow's equation. The calculated results lent strong support to the proposed particle formation mechanism.

8.1.2 Precipitation Cross-linking Polymerization of Acrylic Acid in Supercritical Carbon Dioxide

Cross-linking polymerization of acrylic acid in supercritical carbon dioxide was studied in a batch reactor at 50 °C and 207 bar with tetraallyl pentaerythritol ether and triallyl pentaerythritol ether as the cross-linkers and V-65B as the free radical initiator. All polymers were white, dry, fine powder. SEM showed the polymer morphology was not affected by cross-linking. As the cross-linker concentration in polymerization increased, the polymer glass transition temperature first decreased, then increased. By adjusting the cross-linker concentration, water-soluble and water-insoluble poly(acrylic acid)s (PAA) were synthesized. The polymer thickening effect was measured by a dynamic stress rheometer, and it strongly depended on the concentration of cross-linker in polymerization.

The water-insoluble PAA was neutralized by ammonia gas and sodium hydroxide ethanol solution to make superabsorbent polymers (SAPs). When ammonia gas was used, solvent-free poly(acrylic acid – co – ammonia acrylate) was prepared. Due to the difficulty of diffusion of ammonia into the glassy polymer, the polymer could only be partially neutralized at room temperature. When the polymer was neutralized with a sodium hydroxide alcohol solution, filtration and drying processes had to be used to remove alcohol from the product polymer. However, since the solvent alcohol could swell the polymer to make the diffusion of small molecules into polymer easier, neutralizations close to 100% could be reached easily.

8.2 Recommendations for Future Work

8.2.1 Continuous Precipitation Polymerization of Acrylic Acid in Supercritical Carbon Dioxide

The molecular weight of PAA tends to define the end-use applications [4, 5]. For example, short-chain linear PAA with average molecular weights of 5000 to 20,000 are mainly used as dispersants, while long-chain linear PAA having molecular weights of greater than one million can be used as flocculating agents. The molecular weights of the PAA obtained in our research are in the range from about 7,000 to about 200,000, which are too low to be used in many applications. Further study to increase the polymer molecular weight will be important.

Many acrylic acid polymers are actually copolymers of acrylic acid and other hydrophilic monomers, such as acrylamide and methacrylic acid [5,6]. The introduction of other monomer units can expand the polymer application by changing hydrophile/hydropobe ratio, charge density, etc. For example, the copolymers of acrylic acid and acrylamide are useful as drilling mud additives for oil wells, by enhancing the stability of the clay dispersion in water [5]. In our study, only homopolymer of acrylic acid was produced. Future study on the copolymerization of acrylic acid with other monomers will be interesting too.

The effect of reaction variables on polymer morphology also needs more investigation. We speculate that the polymer morphology mainly depends on the polymerization temperature. If the proposed particle formation mechanism is true, it can be applied to the polymerization of other monomers in $scCO_2$. In addition, new processes can be developed to make polymer particles.

8.2.2 Precipitation Cross-linking Polymerization of Acrylic Acid in Supercritical Carbon Dioxide

In this thesis, most of the cross-linking polymerization experiments were carried out in a 20-ml view cell. The continuous precipitation cross-linking polymerization of acrylic acid in $scCO_2$ has not been studied in detail. Because a continuous process is more suitable for commercial production, study on the continuous cross-linking polymerization of acrylic acid in $scCO_2$ will be important. In addition, a comparison between the homo and the cross-linking polymerizations will be interesting.

Although this thesis has demonstrated that cross-linked water-insoluble PAA can be neutralized to make superabsorbent polymers, only preliminary results have been reported. Further studies, such as investigations on the effect of polymerization variables and neutralization conditions, will be necessary for improving the polymer water-absorption properties.

8.3 References

1. Charpentier, P. A.; DeSimone, J. M.; Roberts, G. W. Ind Eng Chem Res 2000, 39, 4588-4596.
2. Saraf, M. K.; Gerard, S.; Wojcinski, L. W. II; Charpentier, P. A.; DeSimone, J. M.; Roberts, G. W. Macromolecules 2002, 35, 7976 – 7985.
3. Ahmed, T. S.; DeSimone, J. M.; Roberts, G. W. Chem Engng Sci 2004, 59, 5139-5144.
4. Will, R.; Sasano, T. in CEH Market Research Reports; Chemical Economics Handbook – SRI International: 2001; p 582.000 A – 582.005 J.

5. Swift, G. in Encyclopedia of Polymer Science and Technology, 2nd ed.; Bailey, J.; Kroschwitz, J. I. Ed.; Wiley-Interscience: New York, 2003; vol.1, pp 79-96.

6. Buchholz, F. L. in Industrial Polymers Handbook: Products, Processes, Applications; Wilks E. S. Ed.; Wiley-VCH: Weinheim, 2000; Volume 1, pp 565 –585.